

NAVAL POSTGRADUATE SCHOOL MONTEREY, CALIFORNIA



THESIS

POLARIZATION EFFECTS ON INFRARED TARGET CONTRAST

by

Marcos Cesar Pontes

September 1998

Thesis Advisor:
Co-Advisor:

Alfred W. Cooper
David D. Cleary

Approved for public release; distribution is unlimited.

THIS QUANTITY ALLOCATED 1

19980914 024

REPORT DOCUMENTATION PAGE			Form Approved OMB No. 0704-0188	
Public reporting burden for this collection of information is estimated to average 1 hour per response, including the time for reviewing instruction, searching existing data sources, gathering and maintaining the data needed, and completing and reviewing the collection of information. Send comments regarding this burden estimate or any other aspect of this collection of information, including suggestions for reducing this burden, to Washington Headquarters Services, Directorate for Information Operations and Reports, 1215 Jefferson Davis Highway, Suite 1204, Arlington, VA 22202-4302, and to the Office of Management and Budget, Paperwork Reduction Project (0704-0188) Washington DC 20503.				
1. AGENCY USE ONLY (Leave blank)		2. REPORT DATE. September 1998		3. REPORT TYPE AND DATES COVERED Master's Thesis
4. TITLE AND SUBTITLE POLARIZATION EFFECTS ON INFRARED TARGET CONTRAST			5. FUNDING NUMBERS	
6. AUTHOR(S) Marcos Cesar Pontes, Capt.				
7. PERFORMING ORGANIZATION NAME(S) AND ADDRESS(ES) Naval Postgraduate School Monterey CA 93943-5000			8. PERFORMING ORGANIZATION REPORT NUMBER	
9. SPONSORING/MONITORING AGENCY NAME(S) AND ADDRESS(ES)			10. SPONSORING/MONITORING AGENCY REPORT NUMBER	
11. SUPPLEMENTARY NOTES The views expressed in this thesis are those of the author and do not reflect the official policy or position of the Department of Defense or the U.S. Government.				
12a. DISTRIBUTION/AVAILABILITY STATEMENT Approved for public release; distribution is unlimited.			12b. DISTRIBUTION CODE	
13. ABSTRACT (maximum 200 words) An analysis has been carried out of a data base of polarized long wave infrared images of the instrumented Research Vessel POINT SUR recorded over a period of two days during the EOPACE measurements series in San Diego Bay in 1996. The measurements were made from a land site on Point Loma with an AGA780 sensor with internally mounted polarization filters. The objectives of the analysis were to determine a possible influence of target aspect angle on the polarization signature, to compare polarization contrast improvement in San Diego Bay with previous measurements in the North Atlantic, and to validate by measurement the estimation of unpolarized signature from vertical and horizontal components. 5508 images representing 70 cases with vertical, horizontal and unpolarized sequences were analyzed. Using a horizontal polarizer, target to background contrast improvement was found with a mean of 1.08 (8%) compared with the 15% found in previous measurements. Estimated unpolarized signatures from vertical and horizontal components agreed with unpolarized measurements with a slope coefficient of .85 to .99. Target signature for major ship facets and for total ship showed no discernable degree of polarization. A total of 37 IDL programs developed for this analysis can be assembled as a package for future data processing.				
14. SUBJECT TERMS Thermal Imaging, Polarization, Target Contrast, Infrared Radiation			15. NUMBER OF PAGES 189	
			16. PRICE CODE	
17. SECURITY CLASSIFICATION OF REPORT Unclassified	18. SECURITY CLASSIFICATION OF THIS PAGE Unclassified	19. SECURITY CLASSIFICATION OF ABSTRACT Unclassified	20. LIMITATION OF ABSTRACT UL	

NSN 7540-01-280-5500

Standard Form 298 (Rev. 2-89)

Prescribed by ANSI Std. Z39-18 298-102

Approved for public release; distribution is unlimited.

POLARIZATION EFFECTS ON INFRARED TARGET CONTRAST

Marcos Cesar Pontes
Capt., Brazil Air Force
B.S., Brazil Air Force Academy, 1984
Aeronautical Engineer, Aeronautical Institute of Technology, Brazil, 1993

Submitted in partial fulfillment
of the requirements for the degree of

MASTER OF SCIENCE IN SYSTEMS ENGINEERING

from the

NAVAL POSTGRADUATE SCHOOL

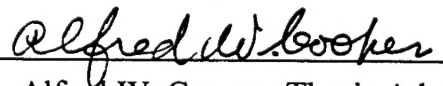
September 1998

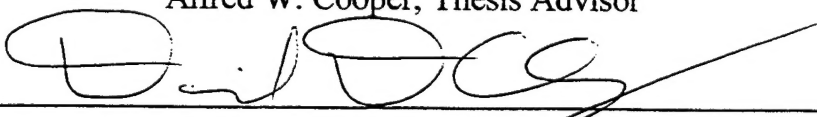
Author:

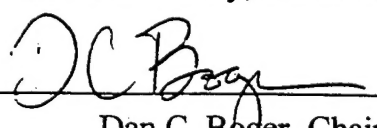


Marcos Cesar Pontes

Approved by:



Alfred W. Cooper, Thesis Advisor

David D. Cleary, Thesis Co-Advisor

Dan C. Boger, Chairman
Electronic Warfare Academic Group

ABSTRACT

An analysis has been carried out of a data base of polarized long wave infrared images of the instrumented Research Vessel POINT SUR recorded over a period of two days during the EOPACE measurements series in San Diego Bay in 1996. The measurements were made from a land site on Point Loma with an AGA780 sensor with internally mounted polarization filters. The objectives of the analysis were to determine a possible influence of target aspect angle on the polarization signature, to compare polarization contrast improvement in San Diego Bay with previous measurements in the North Atlantic, and to validate by measurement the estimation of unpolarized signature from vertical and horizontal components. 5508 images representing 70 cases with vertical, horizontal and unpolarized sequences were analyzed. Using a horizontal polarizer, target to background contrast improvement was found with a mean of 1.08 (8%) compared with the 15% found in previous measurements. Estimated unpolarized signatures from vertical and horizontal components agreed with unpolarized measurements with a slope coefficient of .85 to .99. Target signature for major ship facets and for total ship showed no discernable degree of polarization. A total of 37 IDL programs developed for this analysis can be assembled as a package for future data processing.

TABLE OF CONTENTS

I. INTRODUCTION	1
II. FUNDAMENTALS	3
A. ELECTROMAGNETIC SPECTRUM	3
B. INFRARED TERMINOLOGY AND UNITS	5
C. LAWS OF THERMAL RADIATION	6
1. Black Body	6
2. Planck's Law	8
3. Wien Displacement Law	10
4. Stefan-Boltzmann Law	10
D. ATMOSPHERIC PROPAGATION	11
E. POLARIZATION PHYSICS	12
1. Sea Emission and Reflection	15
2. Sky Emission and Reflection	16
3. Target Emission and Reflection	17
F. TARGET / BACKGROUND CONTRAST	18
III. EXPERIMENT DESCRIPTION	21
A. EQUIPMENT	21
1. AGA-780 Thermovision	21
2. Polarizer Filters	22
3. R/V POINT SUR	23
4. Software	23
a. <i>CEDIP PTRWIN</i>	23
b. <i>Interactive Data Language (IDL)</i>	24
c. <i>ONTAR PCMODTRAN</i>	24
B. EXPERIMENT CONFIGURATION	25

C. ORIGINAL DATA	25
1. Images	25
2. Meteorological Data	27
3. Ship Skin Temperature Data	27
D. PRE-PROCESSED DATA	27
1. Images	29
2. Meteorological Data	30
3. Ship Skin Temperature Data	32
4. Thermal Image Calibration	33
E. ANALYSIS PROGRAMS	36
1. Methodology	37
a. <i>Hotspot.pro</i>	37
b. <i>Areagen.pro</i>	38
c. <i>Horizont.pro</i>	39
d. <i>Threshold.pro</i>	39
e. <i>Elements.pro</i>	41
f. <i>Aspect.pro</i>	42
g. <i>Contrast.pro</i>	43
IV. RESULTS AND ANALYSIS	45
A. IDL PROGRAMS	45
B. RESULTS DESCRIPTION	46
C. SHIP CONTRAST VARIATION IN TIME	46
D. DEGREE OF POLARIZATION AND CONTRAST IMPROVEMENT ..	50
E. GENERATION OF UNPOLARIZED IMAGES	52
F. SHIP ASPECT ANGLE EFFECTS ON POLARIZATION	55
V. CONCLUSIONS AND RECOMMENDATIONS	59

APPENDIX A. EXPERIMENT LOCATION	61
APPENDIX B. POLARIZER PERFORMANCE CURVES	65
APPENDIX C. R/V POINT SUR	69
APPENDIX D. IMAGE FILES	73
1. LIST OF THE SELECTED IMAGE FILES (*.PTW)	73
2. LIST OF THE BASIC IMAGE FILES (*.PTE)	77
APPENDIX E. METEOROLOGICAL DATA	79
1. METOC FILES	79
2. METEOROLOGICAL CONDITIONS	83
APPENDIX F. SHIP SKIN TEMPERATURE	93
APPENDIX G. AGA 780 LABORATORY CALIBRATION CURVES	97
APPENDIX H. ANALYSIS PROGRAMS	101
1. LIST OF THE ANALYSIS PROGRAMS	101
2. HOTSPOT TRACKING	104
3. BOX POSITIONING	106
4. IMAGE SAMPLE	108
5. COMBINED IMAGE / SURFACE / CONTOUR PLOT	110
6. SURFACE PLOT	112
7. NORMALIZATION : PHASE 1	114
8. NORMALIZATION : PHASE 2	116
9. IMAGE ELEMENTS	118
10. SHIP MODEL	120
11. SHIP MODEL : WIREFRAME MODE	122
12. SHIP MODEL'S MAIN PLANES	124
13. MASK APPLICATION EXAMPLE	126
APPENDIX I. RESULT TABLES	129
1. RESULT MATRIX DESCRIPTION	129
2. SUMMARY MATRIX DESCRIPTION	134
3. CONTRAST VARIATION IN TIME	140

4. CONTRAST IMPROVEMENT AND DEGREE OF POLARIZATION	147
APPENDIX J. RESULT GRAPHICS	151
1. CONTRAST VARIATION IN TIME : DATA FILE SAMPLE	151
2. CONTRAST VARIATION IN TIME : STATISTIC DISTRIBUTION	153
3. CONTRAST IMPROVEMENT AND DEGREE OF POLARIZATION	157
4. GENERATION OF UNPOLARIZED IMAGES	160
5. TARGET ASPECT ANGLE EFFECTS	164
LIST OF REFERENCES	173
INITIAL DISTRIBUTION LIST	175

ACKNOWLEDGEMENTS

This research was supported in part by Naval Command, Control and Ocean Surveillance Center, Propagation Division, Code 88 and partly by the Naval Postgraduate Institute for Joint Warfare Analysis.

I wish to express my gratitude to those who contributed to the successful and timely completion of this project. First I would like to thank the participants in the EOPACE measurement series. Special recognition is due the crew of the R/V POINT SUR and the NPS Boundary Layer Meteorology Group, Professor Davidson, Mrs. Tamar Neta, and Mr. Paul Frederickson for their outstanding work during the data acquisition process. I also would like to thank Professor David Cleary for proofreading this work.

My deepest gratitude goes to Professor Alfred Cooper for his patience, constant guidance, cooperation, and most of all, for being a friend whose experience I could always count upon.

Finally, I would like to thank my wife Fatima, my son Fabio and my daughter Ana for their support and understanding as I work in this thesis.

I. INTRODUCTION

Infrared systems have been shown to be among the most important sensors for the future sea warfare scenario. Intensive scientific and technological efforts have been made to improve the performance of those systems. The characteristic operation in a very cluttered environment enforces a requirement to improve the target-to-background contrast to improve discrimination. Analysis of polarization effects in the infrared target contrast provides a promising technology to meet the increasing performance goals in this area.

Previous experiments done at the Naval Postgraduate School have shown that the infrared electric vector of sea radiance near grazing angle appears perpendicularly (horizontally) polarized within regions of direct sun glint and parallel (vertically) polarized otherwise [Ref. 1,2,3]. Sky background and manufactured targets appear much less polarized than sea background. Therefore, polarization filters aligned horizontally while viewing target scenes outside the sun glint can improve the target-to-background contrast. In addition to these works, concerns about the time dependency of contrast results led to the design of a new device to split the scene in two different polarization fields in the same image [Ref. 4].

In this project data from an experimental data set obtained in the Electro Optic Propagation Assessment in the Coastal Environment (EOPACE) multinational measurement series in San Diego Bay in 1996 is analyzed. EOPACE is a program sponsored by ONR and organized by SPAWAR SYSTEMS CENTER, San Diego, Ocean and Atmosphere Sciences Division, Code 543. The overall purpose of the EOPACE

measurements is to quantify infrared (IR) propagation characteristics for near ocean surface transmission and analyze electro-optic (EO) systems performance in the coastal environment condition¹. The basic data analyzed in this thesis were collected by the NPS-Meteorological Group on R/V POINT SUR, NPS-Naval Academic Center for Infrared Technology (NACIT) on R/V POINT SUR and NPS-NACIT at Building 15 of the Naval Command Control and Ocean Surveillance Center (NRAD) in April 9 and April 10, 1996. The data includes 5,508 selected images of the R/V POINT SUR in sets of different ranges and aspect angle, meteorological conditions, Global Positioning System (GPS) data and ship skin temperature. The collected image sets are sequences of horizontally polarized, vertically polarized and unpolarized images taken using an AGA780 camera with internal polarizers. With a greater number of images in comparison to the previous work done, the main objective of this project is to analyze the effect of the target aspect angle on polarized target-to-background contrast. In addition, previously reported results related to target-to-background contrast improvement using a horizontally oriented polarizer will be verified. Assumptions used in those projects about time dependency of contrast results and about generation of unpolarized images by averaging horizontally and vertically polarized images will also be verified.

Chapter II provides the fundamentals of infrared theory. Chapter III describes the relevant conditions to obtain and analyze the data. Results are presented and discussed in Chapter IV, and finally, conclusions and recommendations are provided in Chapter V.

¹ Detailed information about EOPACE measurement series can be found at the internet address www.sunspot.nosc.mil

II. FUNDAMENTALS

In order to build a gradual approach to the objectives of this work, presenting the basic infrared theory is very important. Naturally, there is no intention to develop the topics in full detail. However, the most important points to understand the phenomena associated with infrared radiation will be shown.

A. ELECTROMAGNETIC SPECTRUM

Energy can propagate by spatial and temporal variations of electric and magnetic fields. The relationship between these two fields is represented by Maxwell's equations:

$$\begin{aligned}\nabla \times \mathbf{E} &= -\frac{\partial \mathbf{B}}{\partial t} \\ \nabla \times \mathbf{H} &= \mathbf{J} + \frac{\partial \mathbf{D}}{\partial t} \\ \nabla \cdot \mathbf{D} &= \rho_v \\ \nabla \cdot \mathbf{B} &= 0\end{aligned}\tag{2.1}$$

Where:

\mathbf{E} = Electric field intensity vector (V / m)

\mathbf{D} = Electric flux density vector (C / m²)

\mathbf{H} = Magnetic field intensity vector (A/m)

\mathbf{B} = Magnetic flux density (T)

t = Time (s)

ρ_v = Volume charge density (C / m³)

Therefore, "electromagnetic waves" such as optical, infrared, radar and radio waves have the same nature, being composed of two component fields: electric and

magnetic. Basically, different names are used to distinguish different frequency intervals in the electromagnetic “spectrum.”

The infrared region of the electromagnetic spectrum lies between the visible (shorter wavelength) and the radio (longer wavelength) regions. Figure 2.1 shows this region of the spectrum. Its bandwidth is approximately from $0.7\ \mu\text{m}$ to $1000\ \mu\text{m}$. However, for conventional IR imaging the practical bandwidth is approximately from $1.5\ \mu\text{m}$ to $15\ \mu\text{m}$.

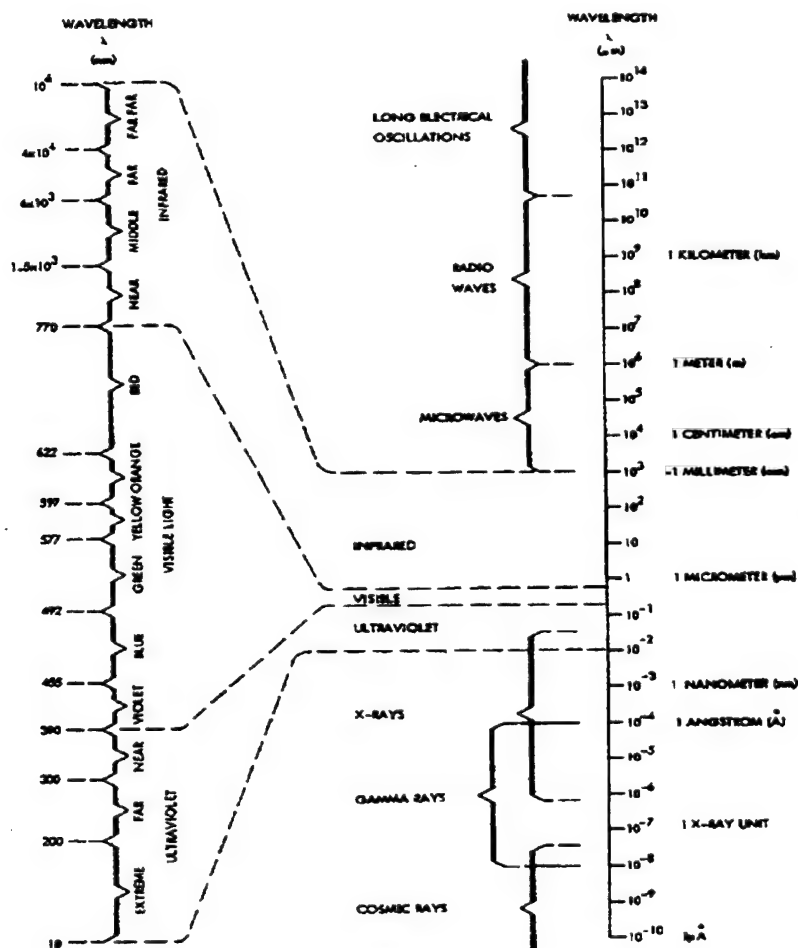


Figure 2.1 - Electromagnetic Spectrum [Ref. 10]

Based on factors such as the form of radiation, methods of detection, and the atmospheric transmission, the infrared part of the spectrum is subdivided into several IR bands. The most common bands are the near-infrared (NIR) $0.7\mu\text{m} - 0.9\mu\text{m}$, the short-wave infrared (SWIR) $1.0\mu\text{m} - 3.0\mu\text{m}$, the mid-wave infrared (MWIR) $3.0\mu\text{m} - 5.0\mu\text{m}$, and the long-wave infrared (LWIR) $8.0\mu\text{m} - 12\mu\text{m}$.

Detectable radiation from $0.7\mu\text{m} - 3.0\mu\text{m}$ is mostly that reflected from the target scene. Night Vision Devices use reflected radiation and can operate in the IR band limited to $1.5\mu\text{m}$ by the detection technology. Infrared radiation with a wavelength beyond $3.0\mu\text{m}$ is called thermal radiation because the emission, dependent on the target temperature, gives most of the detectable signature. Infrared systems such as FLIR (Forward Looking Infrared), IRLS (Infrared Line Scan), andIRST (Infrared Search and Track) use thermal radiation commonly in the MWIR or LWIR band.

B. INFRARED TERMINOLOGY AND UNITS

Since electromagnetic energy comes from a source through the atmosphere until it reaches a sensor, the fundamental radiometric quantities are associated with the characteristic spreading of the infrared radiation. Therefore, they are related to energy, area, solid angle and wavelength units. Table 2.1 shows fundamental radiometric quantities and their units.

TABLE 2.1
RADIOMETRIC QUANTITIES

Symbol	Name	Description	Units (metric)
M	Radiant Flux Density (Exitance)	Radiant Flux leaving an element of a surface per unit area.	Watts/cm ²
E	Irradiance	Radiant power per unit area incident on a surface.	Watts/cm ²
I	Radiant Intensity	Radiant power leaving a point source per unit solid angle.	Watts/Sr
L	Radiance	Radiant power leaving or arriving at a surface at a point in a given direction per solid angle per area normal to that direction.	Watts/cm ² Sr

M characterizes the power leaving the target surface per unit area. Some of this radiation is emitted by the target and some is reflected due to *Irradiance* from another source. The distant transport of the radiant energy from the target is described by the *Radiant Intensity*, which includes the geometrical spreading with range. When the radiation reaches the detector, the *Irradiance* at the receiver of the target radiation is converted into a signal for recording.

C. LAWS OF THERMAL RADIATION

1. Black Body

When radiation is incident upon a target, fractions of the total radiant energy are absorbed, reflected, and transmitted, so that

$$1 = \alpha + \rho + \tau \quad (2.2)$$

where each coefficient represents the respective absorbed, reflected, and transmitted fractions. Kirchoff's law of electromagnetic radiation states that a good absorber is also a good emitter of radiation by the equation:

$$\alpha = \epsilon \quad (2.3)$$

A black body is known simply as an ideal emitter and absorber. Therefore, it has absorptivity (α) = emissivity (ϵ) = 1, so the reflectance (ρ) and transmissivity (τ) = 0. For a black body this is true at all wavelengths. The spectral radiant emittance curve for a black body is shown by Figure 2.2, and is described by Planck's Law.

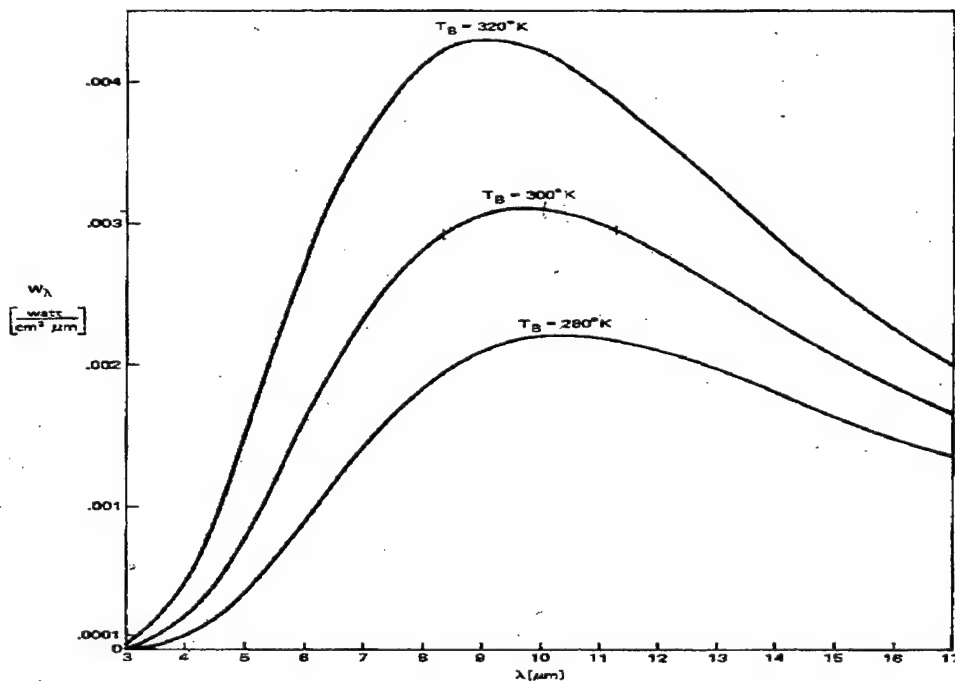


Figure 2.2 - Black Body Radiant Emittance [Ref. 7]

2. Planck's Law

Max Planck theorized that atomic oscillators do not emit radiation continuously but in discrete amounts of energy (quanta). The frequency of the emitted radiation is related to the quantized energy change by the equation:

$$E = h\nu \quad (2.4)$$

Where

E = Energy change (J)

h = Planck's constant ($h = 6.625 \times 10^{-34}$ J s)

ν = frequency (Hz)

From these principles, the equation to represent a black body spectral exitance as function of its temperature was derived. This equation is known as Planck's Law

$$M_{\lambda} (T) = \frac{2\pi c^2 h / \lambda^5}{\left(e^{\frac{hc}{\lambda kT}} - 1 \right)} \quad (2.5)$$

where:

M_{λ} = Spectral exitance (W / cm² / μm)

λ = Wavelength (μm)

k = Boltzmann's constant ($k = 1.38 \times 10^{-23}$ J / K)

c = Velocity of light in the vacuum ($c = 3 \times 10^8$ m / s)

h = Planck's constant ($h = 6.625 \times 10^{-34}$ J s)

T = Temperature of the source (K)

Figure 2.2 shows the graphical representation of Planck's law.

For non black body emitters, the radiant exitance is reduced by the emissivity (ϵ).

The radiant exitance is then:

$$M_{\lambda} = \epsilon_{\lambda} M_{\lambda \text{black-body}} \quad (2.6)$$

Where:

ϵ_{λ} = spectral emissivity ($\epsilon < 1$ for all non black bodies) at wavelength λ .

Some examples of emissivities of practical materials are shown in Table 2.2.

TABLE 2.2
EMISSIVITIES OF COMMON MATERIALS

Material	Emissivity
Polished Al	.05 (373K)
Steel Oxidized	.79 (573K)
Water(frost/ice)	.98/.96 (263K)

If the spectral emissivity (ϵ_{λ}) is a constant, then the body is called a gray body.

Many materials behave as gray bodies over a limited range of wavelength.

3. Wien Displacement Law

Wien's displacement law can be derived by differentiating the radiant exitance M_λ (Eq. 2.5) with respect to wavelength and setting the result equal to zero. This procedure will give the wavelength of maximum exitance as a function of the temperature:

$$\lambda_{\max} T = 2898.78 \quad (2.7)$$

Where:

λ_{\max} = Wavelength for maximum exitance (μm)

T = Temperature of the source (K)

From Wien's Displacement Law it is observed that as the temperature increases, the wavelength corresponding to the maximum exitance decreases.

4. Stefan-Boltzmann Law

If the radiant exitance is integrated over all wavelengths for a given temperature, the total power emitted per unit area can be found. The equation is found to be, for a black body:

$$M(T) = \sigma T^4 \quad (2.8)$$

Where:

σ = Stefan-Boltzmann constant ($\sigma = 5.67 \times 10^{-12} \text{ W / cm}^2 \text{ K}^4$)

T = Temperature of the source (K)

For a gray body the result must be multiplied by the emissivity.

D. ATMOSPHERIC PROPAGATION

The atmosphere is composed by many different elements. Therefore, it emits radiation and interferes with the radiation passing through it. The spectral radiant flux leaving a source at distance R from the sensor will be attenuated by the atmosphere. The attenuation is a function of the distance R and the wavelength of the electromagnetic wave. The atmospheric transmission coefficient τ ($0 < \tau < 1$) represents the general effect of the atmospheric attenuation. τ decreases as the distance increases. On the other hand, the variation of τ with the wavelength is a more complex function and depends on the atmospheric composition. Several standard models are used to predict the influence of the atmosphere. LOWTRAN and MODTRAN are examples of those models. Figure 2.3 shows a characteristic graphic result for atmospheric transmission coefficient generated by MODTRAN for a Mid-Latitude Summer atmosphere, 10 km horizontal path at 100 m altitude over the open sea.

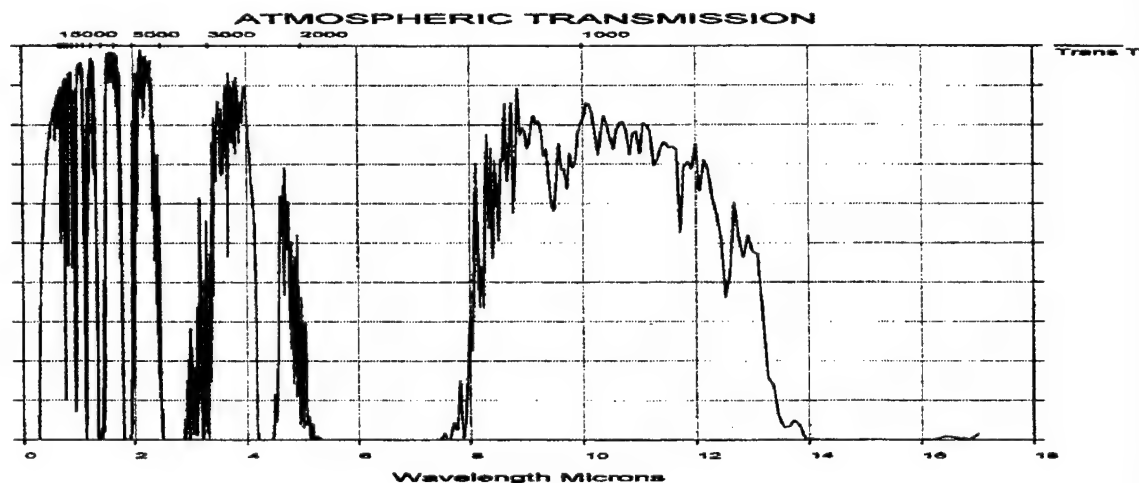


Figure 2.3 - Atmospheric Transmission

Figure 2.3 shows two intervals clearly better in terms of atmospheric transmission: $3.0\mu\text{m} - 5.0\mu\text{m}$ (MWIR) and $8.0\mu\text{m} - 12\mu\text{m}$ (LWIR).

The attenuation dependency on wavelength is an intrinsic characteristic of the atmosphere components associated with two basic mechanisms: scattering and absorption.

The scattering loss mechanism is the redistribution of incident radiation over all directions. The predominant species in this process are suspended aerosol particles for which the particle size is close to the wavelength. Aerosols include dust, fog, salt, ash, and many other airborne particles. Particularly in the marine boundary layer, aerosols include condensed water droplets. The principal effects of scattering are observed at the shorter wavelengths in the IR spectrum (below $1.2\mu\text{m}$). Above $1.2\mu\text{m}$ molecular absorption dominates.

Absorption mechanisms are due to the structure of the molecules and the modes in which they can be excited and thus absorb energy. The predominant absorbing species in the atmosphere are molecules such as H_2O and CO_2 . Basically, they define the observed "windows" used in IR systems (MWIR and LWIR) as seen in Figure 2.3.

E. POLARIZATION PHYSICS

Electromagnetic waves are composed of two fields: electric and magnetic. For a plane wave propagating in the z-direction, the electric field components in the plane perpendicular to the direction of propagation may be represented by:

$$\begin{aligned} E_x(z,t) &= E_{0x} \cos(\omega t + \delta_x) \\ E_y(z,t) &= E_{0y} \cos(\omega t + \delta_y) \end{aligned} \tag{2.9}$$

Where:

E_{ox} = x-component amplitude

E_{oy} = y-component amplitude

δ_x = phase constant of x-component

δ_y = phase constant of y-component

The plane containing the normal to a boundary surface and the direction vector of a propagating wave is called the “plane of incidence.” The direction of the electric field vector in the plane perpendicular to the propagation defines the type of polarization. If the electric field vector is parallel to the plane of incidence, the polarization is called “parallel.” Similarly, if the electric field vector is perpendicular to the plane of incidence, the polarization is called “perpendicular.” In this project, considering the sea surface as a flat horizontal reference, parallel polarization related to it will be called “vertical polarization.” Similarly, perpendicular polarization will be called “horizontal polarization.”

Polarization occurs in the reflected and emitted IR radiation of targets and backgrounds. Reflection and refraction of light are described by the Fresnel equations and Snell’s law. The incident, reflected, and transmitted waves are shown in Figure 2.4.

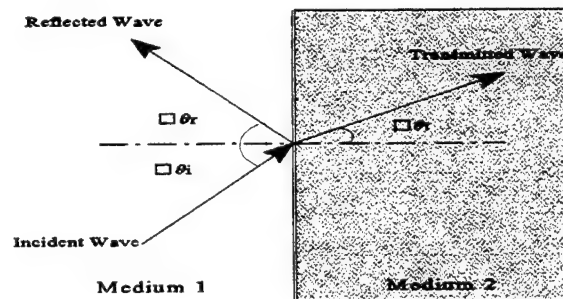


Figure 2.4 - Wave Incidence Geometry

For plane waves incident at a boundary between two media of different complex refractive indices n_1 and n_2 , the angle of reflection equals the angle of incidence. The angle of transmission θ_t as a function of the incidence angle θ_i is given by Snell's law:

$$n_1 \sin(\theta_i) = n_2 \sin(\theta_t) \quad (2.10)$$

For nonmagnetic media, the Fresnel equations can be written:

$$\begin{aligned} r_{\perp} &= -\frac{\sin(\theta_i - \theta_t)}{\sin(\theta_i + \theta_t)} \\ r_{\parallel} &= -\frac{\tan(\theta_i - \theta_t)}{\tan(\theta_i + \theta_t)} \\ t_{\perp} &= 2 \frac{\cos(\theta_i) \sin(\theta_t)}{\sin(\theta_i + \theta_t)} \\ t_{\parallel} &= 2 \frac{\cos(\theta_t) \sin(\theta_i)}{\sin(\theta_i + \theta_t) \cos(\theta_i - \theta_t)} \end{aligned} \quad (2.11)$$

The degree of polarization of the target (or background) can be calculated by:

$$POL = \frac{\langle N_v \rangle - \langle N_h \rangle}{\langle N_v \rangle + \langle N_h \rangle} \quad (2.12)$$

Where:

$\langle N_v \rangle$ = mean radiance with vertical E-field

$\langle N_h \rangle$ = mean radiance with horizontal E-field

For the purposes of this project, three different elements are considered as components of the infrared images: ship (target), sea and sky (background). Each of them has its own polarization characteristics in emitted and reflected radiation.

1. Sea Emission and Reflection

Sea surface polarization characteristics have complex mathematical models.

Extensive studies have been developed to model the sea wave dynamics to improve predictions about the polarization behavior of sea radiance. Many variables influence this process and a probabilistic approach is needed to take into account all their effects. References 6, 11 and 12 present detailed description of some models frequently used for analysis of the polarization characteristics of the sea surface. Previous experiments done by the Naval Postgraduate School have shown that the electric vector of sea radiance appears horizontally polarized within the sun glint regions and vertically polarized otherwise [Ref. 1,2,3]. Figure 2.5 shows the predicted degree of polarization for MWIR and LWIR in and near the sun glint region as a function of solar zenith angle for an observer looking in the vertical plane of the sun [Ref. 3]. The negative values of polarization outside of the sun glint regions indicate parallel polarization.

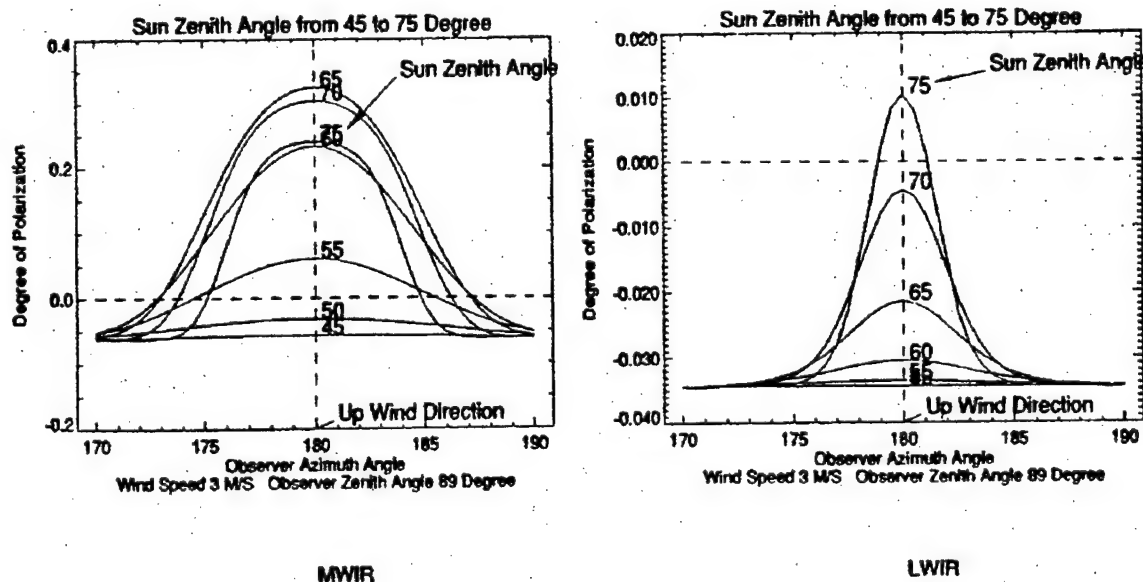


Figure 2.5 - Theoretical polarization in and near sun glint [Ref. 3]

2. Sky Emission and Reflection

The IR radiation from the sky is essentially unpolarized [Ref. 1,2,4]. Therefore, use of static polarized filtering components will not contribute to the contrast improvement measurements when the sky is viewed directly. The sky emission in the image will be subject to attenuation by the polarizing filter to the degree of the unpolarized transmissivity of the filter. Figure 2.6 shows the sky radiance as a function of zenith angle.

Sky radiance increases with zenith angle toward the horizon to that of a black-body with atmospheric temperature. This is due to the maximum thickness of the atmosphere encountered at that angle. Thus, even the small emissivities of the absorbers combine.

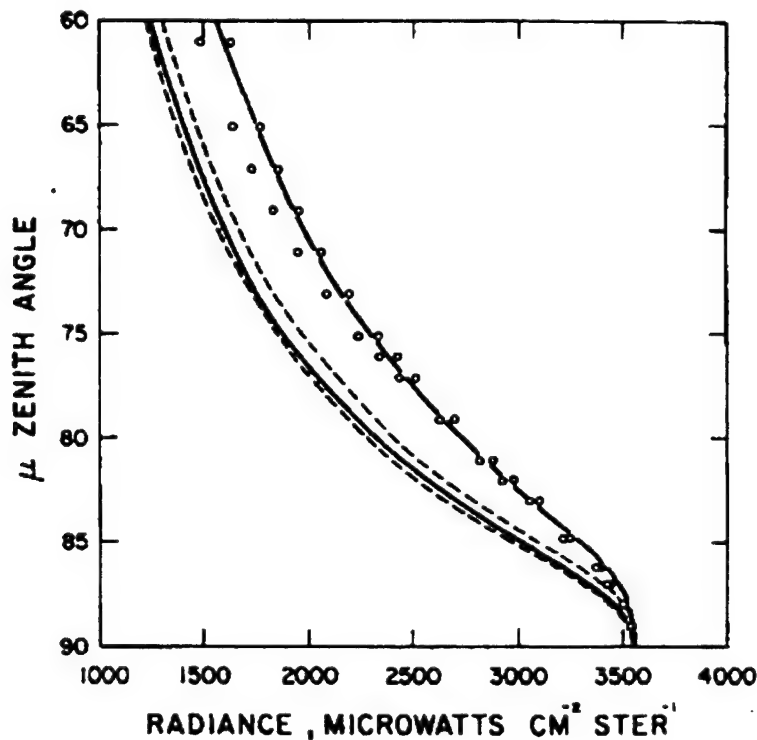
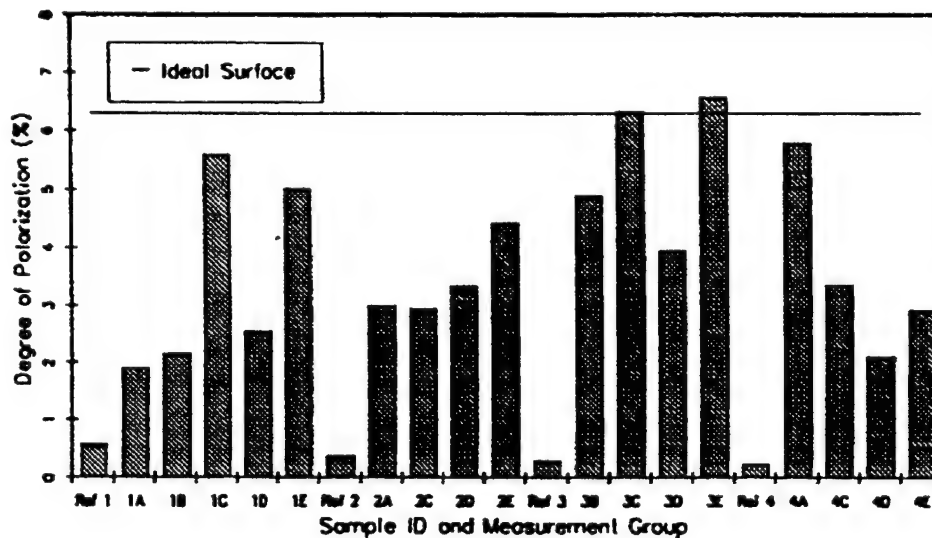


Figure 2.6 - Sky Radiance [Ref. 13]

3. Target Emission and Reflection

Although primary contrast improvement in the sea scenario will be gained by filtering of sea emission polarization, the polarization due to emission from the target itself must be considered. Painted surfaces such as found on all types of vehicles and ships display emission polarization [Ref 14]. Figure 2.7 shows 21 measurements taken on various paint samples ranging from very smooth texture through sand-paint mixtures. The line for an ideal surface in Figure 2.7 denotes polarization that would be seen from a perfect specular reflector. The rougher samples show less polarization than the smoother. The amount of polarization depends on the index of refraction of the paint and any degradation due to surface roughness.



Measured polarized signature components in the 7.5-12 micron band for selected paint samples viewed at 45° from normal.

Figure 2.7 [Ref. 14]

The characteristics of target reflectance follow the same behavior as the sea wave facet reflectance. The difference in the magnitude of the polarized components is a function of the index of refraction of the surface material of the target. The net polarization will be dependent on the balance between thermal emission and reflection of incident radiance.

F. TARGET / BACKGROUND CONTRAST

Depending on application, infrared systems must be able to detect, recognize, and identify a target against a background. The difference between the recorded irradiance from the target and from the background is essential to accomplish those tasks.

The numerical measurement of this difference is called target / background “contrast.” Several methods such as signal processing and polarization filtering can be used to improve the target background contrast.

The absolute contrast (irradiance difference) for any polarization can be written as:

$$\Delta N = \langle N_{target} \rangle - \langle N_{bkgd} \rangle \quad (2.13)$$

Thus, the improvement factor for contrast for horizontal filters over vertical filters is:

$$F = \frac{\Delta N_h - \Delta N_v}{\Delta N_h + \Delta N_v} \quad (2.14)$$

Relative contrast to the background is most commonly defined as:

$$C = \frac{N_{target} - N_{bkgd}}{N_{bkgd}} \quad (2.15)$$

Contrast improvement then is the ratio between polarized contrast and unpolarized contrast,

$$(C_{imp})_{pol} = \frac{C_{pol}}{C_{unp}} \quad (2.16)$$

Previous work [Ref. 3] has shown that target / background contrast outside the sun glint corridor can be improved by using horizontal polarization filters. The filters reduce the predominantly vertically polarized sea background radiance and also, but to a lesser extent, the target radiance. Therefore, an overall improvement in contrast could be observed.

The variation of the target aspect angle was not considered in previous measurements of ship-sea contrast. As presented in section E.3 in this chapter, a variation in the target apparent radiance is expected to be a function of its aspect angle. In this work this factor will be studied using the methods presented in chapter III. In addition, conclusions and assumptions of previous work in respect to the overall contrast improvement, contrast variation and generation of unpolarized images will be verified using a much greater number of analyzed images, and including direct measurement of unpolarized images for comparison.

III. EXPERIMENT DESCRIPTION

In this chapter, all experimental conditions for data acquisition and analysis will be described. Equipment, experiment configuration, data structure, software, and analysis programs comprise the experimental conditions for the experiment. The EOPACE data acquisition of this study was done in April 1996 in San Diego Bay. The analysis covers a total of 5,508 infrared images taken of the R/V POINT SUR in April 9 and April 10, using an AGA-780 Thermovision camera mounted at Point Loma. Polarizer filters were used to get sets of images in three different polarization cases: horizontal, vertical and unpolarized. All images were taken in the LWIR band. Meteorological data, GPS data and ship "skin" temperature data were recorded by instrumentation installed in the ship. Appendix A shows a map of the data acquisition area (San Diego Bay), the GPS ship trajectory and the planned ship trajectory.

A. EQUIPMENT

1. AGA-780 Thermovision

The AGA-780 Thermovision is a two-channel infrared scanning single detector system. It can operate in both the MWIR and LWIR bands using liquid nitrogen cooled InSb and HgCdTe detectors, respectively. The nominal working temperature is 77 K. Scanning is accomplished by two rotating prisms in each channel which scan the image across the detector yielding 1.1 mrad geometric resolution. The input lenses for the long wave infrared (LWIR) used for the experiments consist of anti-reflection coated germanium. Its optical system is f/1.87, with a 7x7 degree field of view.

2. Polarizer Filters

Internal filtering of the radiation after it passes through the imaging system input lenses can be accomplished with the AGA-780 Thermovision Scanning Imaging system by using an existing filter wheel. The original purpose of the filter wheel was to hold various accessory spectral filters in the optical path before the radiation reached the detector. In this experiment polarization filters were installed in the filter wheel. Figure 3.1 shows the internal layout of the AGA-780. One of seven positions of the wheel is selected by rotating the knob on the front face of the unit. The polarization filters used, manufactured by Graseby-Specac; Suffolk, England, each consisted of an aluminum grid superimposed on a 9.5mm diameter x 3mm thick round KRS-5 substrate. The performance specifications provided with the filters are nearly identical. Appendix B shows the performance curves for the two filters installed in filter positions 4 and 5, oriented with passage axis vertical and horizontal, respectively.

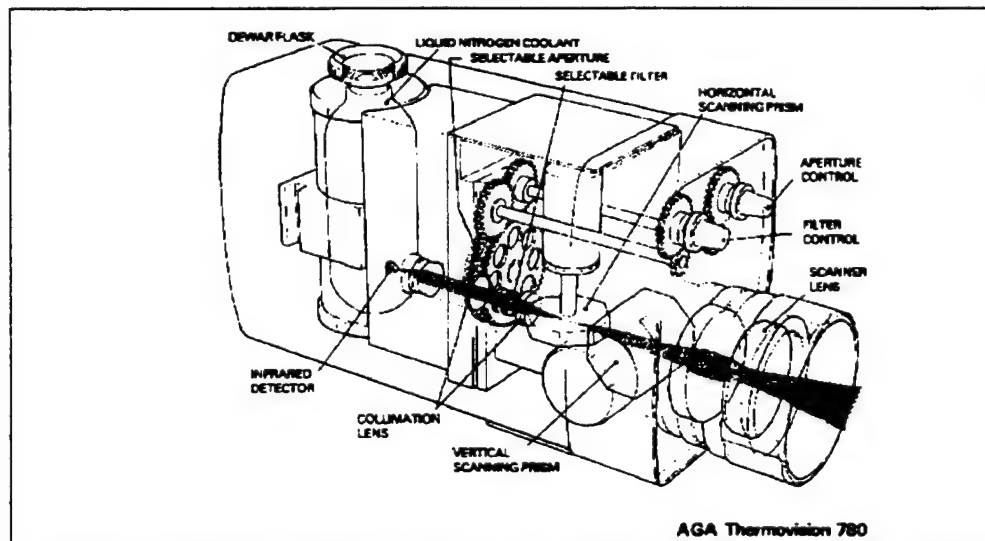


Figure 3.1 Internal Layout of the AGA Thermovision (model with only one IR Band). [Ref 8]

3. R/V POINT SUR

The R/V POINT SUR, owned by the National Science Foundation (NSF), is operated for the Central California Oceanographic Cooperative (CENCAL) by Moss Landing Marine Laboratories, which is on Monterey Bay. It is equipped with the necessary navigational, laboratory and mechanical facilities that support biological, geological, chemical and physical oceanographic research. Setting and recovering current meters, chemical sampling, diving, biological trawling, gear testing and seismic reflection profiling are among a number of operations within the ship's capability. In this project it was used as a cooperative target for infrared imaging as well as for atmospheric sampling functions in the EOPACE experiment. Appendix C presents the ship's general specifications and dimensions (R/V POINT SUR Cruise Planning Manual).

4. Software

a. CEDIP PTRWIN

The analog data provided by the scanning detector is digitized for display, recording and measurement by PTRWIN version 3.16 from CEDIP. This data acquisition and analysis software uses a 12 bit A/D converter for converting the detector signal intensity into a real-time image on a computer screen and for digital image recording. In addition, the PTRWIN software was used as a visualization tool to select images to be analyzed. Although PTRWIN also offers good analysis tools, it works interactively analyzing only one image a time. Thus, this software package is not adequate to be used as analysis software in this project due the large number of images to be analyzed.

b. Interactive Data Language (IDL)

IDL is a complete computing environment for the interactive analysis and visualization of data, integrating an array-oriented language with mathematical analysis and graphical display techniques. All image analyses in this project were performed using programs written in IDL 5.0.3 from Research Systems Inc., Boulder, CO.

c. ONTAR PCMODTRAN

PCMODTRAN 3 from Ontar Inc. was used in this project to calculate the average atmospheric transmission from the available meteorological data. It can operate in MODTRAN 3 or LOWTRAN 7 modes. All calculations were performed in MODTRAN 3 mode using meteorological data (METOC) collected during the experiment. Appendix E.2 presents the METOC information for each data analysis file. The following input parameters were used in the atmospheric transmission calculations:

1. Atmosphere model: Midlatitude summer
2. Aerosol model: Navy maritime
3. Air mass parameter: 3
4. Geometry: horizontal path at 10 m above sea level.
5. Distance between sensor and target: from GPS information
6. Wind speed: from METOC information
7. Pressure: from METOC information
8. Temperature: from METOC information
9. Relative humidity: from METOC information

B. EXPERIMENT CONFIGURATION

The experiment was set in San Diego Bay at Point Loma. Appendix A.1 shows a map of the area. The basic components in the experiment configuration were the sensor (camera AGA 780) and the target (R/V POINT SUR). The sensor was located at building 15 in NRaD, Point Loma. Its geographic coordinates were N 32° 39' 36", W 117° 14' 22". The ship positioning was planned to correspond to a pattern of radial bearings with stationary points spaced at 0.5 nm intervals. At each stationary point, the ship should maneuver to be at different heading for each image sequence (3 polarization cases) taken. Both ship GPS location and sensor position are known, so the bearing is computed. From ship heading and bearing information, the target aspect angle can be calculated. Appendix A presents the planned ship positioning for the experiment.

C. ORIGINAL DATA

1. Images

The sets of images were recorded sequentially for three different polarization cases: horizontal, vertical and unpolarized. Each polarization case has an average of 26 images (frames). Horizontal and vertical cases were recorded in the same file whereas each unpolarized case was recorded in a separate file. The frames are composed of 4 interlaced fields with dimensions 125x64 pixels each. Therefore, each frame is an array of 125x256 pixels. A total of 5,508 images were analyzed. Image data taking was implemented with the AGA 780 mounted on a remotely controlled pan-tilt head outside the south looking window of Building 15 in Point Loma. The data were digitalized and recorded with the PTRWIN acquisition boards installed in the docking station of an NEC

laptop computer. For storage, the files were transferred to a second portable computer and stored on optical disk. The original image files from PTRWIN are identified by the extension *.PTW. Table 3.1 presents the *.PTW binary file structure.

TABLE 3.1
ORIGINAL IMAGE FILES (*.PTW) STRUCTURE

DATA		OFFSET (bytes)
Main Header (65,536 bytes)	General Parameters	0
	Scanner Parameters	44
	Display Parameters	245
	Digitalization Parameters	375
	Comments	563
	Setup File Name	1563
1st Frame Header (1,536 bytes)	Level	0
	Time	80
	Comments	180
1st Frame (64,000 bytes)	1st Field	0
	2nd Field	16,000
	3rd Field	32,000
	4th Field	48,000
2nd Frame Header (1,536 bytes)	Level	0
	Time	80
	Comments	180
2nd Frame (64,000 bytes)	1st Field	0
	2nd Field	16,000
	3rd Field	32,000
	4th Field	48,000
The Frame Structure above is repeated until the last frame in the image sequence.		

Appendix D.1 presents a list of the selected *.PTW files.

2. Meteorological Data

Meteorological data were collected by the NPS Boundary Layer Meteorology Group on 2 meteorological towers (METOC 1 and METOC 2) installed on the ship. The data were recorded at 30 second intervals. Ship GPS data are included in the METOC files. Appendix E.1 describes and presents the format used to record the data. METOC 1 tower was located above the ship bridge (38 ft above sea surface) and METOC 2 tower was located at the ship bow (24 ft above sea surface). Meteorological conditions for each analysis file are presented in Appendix E.2 whereas timing and positioning data are presented in Appendix E.3.

3. Ship Skin Temperature Data

The temperature of the ship "skin" was measured by 16 thermistors installed by NPS-NACIT in different points of the ship. The data were recorded at a 20 second rate. Appendix F presents the position for each thermistor and the format used to record the data.

D. PRE-PROCESSED DATA

All files recorded under the PTRWIN program were stored in *.PTW format. The original format used to store the images (*.PTW) has some inconveniences for use as a data base for the analysis programs:

- Polarization cases for one test condition are divided in two different files.

Consequences : programs would have to open two different files for analysis, increasing the time and memory resources needed.

- Headers have much information that is not used for the analysis.

Consequences : increase in reading time and memory resources needed.

- Field interlace sequence is not constant for all files.

Consequences : before each analysis the interlace sequence should be verified and corrected by the user interactively for each analysis phase, increasing the analysis time.

- File structure is specific for the camera settings.

Consequences: the analysis programs could be used only for this specific format.

Converting another format (a single JPEG or BMP image for example) to the original image format (*.PTW) is not easy.

In order to solve these problems, all original image files (*.PTW) were converted into a new format (*.PTE) with the following properties:

- All polarization cases included in one file (each file represents one test condition).
- Images are integer arrays (in this project their dimensions are 125x256).
- Only the essential information for the analysis programs is included. This information is given as an integer matrix.
- All analysis results are included in the same data file as a floating point matrix.
- Converting any image format into a “*.PTE” file format is easy.

Therefore, the analysis programs do not need modification to be used to analyze images recorded in other formats.

The file structure for “*.PTE” files is described in the next item.

1. Images

140 selected original image files (*.PTW) were converted into 70 "basic image files" (*.PTE) using the program BASEGEN.PRO (appendix H) written in IDL. Appendix D.2 presents a list of the generated basic files. The denomination "basic file" is used because they are the "data base" for the analysis programs. The basic files (*.PTE) were named sequentially using the root name "BASE" followed by a number. For example, the basic file corresponding to the 10th analyzed test condition (3 polarization cases) is BASE10.PTE. This technique was adopted to simplify the reading of all files sequentially. All analysis programs will recognize basic file structures for any dimensions of image arrays and any number of polarization cases.

The basic files structure for 3 polarization cases is presented in Table 3.2.

TABLE 3.2
BASIC FILES (*.PTE) STRUCTURE

Variable	Type
Name of original (*.PTW) file	string (20)
Information vector	integer (1,13) ¹
Frame time : horizontal polarization	integer (4, # frames hor. case)
Frame time : vertical polarization	integer (4, # frames ver. case)
Frame time : unpolarized	integer (4, # frames unp. case)
Image set (frames) : horizontal polarization	integer (125, 256, # frames hor. case)
Image set (frames) : vertical polarization	integer (125, 256, # frames ver. case)
Image set (frames) : unpolarized	integer (125, 256, # frames unp. case)
Results : horizontal polarization	float (100, # frames hor. case)
Results : vertical polarization	float (100, # frames ver. case)
Results : unpolarized	float (100, # frames unp. case)

¹ In IDL, the first matrix index is column number and the second is line number.

Table 3.3 presents the structure for the information vector variable referred to in Table 3.2.

TABLE 3.3
INFORMATION VECTOR

Line	Data	Example
0	Recording Date : Day	9
1	Recording Date : Month	4
2	Recording Date : Year	96
3	First Frame Recording Time : Hour	12
4	First Frame Recording Time : Minute	45
5	First Frame Recording Time : Second	27
6	First Frame Recording Time : Hundredths of sec.	77
7	Number of polarization cases	3
8	Number of pixels per line	125
9	Number of lines	256
10	Number of frames : horizontal polarization	27
11	Number of frames : vertical polarization	25
12	Number of frames : unpolarized	29

Time matrices have 4 columns to describe the time for each frame recording: hour, minute, second and hundredths of second..

2. Meteorological Data

The original meteorological data were converted into a float matrix with dimensions $9 \times 2882 \times 2$ where the 9 columns represent the average values for measurements performed on the 2 different meteorological towers on the ship. Each line

corresponds to a data sample and each layer corresponds to one day (April 9 and April 10). Table 3.4 presents the parameter's columns in this matrix ("METDATA.PTE").

TABLE 3.4
COLUMNS OF THE METEOROLOGICAL DATA MATRIX (METDATA.PTE)

Column	Data	Example
0	Elapsed time from 00:00 (s)	48,356.76
1	Ship latitude (min)	1,958.00
2	Ship longitude (min)	7035.40
3	GPS antenna height (m)	2.45
4	Air temperature (C)	15.60
5	Relative humidity (%)	82.45
6	Air pressure (mb)	1018.35
7	Wind speed (m/s)	5.50
8	Sea surface temperature (C)	17.30

Another matrix ("AVEMET.DAT") was also created to summarize meteorological data, ship positioning and average atmospheric transmission for all 70 basic files. These matrix data are presented in Appendix E.2. Table 3.5 presents a sample of the AVEMET.DAT data (BASE01.PTE).

TABLE 3.5
COLUMNS OF THE AVEMET.DAT MATRIX (SAMPLE BASE01.PTE)

Column	Data	Example
0	File number	1
1	Day of Recording (April / 96)	9
2	Time of Recording (elapsed time from 00:00 h local in seconds)	44018.00
3	Ship GPS Antenna : Latitude (minutes)	1959.20
4	Ship GPS Antenna : Longitude (minutes)	7034.80
5	Ship GPS Antenna : Height (m)	-27.01
6	Air Temperature (C)	15.30
7	Relative Humidity (%)	72.00
8	Air pressure (mb)	1018.25
9	Wind speed (m/s)	6.50
10	Sea surface temperature (C)	18.55
11	Range (distance sensor / ship in meters)	998.52
12	Theta (angle between the vertical vector fixed at the sensor and the sensor to the ship vector in radians)	1.62
13	Phi (angle between the True North pointing vector fixed at the sensor and the horizontal projection of the sensor to the ship vector in radians)	2.41
14	Atmospheric Transmittance	0.82

3. Ship Skin Temperature Data

The original skin temperature data recorded by NPS-NACIT on the R/V POINT SUR were converted into a floating point matrix ("SKINDATA.PTE") with dimensions 17 x 4321 x 2. Its first column represents the elapsed time in seconds from 00:00 h local of the corresponding day. The 16 other columns represent the temperature measured by each thermistor. Each line corresponds to a data sample and each layer corresponds to one day (April 9 and April 10).

4. Thermal Image Calibration

During the image acquisition process, the detector signal related to a given point of the scene is converted to a digital number at the correspondent point in the image. The digital number recorded by the digitalization software is called “thermal level.” Although the intensity of radiation received at the detector is presumed to be proportional to the system’s thermal level, this signal is a nonlinear function of temperature. Thus, in order to have a correct correspondence between thermal level and temperature, the AGA 780 requires calibration with a laboratory blackbody source. The system output of thermal level is recorded against the source blackbody temperature through a range of temperatures and the calibration curve is generated through a least squares fit method and is of the form [Ref. 8]:

$$TL = \frac{A}{C e^{B/T} - 1} - OS \quad (3.1)$$

Where:

- A, B, and C = Constants determined by the curve fitting
- OS = Offset correction to adjust for detector response drift [Ref. 1]
- T = Temperature (K).

Appendix G presents the laboratory calibration curves for the 3 analyzed polarization cases. Thermal level values are used to calculate the image contrast. The camera was set to atmospheric transmittance and target emissivity equal to 1.0. Since the images are taken at different distances and the target is not a blackbody, their thermal level

values must be calibrated before the analysis process. Since the skin temperature was available, the image calibration procedure described in the AGA Operating Manual using a known temperature reference source was used. In this process, the calibrated thermal level is calculated by the following equation:

$$I_c = \frac{\Delta I_{or}}{\tau_a \epsilon_0} + I_r \quad (3.2)$$

Where:

- ΔI_{or} = Difference between a point thermal level and the recorded thermal level at the reference point

- τ_a = Average atmospheric transmission

- ϵ_0 = Target Emissivity

- I_r = Calibrated thermal level at the reference point in the target (eq. 3.1).

The calibration process can be described as follows:

- The recorded image is composed by a matrix of uncalibrated thermal level values (one for each image pixel).

- The stored thermal level values are assumed to be proportional to the apparent radiance at each given pixel.

- The skin temperature at a reference point (stack) on the target is known.

- From the laboratory calibration curve for that polarization case, a thermal level value corresponding to the reference point temperature is calculated and the calibrated thermal level for any point is calculated using Equation 3.2. The thermal level

value at the reference point, calibrated by the calibration curve, is called “reference thermal level (L_r).” It considers the target as a blackbody and it is related to the real temperature (it does not consider the distance between the sensor and the target). The idea behind the calibration process is to relate each thermal level value in the image to the reference thermal level conditions (blackbody at short distance). Although the mathematical derivation of the Equation 3.2 can be followed in the reference 8, its physical meaning can be explained using simple ideas:

- The calibrated thermal level at the reference point (reference thermal level) considers the target as a blackbody at short distance.
- To be calibrated, the recorded thermal level at any point is going to be brought at the same conditions of the reference thermal level (blackbody at short distance).
- The target is assumed to be a gray body. Therefore, to correct the recorded thermal level of the target points for the blackbody condition, it is necessary to divide its values by the target emissivity.
- Since the recorded thermal level is assumed to be proportional to the radiance, to correct it for the target distance to the sensor, it is necessary to divide its values by the atmospheric transmission coefficient.
- Since the reference point is in the target, the path radiance has the same value for the reference and the other points. Therefore, by subtracting the reference thermal level from a point calibrated thermal value, the path radiance is canceled and thus, it is not present in Equation 3.2.

E. ANALYSIS PROGRAMS

The purpose of the analysis carried out was to analyze statistically the sequence of frames with each polarization for a given case, so as to compute;

- Averaged degree of polarization for ship, sea background and sky background.
- Temporal variability of each and temporal trend if any.
- Target to background contrast for each polarization.
- Contrast improvement for horizontal and vertical polarization cases.
- Degree of polarization of the ship and of its major planes as functions of aspect angle.

To carry out this analysis it was necessary to develop a set of computer programs. All programs were written in IDL. The complete set comprises 37 different programs that can be divided in 3 categories:

- Auxiliary programs: specialized functions used to perform common tasks for other programs.
- Data management programs: programs used to perform data format conversion and results summarization
- Executive programs: programs used to calculate results from the available data.

Appendix H.1 presents a summary table of the program's name, type and objective.

1. Methodology

All programs are completely commented in their text sources to help the user to understand and modify them for future analysis². The set of programs runs in a sequence given by PONTES.PRO program for each image sequence (polarization case):

- HOTSPOT.PRO: Finds and Tracks the ship hotspot (stack).
- AREAGEN.PRO: Defines an “analysis box” around the ship.
- HORIZON.PRO: Determines the horizon line equation.
- NORMALIZE.PRO: Normalizes the image to threshold the ship.
- ELEMENTS.PRO: Isolates each image main component (ship, sea, sky).
- ASPECT.PRO: Estimates the ship aspect angle.
- CONTRAST.PRO: Calculates ship (and its major planes) to background

contrast and degree of polarization for each image main components.

Although they are commented in their text sources, because of special characteristics or methodology, it is interesting to make complementary comments about some of them.

a. Hotspot.pro

HOTSPOT.PRO is the first executive program in the analysis sequence. It has the basic interactive concept used for all programs which need any kind of user initial input. In this concept, the user will be asked to provide initial input data for the first frame of the set. The program performs the calculation for all other frames of the set and then

² All programs used in this work are available with Prof. Alfred W. Cooper, PhD at NPS Physics Department

shows its results graphically. The user can either accept the computer results or modify them (any frame). Finally, the program shows the final result, including the user's modifications. For HOTSPOT.PRO, the initial data requested from the user are the definition of a rectangular area using the mouse on the first frame image. The program searches for the hottest point inside that area and records its thermal value and position. For the next frame it translates the center of the search area to the position of the previous hotspot (last frame). This technique allows usage of cluttered images (other "hot" targets in the image) for analysis and permits the program to keep the "tracking" on the ship hotspot (stack normally) even if it is in motion. Appendix H.2 presents a sequence of frames showing a hotspot in a moving target being tracked in a cluttered image.

b. Areagen.pro

AREAGEN.PRO generates the coordinates for two corners (diagonal end points) of a rectangle around the ship. This rectangle is called the "analysis box" and will be used as image object by the other analysis programs. This technique allows the analysis to be performed only in the neighborhood of the ship, excluding any possible secondary target and so permitting cluttered images to be used. The presence of a secondary target inside the analysis region can cause poor results because the thresholded "target" pixels might include the secondary target, altering the real target characteristics. Alternatively, the secondary target could be computed as "background" pixels, giving a false higher average background radiance. AREAGEN.PRO uses the hotspot position as a reference to locate the analysis box for each frame. Therefore, if the ship moves, the box will move with it. Appendix H.3 presents a sequence of frames showing the box moving along a target in a cluttered image.

c. Horizont.pro

HORIZONT.PRO calculates the coefficients for the horizon line equation by linear regression using 3 points at the horizon line: one point at the middle “x” value of the image and two at extreme “x” values (0 and x size of the image). For each point, the “y” position is calculated using the natural change in the image thermal level gradient in “y” direction at the horizon plane. This change in the gradient can be seen as a “wall” in the surface plot of a typical image in appendices H.5 and H.6. Immediately above the horizon, the sky radiance is much higher than the sea radiance. This difference in radiance is detected by the program during the process of horizon “y” position searching. The initial user input is used to limit the searching interval, assuring that secondary targets at the edges of the image will not interfere with the gradient verification process. The idea is similar to the hotspot searching, but unidimensional.

d. Threshold.pro

THRESHOLD.PRO is used to isolate the ship from the background. The basic concept used in this program is the sudden increase in the number of “target pixels” (pixels with thermal value above a “testing threshold level”) when the “testing threshold level” drops into the background level. In order to apply this concept, the interval between the maximum and the minimum thermal values in the image is divided into 100 “testing threshold levels.” Starting from the highest testing threshold level, the number of pixels above the threshold value is computed and recorded for each one of the 100 defined levels. The number of pixels above threshold as a function of the testing threshold level is then analyzed. The biggest positive variation in number of pixels is detected and the

optimal threshold level is determined. Although the concept is very simple, some important points must be taken into consideration to assure good performance of the program in detecting the ship with the minimum shape distortion. The most influential of them is about the characteristic high radiation level of the sky. As commented in the previous item, the increase in the thermal level immediately above the horizon line is seen as a “wall” in the surface plot of a typical image in Appendices H.5 and H.6. The thermal level of the sky portion in the image is much higher than the thermal level in the sea portion. Compared with the ship’s thermal level, the sky’s thermal level is normally smaller, but as the distance between ship and camera increases, the sky thermal level can become higher than the ship (target) thermal level. This is a clear problem to apply directly the threshold concept to the original image. By doing this, it would be very likely to reduce the thresholded ship area significantly or even to reduce it to zero (detection of the sky instead) when the ship distance was enough to make its thermal level less than the sky thermal level. To solve this problem, the program “NORMA.PRO” was created. This program uses the natural characteristics of the sky (and sea) thermal level variation in the “x” direction (horizontal) to normalize the entire image and to eliminate the difference between the thermal level of the sky and sea portion without distorting the shape of the ship. Observing the surface plot of a typical image in Appendix H.6, the horizon can be identified by the base of the “wall” created by the much higher thermal level immediately above the horizon when compared with the sea thermal level. In the same picture, since the horizon has been identified, it can be seen that the sky and sea thermal level have practically no variation in “x” direction (horizontal). This statement is true except for the

image's lines where for the ship (target) is seen to be. Therefore, the normalization process starts considering the "horizontal" direction by dividing each pixel's thermal value of the image by the average thermal value of its entire line. This first phase will bring the sky thermal level and the sea thermal level near to one for all lines "without target in." The target pixels will have thermal level values bigger than one and the background lines (sea or sky) "with a target in" will have thermal level values less than one. This effect on the background lines that contain the target is seen as a horizontal "depression" in the surface plot for normalization phase one in appendix H.7. In a second normalization phase, the same process is performed in "y" direction (vertical) dividing each pixel's thermal value of the image by the average thermal value of its entire column. These two phases comprise the normalization used during the threshold process. Appendix H.8 shows the surface plot for normalization phase 2.

e. Elements.pro

ELEMENTS.PRO is used to separate the main elements of the image: ship, sky and sea. The program uses data from HORIZONT.PRO and THRESHOLD.PRO to generate "masks" for each element. "Masks" are images with the same dimensions of their object analysis box image, but with pixel values equal to 1 for the corresponding element and zero anywhere else. Thus, when a mask image is multiplied by its object image, only those pixels covered by the mask (its pixels with value 1) will have the original value. All others will be zero. Appendix H.9 shows an example of object analysis box, its masks and its corresponding elements separated by the process.

f. Aspect.pro

The ship heading information recording system had a problem during the data acquisition process so this information was not available in the 30 second rate METOC data files. The ship aspect angle is necessary data to the analysis performed in this project. Thus, the program “ASPECT.PRO” was written to estimate the ship aspect angle using user provided initial information to start the estimation process which is based on target / model shape correlation and aspect ratio comparison. The initial information about the ship’s aspect angle comes from the notes taken during the experiment by the imager operators by radio contact with the ship. These notes contain information about polarizer used, ship magnetic bearing and ship magnetic heading. From this information, an estimated ship aspect angle can be calculated. ASPECT.PRO searches for the best matching in shape and aspect angle turning a scaled model 20 degrees around the initial estimation. Calculated results are then shown to the user to be verified and modified if necessary.

The model used by this program is a scaled model of the ship composed of flat surfaces (planes). A total of 32 planes defined by 76 vertices comprise the model. The vertices are defined by three coordinates (x,y,z) and their values correspond to the ship dimensions in feet. Although only the four main planes that define the hull sides of the model are used for contrast calculations, the other planes used to model the upper decks are necessary for the shape matching process used by ASPECT.PRO. The model is generated by “MODELE.PRO” and “DRAW_MDL.PRO” and it can be viewed at any combination of elevation and azimuth angle. Appendix H.10 presents the model viewed at

different angles. The model can also be drawn as a wireframe structure. The wireframe model is used to superimpose the model on the ship image to verify the shape matching and model positioning. Appendix H.11 shows the wireframe model superimposed on a ship image.

g. Contrast.pro

CONTRAST.PRO is used to calculate the contrast for the ship and its “main planes.” The ship’s “main planes” are the four biggest planes that comprise the superstructure of the ship model. Appendix H.12 presents a picture showing the ship’s main planes. The ship/background contrast is calculated by considering the contrast between the ship’s image portion above the horizon against the sky and the ship’s image portion below the horizon against the sea. In order to calculate the contrast for each main plane separated, the scaled model in “mask” mode is turned to match the ship aspect angle. “Mask” mode is an available feature of “MODELE.PRO” which generates the model as a “mask” for a given plane. The “mask” is just a part of the image where the pixels have value equal to 1. All other pixels have value equal to zero. Therefore, the process to isolate a part of an image using a mask image is described as follows:

- A ship image is represented by an integer matrix where each element represents a pixel.
- Suppose it is necessary to isolate the main “plane 0” of the ship image.
- The ship model is turned to match the ship image in size and aspect angle.
- The ship model in mask mode is an image represented by an integer matrix where only the pixels corresponding to the main “plane 0” have value equal to 1.

All other pixels (image matrix elements) have value equal to zero.

- By multiplying the ship image matrix by the ship model matrix (mask), only those pixels in the ship image corresponding to the main "plane 0" will keep their original values. All other pixels will have value zero. Therefore, by this process the main "plane 0" is isolated from the rest of the ship image.

Appendix H.13 presents a figure showing plane mask being applied on a ship image. For each of the 4 main planes, the contrast is calculated against the average background. Depending on the ship aspect angle some planes are not visible.

IV. RESULTS AND ANALYSES

In this chapter, all experimental results will be described and analyzed. In addition, the IDL programs used in this project will also be analyzed. Although these programs were used as an analysis tool in this project, they comprise a very useful package for future analysis. Thus, improving their performances and interfaces is important.

A. IDL PROGRAMS

The programs have shown good performance in terms of stability and quality of results. However, it was observed that the execution time and the user interface still need improvements to be used as an analysis package. The average time to process one file (*.pte) is 40 minutes and there are too many keyboard inputs requested from the user. Therefore the following improvements are recommended for future versions to optimize an analysis package:

- Use of "WIDGETS"¹ to integrate the programs.
- Optimization of array treatment to reduce the number of "loops" in the programs.
- Inclusion of "PTRWIN" (from CEDIP) as an external program that can be accessed from the main program in the package.

¹ IDL graphic tools. These tools permit generation of "windows" type applications.

B. RESULTS DESCRIPTION

The results are systematically stored during the analysis process in three matrices (one for each polarization case). These matrices are called “result matrices” and have 100 columns and a number of rows equal to the number of frames for the analyzed polarization case. Appendix I.1 presents the format (column description) of the result matrices.

After analyzing all 70 files, their corresponding result matrices (three each file) were summarized by averaging the frame values. The summarized values were then collected in one summary matrix with 130 columns (parameters) and 70 rows (files). The format of this matrix (column description) is presented in Appendix I.2. The summary matrix is too big to be presented completely. However, its contents are presented partially in Appendix I in the tables referred to in the next analysis items.

C. SHIP CONTRAST VARIATION IN TIME

In this and in previous projects, image sets of different polarization were taken sequentially. This means that the image recording starts with the horizontal polarizer setting for approximately 8 seconds. Then, the polarizer is switched manually to the vertical setting. Finally the unpolarized case is selected on the camera. This change from polarized to unpolarized requires resetting the thermal level range controls and recording these in the computer. This process involves a significant time lag as seen in Figure 4.1 (sample from BASE01.PTE).

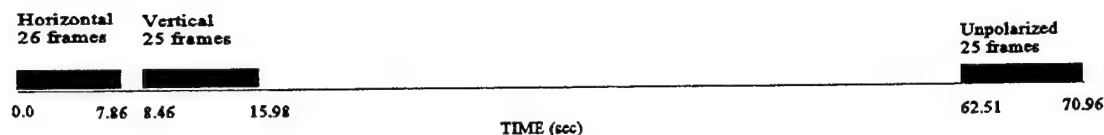


Figure 4.1 Example of image set time line (BASE01.PTE)

Since comparisons between the horizontal and the vertical polarization cases have to be made, there were concerns about the validity of these comparisons because of the possible time variations in the contrast during recording time for those cases. To verify the validity of those comparisons, the contrast variation for the three polarization cases was analyzed by calculating the contrast for each frame. The results were plotted against the elapsed time and a straight line was fitted to the points for each case. The basic parameters to be observed in this analysis are the angular coefficient and the correlation coefficient for the line fitting. The angular coefficient shows how the contrast increases or decreases in time. Thus, an angular coefficient near zero would represent that the contrast does not vary significantly in the analyzed interval of time. The correlation coefficient shows how well the contrast variation can be represented by a straight line and so how well it can be extrapolated in time. For each set of frames, the contrast's mean and standard deviation are also calculated. These parameters are useful to analyze the contrast fluctuation during the recording interval of time. Statistical considerations about the results are analyzed by calculating results for all 70 files and plotting a histogram for each analysis parameter. Appendix I.3 presents the tabulated results for the curve fitting process to the ship contrast variation data. Each table shows the results for all 70 files for each polarization

case: horizontal, vertical and unpolarized. Appendix J.1 graphically presents a sample of the line fitting process for one file (BASE01.PTE). As an example of this process, Figure 4.2 presents the line fitting results for the vertically polarized case in BASE01.PTE.

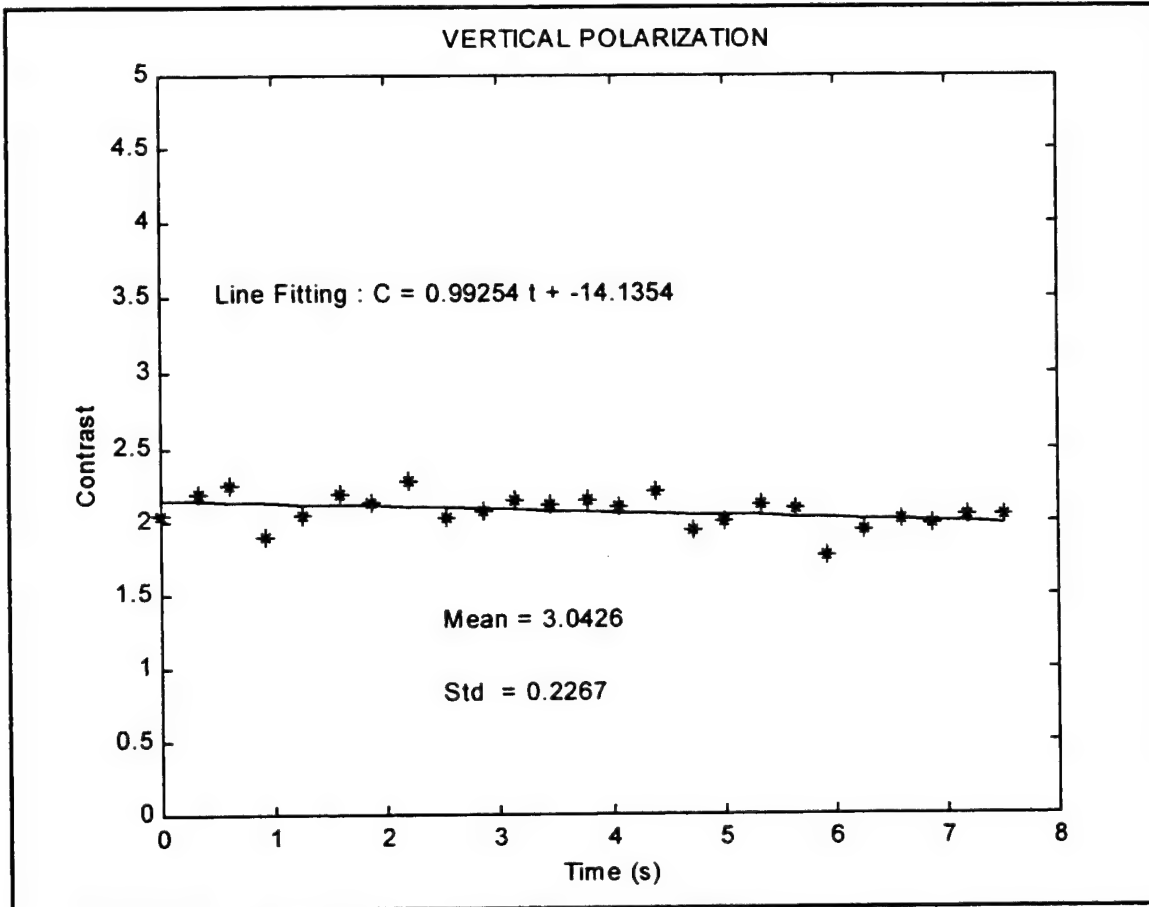


Figure 4.2 Example of line fitting process (BASE01.PTE)

Appendix J.2 presents the statistical distribution (histograms) of the fitting coefficients for horizontal, vertical and unpolarized cases. Those histograms summarize the results calculated for all 70 files. From the histograms it is possible to obtain Table 4.1 which represents each parameter as a statistical population with 70 samples.

TABLE 4.1
SHIP CONTRAST VARIATION: HISTOGRAMS RESULTS

Parameter		Horizontal Polarization	Vertical Polarization	Unpolarized
Line Fitting: Linear Coefficient	Mean	3.127	2.176	3.121
	Standard Dev.	2.047	1.297	1.857
Line Fitting: Angular Coefficient	Mean	-0.006	0.006	-0.015
	Standard Dev.	0.077	0.041	0.139
Line Fitting: Correlation Coeff.	Mean	0.863	0.807	0.802
	Standard Dev.	0.087	0.146	0.149
Contrast Fluctuation: Standard Deviation	Mean	0.379	0.301	0.430
	Standard Dev.	0.248	0.205	0.469

Table 4.1 : Statistical distribution of curve fitting parameters for all 70 analyzed files.²

Analyzing the results, the following observations can be made:

- The correlation coefficient for the three polarization cases is greater than 0.8. Thus, the contrast variation in time for the three polarization cases has linear behavior.

- For the three polarization cases, the angular coefficient has mean value very close to zero and small standard deviation. This demonstrates that the contrast does not have significant variation in time.

- The analysis of the standard deviation of the contrast distribution shows that the unpolarized case has bigger contrast fluctuation in comparison with the vertical and horizontal polarization cases. This can be explained by the polarizer effect in reducing fluctuation of the radiance components for the horizontal and vertical polarization cases.

² Appendix E.2 presents all specific conditions for each one of the 70 analyzed files

These analyses support the validity of the results from previous work by comparing horizontally and vertically polarized images taken sequentially.

D. DEGREE OF POLARIZATION AND CONTRAST IMPROVEMENT

Previous projects have shown that using a horizontal polarizer it is possible to improve the target to background contrast for sea / ship targets by up to 15% [Ref 1,2]. In this project, using a larger number of images and different meteorological environment, it is possible to verify those results with a good statistical confidence. A total of 5,508 images were analyzed and their results were summarized in 70 files. Appendix I.4 presents the target degree of polarization and the target to background contrast improvement for horizontal and vertical polarization cases for each one of the 70 analyzed files.

Appendix J.3 shows the statistical distribution of the contrast improvement factor obtained with a horizontal and vertical polarizing filters. Whereas in the MAPTIP measurements off the Dutch coast in the late fall the observed contrast improvement ranged only above 1 up to 1.5 with the horizontal filter, the EOPACE San Diego measurements analyzed here range from 0.5 to 1.8, with a mean of 1.08. This implies that use of the horizontal filter to reject the sea surface polarization gives on the average an 8% contrast improvement, as opposed to 15% in the MAPTIP work.

The histograms of degree of polarization for the ship target, the sea and the sky are also shown in Appendix J.3. For analyzing those results it must be observed that a positive degree of polarization shows a predominance of vertically polarized radiation whereas a negative degree of polarization means a predominance of horizontally polarized radiation. The sea surface shows rather consistent vertical polarization with mean at 0.1218, while

the ship shows a very narrow distribution centered effectively at zero. The sky polarization is apparently random with widely spaced outliers on both sides.

Table 4.2 summarizes all the results from the histograms shown in Appendix J.3.

TABLE 4.2
DEGREE OF POLARIZATION AND SHIP CONTRAST IMPROVEMENT

Parameter		Value
Ship: Degree of Polarization	Mean	-0.003
	Standard Deviation	0.029
Sea: Degree of Polarization	Mean	0.128
	Standard Deviation	0.096
Sky: Degree of Polarization	Mean	-0.029
	Standard Deviation	0.242
Horizontal Polarization: Ship to Background Contrast Improvement	Mean	1.081
	Standard Deviation	0.266
Vertical Polarization: Ship to Background Contrast Improvement	Mean	0.811
	Standard Deviation	0.242

Table 4.2: Statistical distribution of degree of polarization and contrast improvement for all 70 analyzed files.³

From the analyses, the following observations can be made:

- Ship and sky degree of polarization have mean value very close to zero.

Thus, neither horizontal nor vertical polarization is predominant in the radiation from the sky or from the ship.

- Positive mean value for sea degree of polarization demonstrates that sea radiation is partially vertically polarized over the testing conditions.

- Mean value for contrast improvement using horizontally oriented

³ Appendix E.2 presents all specific conditions for each one of the 70 analyzed files

polarizer shows a gain of 8% (1.081) in contrast in this polarization case. This value is smaller than previous results (15%). A higher average sea surface temperature could be a factor in this difference. For the analyzed data set, the average sea surface temperature was 17.2 C (Appendix E.2) against 11.5 C in previous reports [Ref. 1].

These analyses demonstrate that the results from previous work in terms of contrast improvement using a horizontal polarizer are qualitatively valid.

E. GENERATION OF UNPOLARIZED IMAGES

In previous projects, unpolarized images were generated by averaging the thermal level values for horizontal and vertical polarization cases. In the analysis of the Monterey Bay and MAPTIP polarization measurements, the Contrast Improvement Factor (relative to the unpolarized case) was calculated by constructing an effective unpolarized image as the average of the two polarized components. This process is subject to uncertainties caused by the presence of the filter with possible transmission extinction loss and thermal emission and reflection from the back of the filter. In this project, three polarization cases were recorded and analyzed: horizontal, vertical and unpolarized. Therefore it is possible to verify the validity of the previous assumption used for composing unpolarized images. Appendix J.4 presents plots of the mean thermal level for the unpolarized images against the calculated average value using the horizontal and the vertical polarized images. Those plots represent the results for the main components of the image: ship, sea and sky respectively. Each plot contains 70 points corresponding to the 70 analyzed files. A linear fitting process was done to the points in each plot. An angular coefficient close to 1 (45 degrees) would show that the average assumption was correct. Histograms showing the

difference distributions are also presented in the same graphics. In order to illustrate the comparison process by line slope, a sample plot for the Sea Thermal Level, the most sensitive case, is shown as Figure 4.3. The plot indicates that the average value slightly exceeds the unpolarized case, with slope of 0.839 in place of 1.

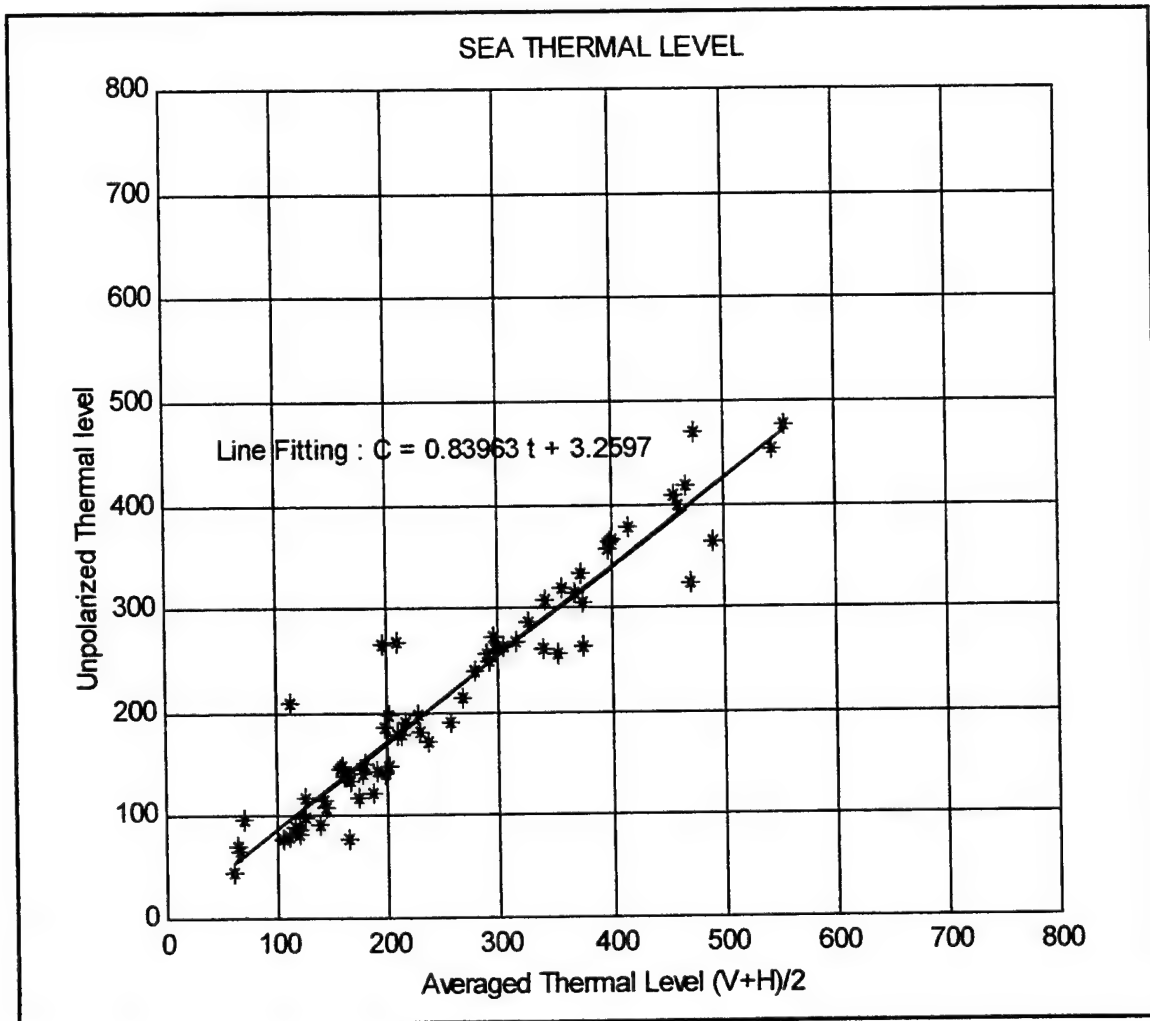


Figure 4.3 Sea Thermal Level

Table 4.3 presents the numerical results from the linear fitting process and from the histograms in Appendix J.4 .

TABLE 4.3
COMPOSITION OF UNPOLARIZED IMAGES

Parameter		Ship	Sea	Sky
Linear Fitting	Linear Coeff.	-5.947	3.259	-14.135
	Angular Coeff.	0.975	0.839	0.993
Difference: Average - Unpolarized	Mean	31.354	38.025	18.887
	Standard Dev.	42.029	38.274	63.461

Table 4.3: Linear fitting for unpolarized image generation by averaging vertical and horizontal polarization thermal levels for all 70 analyzed files.⁴

Analyzing the results, the following observations can be made:

- For all components the mean difference between average and unpolarized value is positive. Therefore, the average value is slightly bigger than the unpolarized value.
- The biggest difference is found to occur for the sea thermal values. This fact can be observed by the bigger mean difference value or by the smaller angular coefficient when compared with the ship or the sky values.
- The angular coefficient for the three main components is close to 1.0.

These analyses demonstrate that the assumption used in previous work in terms of unpolarized image generation by averaging horizontal and vertical polarization cases is satisfactory.

⁴ Appendix E.2 presents all specific conditions for each one of the 70 analyzed files

F. SHIP ASPECT ANGLE EFFECTS ON POLARIZATION

In this project, considering results from all 70 analyzed files, the sea radiation has shown a vertical polarization predominance whereas the sky and the ship radiation have shown no polarization predominance. The average ship target image has not been shown to exhibit any significant degree of polarization in either of the previous measurements series. However, literature references have found plane painted surfaces to exhibit considerable emission polarization, strongly dependent on angle. It would be expected thus that the ship target would show polarization signature varying with the orientation of each facet of the ship surface. Thus the overall polarization of the ship radiance (combined emission and reflection) is likely affected by the ship aspect angle. In order to verify this relationship the ship was modeled as a set of facets, or planes, as described on item 3.E.1.f on page 41 and in Appendix H10 to H12. Figure 4.4 presents a view of the ship model.

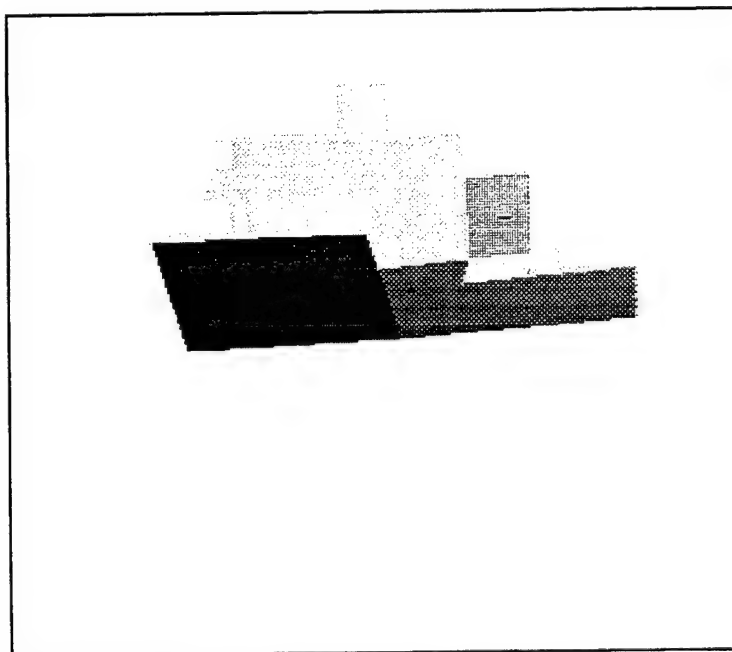


Figure 4.4 Ship Model View

The basic idea is to analyze the variation of the degree of polarization of the ship and its main planes with their corresponding aspect angle. A major portion of the experimentation with the R/V POINT SUR was devoted to evaluation of degree of polarization versus aspect angle. The programs ASPECT.PRO, MODELE.PRO and CONTRAST.PRO were developed to evaluate separately for each of the major facets of the ship the polarization and the contrast for each measurement case. The data for the 70 files were analyzed with respect to major planes 0,1,2, and 3 as defined in Appendix H.12, and also with respect to range. Planes 0 and 3 constitute the port and starboard bow quarter of the ship respectively, while planes 1 and 2 represent the port and starboard beam. The radiance from these planes was selected using the “mask” procedure explained in item 3.E.1.g. Appendix J.5 presents plots of the degree of polarization of the ship and its main planes against the aspect angle for different ranges. A variation of degree of polarization mostly at the vicinity of the Brewster angle was expected to be observed. However, analyzing the graphics in Appendix J.5 it is observed that the points for any range are spread around the “x” axis. These results show no strong evidence of any functional relationship that could represent a variation of the degree of polarization with the target aspect angle in the testing conditions⁵. The aspect angle has certainly a partial influence on the ship degree of polarization. However, over the experiment conditions other factors and testing uncertainties can have influence strong enough to cover any possible observation of the aspect angle influence on the degree of polarization. Basically three factors in the data processing contributed to the uncertainties in this project: ship

⁵ Appendix E.2 presents all specific conditions for each one of the 70 analyzed files

modeling using planes, ships' oscillation due to wave movements and lack of ship heading information at an adequate sample rate. The aspect angle of each main plane used to model the ship's hull certainly can represent the median aspect angle of the corresponding part. However, since the hull's surfaces are generally curved, there is an angular error for each point on the hull surface. Considering the ship's geometry and the main planes positioning, the maximum error due to this factor occurs at the planes 0 and 3 and it is estimated to be 10 degrees. The ships' oscillation is not followed by the ship model. Therefore, the angular variations due this factor are not computed in the data process. The ship's heading information was available at 10 minutes sample interval. This was not sufficient in terms of precision for the image's aspect angle information since each frame takes 0.3 seconds. ASPECT.PRO program was then used to estimate the ship heading using aspect ratio and shape correlation. In order to test the accuracy of this program, four observed headings were compared with the corresponding estimated headings. Table 4.4 presents the results of the comparison.

TABLE 4.4
ASPECT.PRO RESULTS VERIFICATION

Sample	Heading data (degrees)	Aspect.pro Result (degrees)	Difference (degrees)
1	152	156	+4
2	109	115	+6
3	131	128	-3
4	128	117	-11

Table 4.4: Comparison between results from program aspect.pro and recorded ship heading information

Results in Table 4.4 show an angular error comparable to the plane modeling error. The greatest difference (11 degrees) occurred at the longest range (5 km). This is a limitation of the program methodology, since it is based on target image contour which loses definition with the distance. In order to observe the aspect angle effect, a more specific experiment can be designed to reduce the influence of other factors as well the uncertainties of this project. For example, a ship carrying a special target could be used for this specific experiment. The target would be a metallic plane with known surface temperature. The temperature should be controlled to be constant and higher than the ship's stack temperature. A stabilized gyro platform mounted on the target and a GPS would give the target's angular data and the ship's positioning to be recorded at least at 1 Hz sample rate.

By performing this experiment the uncertainties would certainly be reduced. However, the operational meaning of it would be debatable, since it represents conditions very unlikely to be found in a real engagement scenario. From this point of view, the results of this project, showing no strong evidence that the aspect angle affects the target degree of polarization, can be interpreted as a first indication that the target aspect angle should not be considered as a primary factor in designing an IR sensor improved by polarizers. Another consideration that must still be done is the fact that all results in this project are related to the R/V POINT SUR as a target. Therefore, further experimentation and modeling work for different targets will be required for final results validation.

V. CONCLUSIONS AND RECOMMENDATIONS

The main objectives of this project were to determine a possible influence of the target aspect angle on the degree of polarization of the target radiation and also to verify previous work results and assumptions related to the target to background contrast improvement using horizontal polarizers on the sensor, the time dependency of contrast results and the methodology for unpolarized image generation by averaging vertically and horizontally polarized images. From the analyses done, the following conclusions were drawn:

1. Although it was theoretically expected, the target degree of polarization has shown no strong evidence of any observable dependency of the target aspect angle. Therefore, it was concluded that within the experimental conditions other factors and testing uncertainties had influence strong enough to cover any possible observation of the aspect angle influence on the degree of polarization. In order to observe the aspect angle effect, a more specific experiment is proposed, but the operational meaning of it would be debatable, since it represents conditions very unlikely to be found in a real engagement scenario. From this point of view, the results of this project show no strong evidence that the aspect angle affects the target degree of polarization and can be interpreted as a first indication that the target aspect angle should not be considered as a primary factor in designing an IR sensor improved by polarizers.

2. The average contrast improvement achieved by using a horizontal polarizer on the sensor was found to be 8%. This value is smaller than previous results (15%). A higher average sea surface temperature is presented as an important factor for explaining this difference. For the analyzed data set, the average sea surface temperature

was 17.2 C against 11.5 C in previous reports [Ref. 1]. Therefore, the analyses support the results from previous work in terms of contrast improvement using a horizontal polarizer.

3. The contrast time variation was not shown to be significant during the image recording time. This demonstrated that the results from this and previous work by comparing horizontally and vertically polarized images taken sequentially are valid. In addition, the analysis of the standard deviation of the contrast distribution has shown that the unpolarized case has bigger contrast fluctuation in comparison with the vertical and horizontal polarization cases. This fact was interpreted by the polarizer effect in reducing fluctuation of the radiation components for the horizontal and vertical polarization cases.

4. Generation of unpolarized images by averaging horizontal and vertical polarization cases has shown to be satisfactory. This was an assumption used in previous work. Therefore, the results of previous work are validated.

Besides the data analysis results, the set of programs used for the analyses have been shown to be useful as an analysis package for future work. However, in order to improve their performance and user interface, some recommendations were made:

- Use of "WIDGETS"¹ to integrate the programs.
- Optimization of array treatment to reduce the number of "loops" in the programs.
- Inclusion of "PTRWIN" (from CEDIP) as an external program that can be accessed from the main program in the package.

¹ IDL graphic tools. These tools permit generation of "windows" type applications.

APPENDIX A

EXPERIMENT LOCATION

Description :

Map of the San Diego Bay.

Plots of the GPS information of the ship trajectory during the experiment in April 9 and April 10, 1996. Image set recording points are marked as diamonds in this figure.

Map showing the planned ship positioning and desired ship heading in each station location.

Conditions :

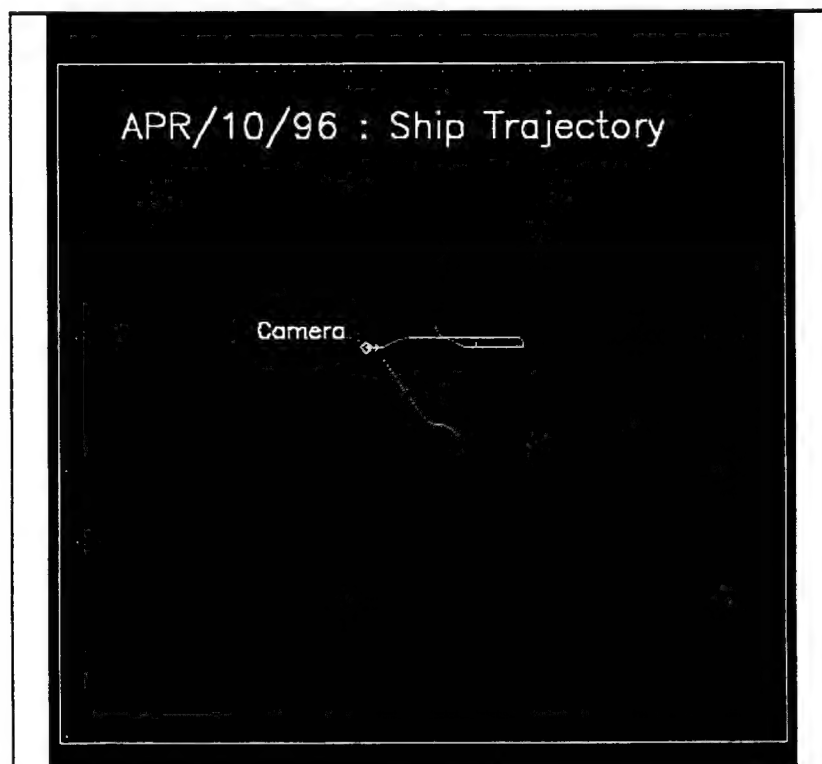
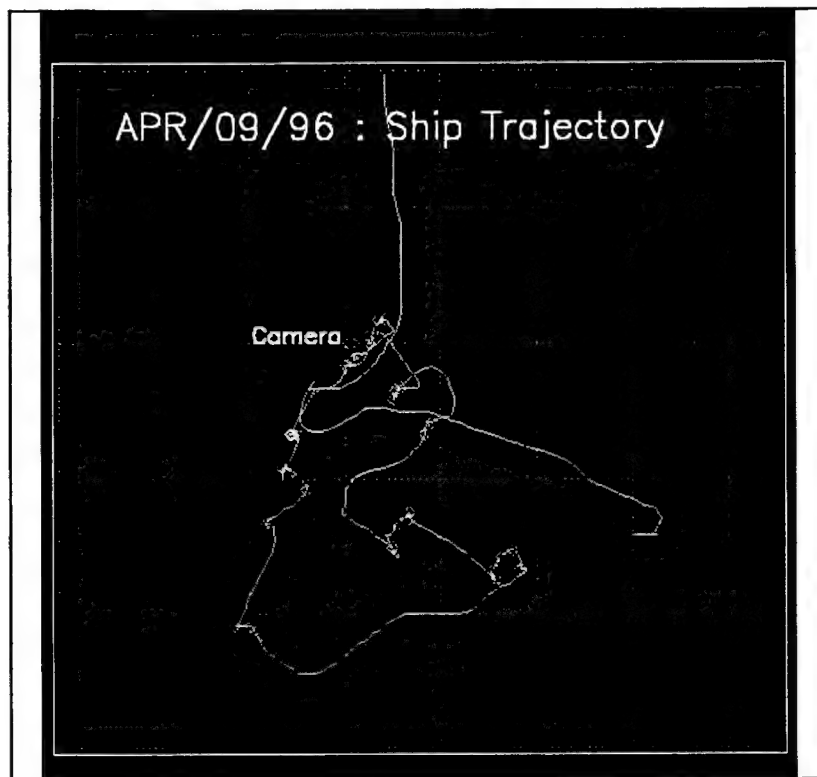
The camera (AGA 780) was located at the Building 15 of the NCCOSC-NRaD in Point Loma. Its geographic coordinates were N 32 39 35.8 , W 117 14 22.2. It was mounted on a table projecting from the window, and directed using a remote pan-tilt head. The ship maneuvered in reference to the camera position according to five planned magnetic bearings (camera to ship) ranging from 135 to 200 degrees. For each bearing there are 5 station locations at ranges from 0.5 to 3.0 nm. In each station location the ship is supposed to turn to the indicated magnetic headings and stay still during the time needed for the image recording process.

Notes :

Both ship GPS position and camera location are known, so bearing is computed. Thus, ship heading information is used with the bearing information to give the aspect angle of the target.

Range to the shore station and ship heading were reported from the ship at irregular intervals and recorded at the sensor. Magnetic bearings to the ship were recorded on land in the sensor log.





APPENDIX B

POLARIZERS PERFORMANCE CURVES

Description :

Two figures showing the performance curves for the KRS-5 , 9.5mm polarizers used in the camera setting positions 4 and 5 respectively.

Conditions :

The data were provided by the manufacturer of the polarizers, Graseby-Specac. The measurements were taken with a spectrometer using the actual filter shipped. Where two filters were required for the crossed-grid measurement (trace 3), another polarizer nearly identical to the one shipped is used. The filter performance specifications require 85% transmission efficiency over the range 1-12 μm and 98% polarization effectiveness.

Notes :

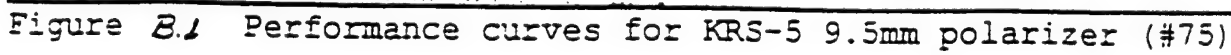
Trace 1 : Transmittance with grid perpendicular to the E vector of the incident radiation

Trace 2 : Transmittance with grid parallel to the E vector of the incident radiation

Trace 3 : Transmittance of two filters with grids crossed

Vertical axis : Wavenumber/wavelength

Horizontal axis: Transmittance



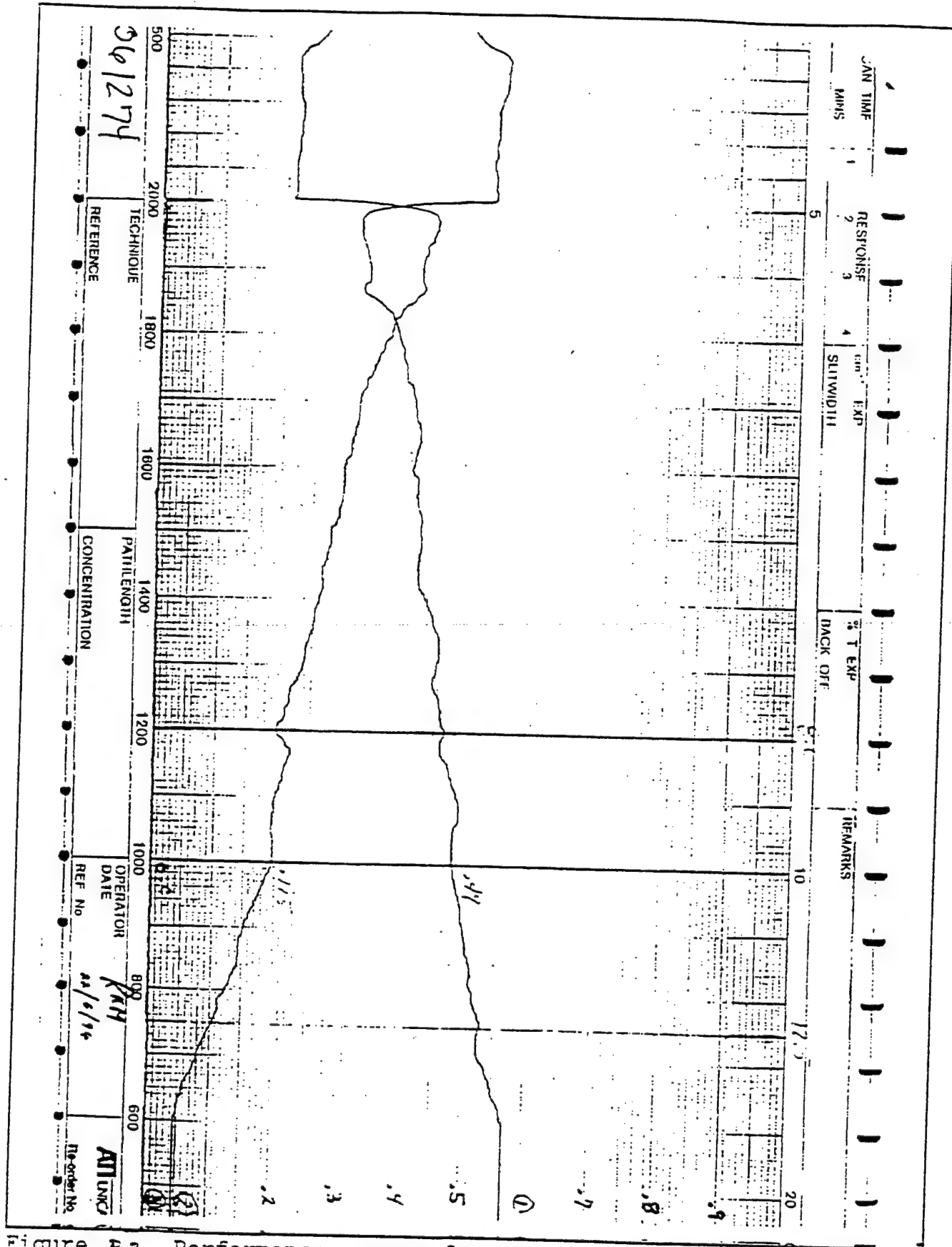


Figure 8.2 Performance curves for KRS-5 9.5mm polarizer (#74)

APPENDIX C
R/V POINT SUR

Description :

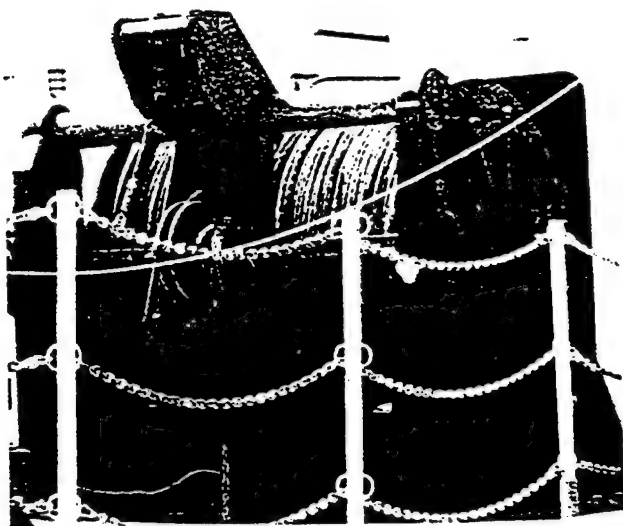
R/V POINT SUR general specifications and dimensions.

Conditions :

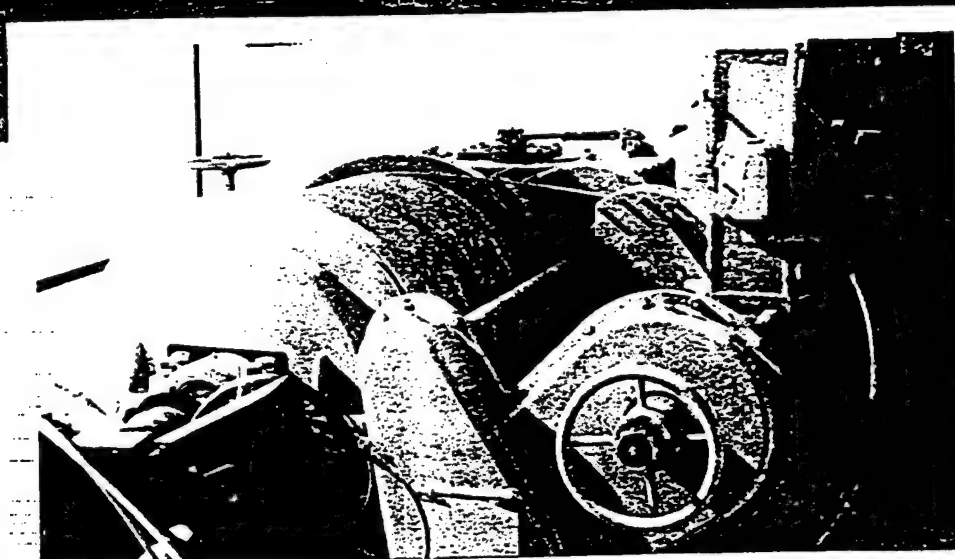
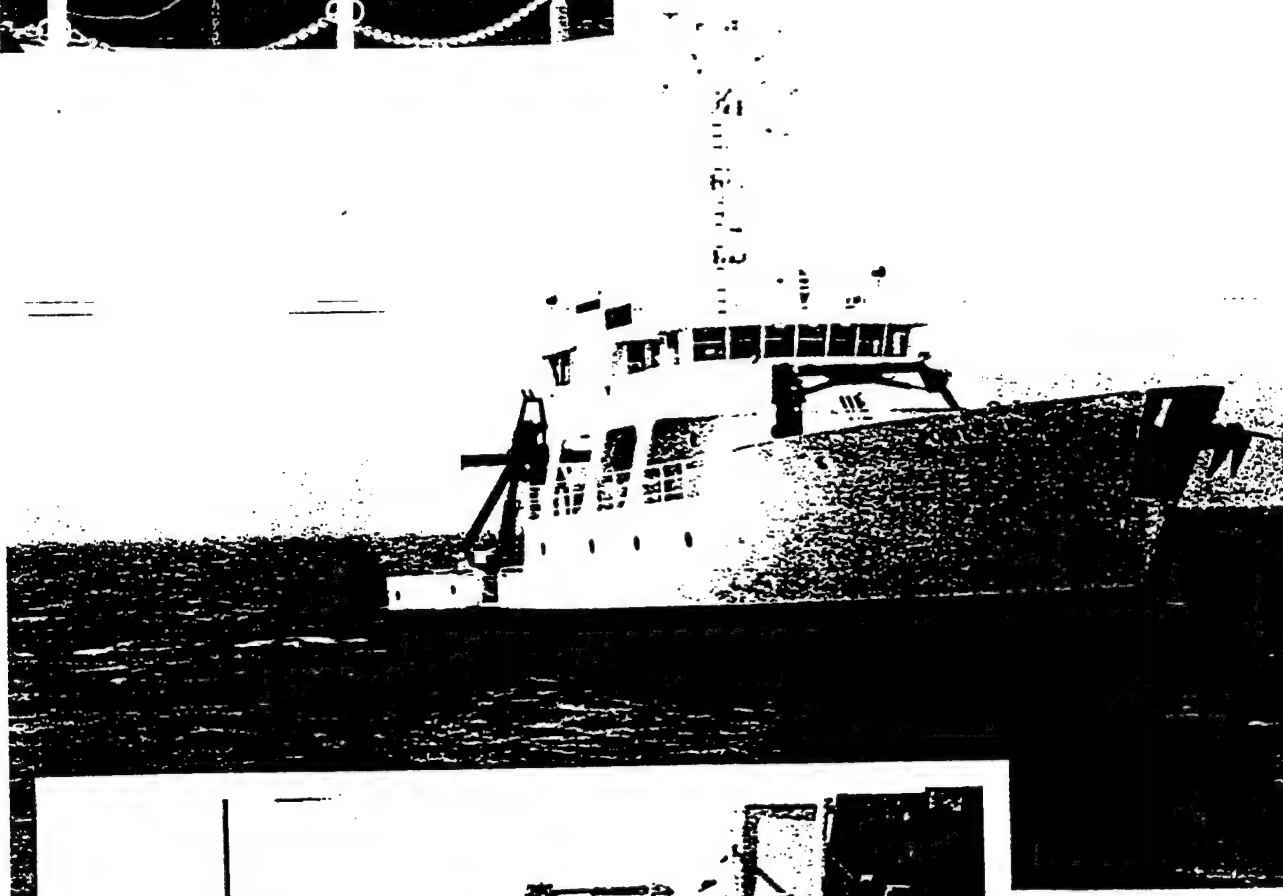
Data extracted from R/V POINT SUR Cruise Planning Manual.

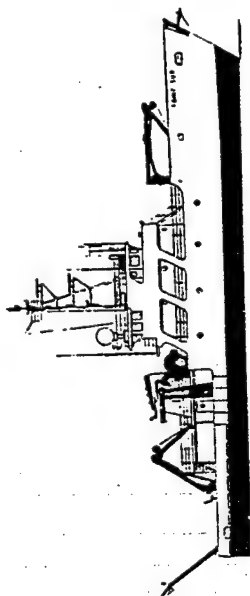
Notes :

None



THE SHIP
Section 1





GENERAL DATA:

Length overall: 135 feet
Length between perpendiculars: 124 feet
Beam: 32 feet
Draft (full load): 9 feet
Displacement: 294 tons
Displacement (full load): 539 light tons
Maximum sustained speed: 11.5 knots
Maneuvering speed: 0-10 knots
Cruising range (normal): 5,000 nautical miles
Endurance (normal): 21 days
Weather limitations: #6 high (12-20 ft. waves)
#8 gale (14-40 kts.)
#5 very rough (8-12 ft. waves)
#7 moderate gale (28-33 kts.)
Crew: Nine
Scientific Berthing: Twelve
Scientist (maximum): Forty, Day Cruise only (limited by number of life jackets)
Laboratory Area: 480 sq. ft., main deck/equipment benches installed on a modular system as required, two single sinks
Electronics Lab: 120 sq. ft., main deck/equipment with MK37 gyro repeater, G.P.S. readout, benches and/or electronic racks as required
Wet Lab: 100 sq. ft., main deck, benches, sink installed as required
Mainmast: Instrument platform 12 ft. long, 50 ft. above waterline
Workboat: 14 ft. Rhadial, 15 hp outboard motor
Deck Handling Equipment: Trawl Winch, Hydro Winch, CTD Winch, Fwd. Deck Crane, Aft Deck Crane, Captain, Stern A-Frame, Stod. Galleys Frame (see section on deck handling gear for more details)
Owner: National Science Foundation
Built: Moss Landing Marine Laboratory
Home Port: Moss Landing, California
Radio Call Signal: WSC2278

0 1 DECK

MAIN DECK

LOWER DECK

APPENDIX D

IMAGE FILES

1. LIST OF THE SELECTED IMAGE FILES (*.PTW)

Description :

List of the *.PTW files showing their size, last modification date (creation date).

Conditions :

The list was generated directly from the Norton File Manager.

Notes :

None.

Name	Size	Created On
<>		1/1/01
NSA1001.PTW	3,604,480	3/9/98 11:22:30 AM
NSA1002.PTW	1,703,936	4/10/96 8:27:24 AM
NSA1004.PTW	3,538,944	4/10/96 8:28:48 AM
NSB1000.PTW	1,703,936	4/10/96 8:32:54 AM
NSB1002.PTW	3,604,480	4/10/96 8:35:02 AM
NSB1003.PTW	1,703,936	4/10/96 8:35:00 AM
NSB1005.PTW	3,473,408	4/10/96 8:36:48 AM
NSB1006.PTW	1,769,472	4/10/96 8:37:20 AM
NSB1008.PTW	3,538,944	4/10/96 8:38:34 AM
NSB1009.PTW	1,835,008	4/10/96 8:39:44 AM
NSB1011.PTW	3,670,016	3/9/98 11:51:48 AM
NSB1012.PTW	1,703,936	4/10/96 8:41:42 AM
NSB1015.PTW	3,538,944	4/10/96 8:49:46 AM
NSB1016.PTW	1,769,472	4/10/96 8:49:48 AM
NSB1018.PTW	3,604,480	4/10/96 8:52:00 AM
NSB1019.PTW	1,703,936	4/10/96 8:52:14 AM
NSCA0912.PTW	3,473,408	4/9/96 12:13:28 PM
NSCA0913.PTW	1,703,936	4/9/96 12:14:32 PM
NSCA0915.PTW	3,473,408	4/9/96 12:18:00 PM
NSCA0916.PTW	1,703,936	4/9/96 12:20:08 PM
NSCA0918.PTW	3,538,944	4/9/96 12:23:56 PM
NSCA0919.PTW	1,835,008	4/9/96 12:25:34 PM
NSCA0927.PTW	3,801,088	4/9/96 12:41:04 PM
NSCA0928.PTW	1,835,008	4/9/96 12:41:38 PM
NSCA0930.PTW	3,932,160	4/9/96 12:44:30 PM
NSCA0931.PTW	1,769,472	4/9/96 12:44:48 PM
NSCA0933.PTW	3,997,696	4/9/96 12:46:30 PM
NSCA0934.PTW	1,900,544	4/9/96 12:47:06 PM
NSCA0936.PTW	3,670,016	4/9/96 12:51:06 PM
NSCA0937.PTW	1,835,008	4/9/96 12:51:20 PM
NSCA0938.PTW	3,473,408	4/9/96 1:03:50 PM
NSCA0939.PTW	1,769,472	4/9/96 1:05:08 PM
NSCA0940.PTW	3,473,408	4/9/96 1:07:06 PM
NSCA0941.PTW	1,769,472	4/9/96 1:08:42 PM
NSCA0942.PTW	3,407,872	4/9/96 1:10:34 PM
NSCA0943.PTW	1,769,472	4/9/96 1:11:38 PM
NSCA0944.PTW	3,538,944	4/9/96 1:15:00 PM
NSCA0945.PTW	1,769,472	4/9/96 1:15:40 PM
NSCA0946.PTW	3,473,408	4/9/96 1:19:44 PM
NSCA0947.PTW	1,769,472	4/9/96 1:20:12 PM
NSCA0948.PTW	3,604,480	4/9/96 1:27:42 PM
NSCA0949.PTW	1,835,008	4/9/96 1:29:00 PM
NSCA0950.PTW	3,932,160	4/9/96 1:30:28 PM
NSCA0951.PTW	1,835,008	4/9/96 1:31:24 PM
NSCA0952.PTW	3,407,872	4/9/96 1:34:24 PM
NSCA0953.PTW	1,769,472	4/9/96 1:35:26 PM
NSCA0954.PTW	3,473,408	4/9/96 1:37:30 PM
NSCA0955.PTW	1,769,472	4/9/96 1:38:38 PM
NSCA0956.PTW	3,473,408	4/9/96 1:40:30 PM
NSCA0957.PTW	1,835,008	4/9/96 1:41:18 PM
NSCA0958.PTW	3,604,480	4/9/96 1:52:56 PM
NSCA0959.PTW	1,835,008	4/9/96 1:53:18 PM
NSCA0962.PTW	3,538,944	4/9/96 1:58:56 PM
NSCA0963.PTW	1,835,008	4/9/96 1:59:54 PM
NSCA0964.PTW	3,604,480	4/9/96 2:01:50 PM

Name	Size	Created On	
NSCA0965.PTW	1,835,008	4/9/96	2:03:40 PM
NSCA0966.PTW	3,473,408	4/9/96	2:38:14 PM
NSCA0967.PTW	1,835,008	4/9/96	2:39:56 PM
NSCA0968.PTW	3,801,088	4/9/96	2:41:52 PM
NSCA0969.PTW	1,703,936	4/9/96	2:42:24 PM
NSCA0970.PTW	3,801,088	4/9/96	2:44:26 PM
NSCA0971.PTW	1,703,936	4/9/96	2:45:48 PM
NSCA0972.PTW	3,670,016	4/9/96	2:46:40 PM
NSCA0973.PTW	1,835,008	4/9/96	2:47:18 PM
NSCA0974.PTW	3,866,624	4/9/96	2:49:44 PM
NSCA0975.PTW	1,835,008	4/9/96	2:50:40 PM
NSCA0976.PTW	3,997,696	4/9/96	2:52:00 PM
NSCA0977.PTW	1,900,544	4/9/96	2:52:28 PM
NSCA0978.PTW	3,735,552	4/9/96	3:04:40 PM
NSCA0979.PTW	1,769,472	4/9/96	3:05:24 PM
NSCA0980.PTW	3,735,552	4/9/96	3:06:30 PM
NSCA0981.PTW	1,703,936	4/9/96	3:07:14 PM
NSCA0982.PTW	3,538,944	4/9/96	3:09:34 PM
NSCA0983.PTW	1,835,008	4/9/96	3:10:14 PM
NSCA0988.PTW	3,670,016	4/9/96	3:18:04 PM
NSCA0989.PTW	1,769,472	4/9/96	3:19:38 PM
NSCA0990.PTW	3,670,016	4/9/96	3:44:46 PM
NSCA0991.PTW	1,835,008	4/9/96	3:45:02 PM
NSCA0993.PTW	3,735,552	4/9/96	3:50:22 PM
NSCA0994.PTW	1,835,008	4/9/96	3:51:46 PM
NSCA0996.PTW	4,194,304	4/9/96	3:53:44 PM
NSCA0997.PTW	1,835,008	4/9/96	3:55:00 PM
NSCA0999.PTW	3,801,088	4/9/96	3:56:48 PM
NSCA1086.PTW	3,604,480	4/10/96	8:10:12 AM
NSCA1087.PTW	1,835,008	4/10/96	8:10:20 AM
NSCA1089.PTW	3,932,160	4/10/96	8:17:14 AM
NSCA1090.PTW	1,769,472	4/10/96	8:18:04 AM
NSCA1092.PTW	4,063,232	4/10/96	8:19:20 AM
NSCA1093.PTW	1,769,472	4/10/96	8:20:32 AM
NSCA1095.PTW	3,473,408	4/10/96	8:21:26 AM
NSCA1096.PTW	1,769,472	4/10/96	8:22:28 AM
NSCA1098.PTW	3,538,944	4/10/96	8:24:36 AM
NSCA1099.PTW	1,703,936	4/10/96	8:24:32 AM
NSCA900.PTW	1,769,472	4/9/96	3:58:32 PM
NSCA902.PTW	3,670,016	4/9/96	4:01:06 PM
NSCA903.PTW	1,769,472	4/9/96	4:01:22 PM
NSCA905.PTW	3,604,480	4/9/96	4:03:14 PM
NSCA906.PTW	1,900,544	4/9/96	4:04:52 PM
NSCA911.PTW	3,538,944	4/9/96	4:20:16 PM
NSCA912.PTW	1,835,008	4/9/96	4:21:28 PM
NSCA914.PTW	3,473,408	4/9/96	4:23:32 PM
NSCA915.PTW	1,835,008	4/9/96	4:23:32 PM
NSCA917.PTW	3,670,016	4/9/96	4:26:08 PM
NSCA918.PTW	1,769,472	4/9/96	4:26:08 PM
NSCA920.PTW	3,604,480	4/9/96	4:28:12 PM
NSCA921.PTW	1,769,472	4/9/96	4:28:20 PM
NSCA923.PTW	3,670,016	4/9/96	4:31:30 PM
NSCA924.PTW	1,769,472	4/9/96	4:31:28 PM
NSCA926.PTW	3,735,552	4/9/96	4:33:44 PM
NSCA927.PTW	1,835,008	4/9/96	4:33:40 PM
NSCA929.PTW	3,538,944	4/9/96	4:51:06 PM

Name	Size	Created On	
NSCA930.PTW	1,769,472	4/9/96	4:51:20 PM
NSCA932.PTW	3,735,552	4/9/96	4:54:02 PM
NSCA933.PTW	1,900,544	4/9/96	4:54:12 PM
NSCA935.PTW	3,604,480	4/9/96	4:55:38 PM
NSCA936.PTW	1,769,472	4/9/96	4:56:36 PM
NSCA938.PTW	3,538,944	4/9/96	4:57:44 PM
NSCA939.PTW	1,703,936	4/9/96	4:58:46 PM
NSCA941.PTW	3,670,016	4/9/96	5:00:16 PM
NSCA942.PTW	1,835,008	4/9/96	5:01:22 PM
NSCA944.PTW	3,670,016	4/9/96	5:13:34 PM
NSCA945.PTW	1,769,472	4/9/96	5:15:00 PM
NSCA947.PTW	3,735,552	4/9/96	5:16:28 PM
NSCA948.PTW	1,769,472	4/9/96	5:16:24 PM
NSCA958.PTW	3,735,552	4/9/96	5:30:28 PM
NSCA959.PTW	1,769,472	4/9/96	5:31:20 PM
NSCA961.PTW	3,670,016	4/9/96	5:33:16 PM
NSCA962.PTW	1,703,936	4/9/96	5:34:34 PM
NSCA964.PTW	3,801,088	4/9/96	5:43:36 PM
NSCA965.PTW	3,407,872	4/9/96	5:43:36 PM
NSCA967.PTW	3,473,408	4/9/96	5:45:16 PM
NSCA968.PTW	1,703,936	4/9/96	5:46:40 PM
NSCA971.PTW	3,538,944	4/9/96	5:48:08 PM
NSCA972.PTW	1,835,008	4/9/96	5:49:40 PM
NSCA974.PTW	3,604,480	4/9/96	5:51:16 PM
NSCA975.PTW	1,835,008	4/9/96	5:51:20 PM
NSCA977.PTW	3,670,016	4/9/96	5:53:56 PM
NSCA978.PTW	1,703,936	4/9/96	5:53:52 PM
NSCA980.PTW	3,670,016	4/9/96	5:55:56 PM
NSCA981.PTW	1,769,472	4/9/96	5:56:02 PM
NSCA983.PTW	3,538,944	4/9/96	5:57:12 PM

2. LIST OF THE BASIC IMAGE FILES (*.PTE)

Description :

List of the *.PTE files showing their size, last modification date.

Conditions :

The list was generated directly from the Norton File Manager.

Notes :

None.

Name	Type	Size	Last Modified
BASE01.PTE	PTE File	4,896,254	5/21/98 10:03:32 AM
BASE02.PTE	PTE File	4,896,254	5/21/98 10:36:08 AM
BASE03.PTE	PTE File	5,025,070	5/21/98 4:58:38 PM
BASE04.PTE	PTE File	5,347,110	5/21/98 5:15:06 PM
BASE05.PTE	PTE File	5,347,110	5/21/98 5:31:48 PM
BASE06.PTE	PTE File	5,540,334	5/21/98 5:49:08 PM
BASE07.PTE	PTE File	5,089,478	5/21/98 6:04:54 PM
BASE08.PTE	PTE File	4,831,846	5/21/98 6:19:48 PM
BASE09.PTE	PTE File	4,831,846	5/21/98 6:37:48 PM
BASE10.PTE	PTE File	4,767,438	5/21/98 9:18:24 PM
BASE11.PTE	PTE File	4,896,254	5/21/98 9:34:38 PM
BASE12.PTE	PTE File	4,896,254	5/21/98 9:49:48 PM
BASE13.PTE	PTE File	5,089,478	5/21/98 10:05:36 PM
BASE14.PTE	PTE File	5,411,518	5/21/98 10:23:16 PM
BASE15.PTE	PTE File	4,831,846	5/21/98 10:38:54 PM
BASE16.PTE	PTE File	4,960,662	5/21/98 10:55:00 PM
BASE17.PTE	PTE File	4,896,254	5/22/98 11:27:10 AM
BASE18.PTE	PTE File	5,025,070	5/22/98 11:42:04 AM
BASE19.PTE	PTE File	5,025,070	5/22/98 11:57:20 AM
BASE20.PTE	PTE File	5,089,478	5/22/98 12:12:10 PM
BASE21.PTE	PTE File	4,896,254	5/24/98 9:44:50 AM
BASE22.PTE	PTE File	5,089,478	5/24/98 10:00:46 AM
BASE23.PTE	PTE File	5,089,478	5/24/98 5:52:10 PM
BASE24.PTE	PTE File	5,089,478	5/24/98 6:08:38 PM
BASE25.PTE	PTE File	5,282,702	5/24/98 6:24:48 PM
BASE26.PTE	PTE File	5,475,926	5/24/98 6:41:20 PM
BASE27.PTE	PTE File	5,218,294	5/24/98 6:57:34 PM
BASE28.PTE	PTE File	5,025,070	5/24/98 7:13:36 PM
BASE29.PTE	PTE File	4,960,662	5/24/98 7:29:18 PM
BASE30.PTE	PTE File	5,025,070	5/24/98 7:44:32 PM
BASE31.PTE	PTE File	5,089,478	5/25/98 10:36:08 PM
BASE32.PTE	PTE File	5,153,886	5/25/98 10:52:28 PM
BASE33.PTE	PTE File	5,540,334	5/25/98 11:09:34 PM
BASE34.PTE	PTE File	5,153,886	5/25/98 11:25:44 PM
BASE35.PTE	PTE File	5,025,070	5/25/98 11:41:38 PM
BASE36.PTE	PTE File	5,089,478	5/25/98 11:57:40 PM
BASE37.PTE	PTE File	5,025,070	5/26/98 12:13:34 AM
BASE38.PTE	PTE File	4,896,254	5/26/98 12:28:58 AM
BASE39.PTE	PTE File	5,025,070	5/26/98 12:45:10 AM
BASE40.PTE	PTE File	5,025,070	5/26/98 1:01:20 AM
BASE41.PTE	PTE File	5,025,070	5/26/98 1:17:42 AM
BASE42.PTE	PTE File	5,153,886	5/26/98 1:33:48 AM
BASE43.PTE	PTE File	4,960,662	5/26/98 1:49:54 AM
BASE44.PTE	PTE File	5,282,702	5/26/98 2:07:32 AM
BASE45.PTE	PTE File	5,089,478	5/26/98 2:27:58 AM
BASE46.PTE	PTE File	4,831,846	5/26/98 2:43:56 AM
BASE47.PTE	PTE File	5,089,478	5/26/98 2:59:46 AM
BASE48.PTE	PTE File	5,025,070	5/26/98 3:15:36 AM
BASE49.PTE	PTE File	5,153,886	5/26/98 3:32:34 AM
BASE50.PTE	PTE File	5,089,478	5/26/98 3:49:20 AM
BASE51.PTE	PTE File	5,025,070	5/26/98 4:05:48 AM
BASE52.PTE	PTE File	5,797,966	5/26/98 4:24:14 AM
BASE53.PTE	PTE File	4,767,438	5/26/98 4:39:16 AM
BASE54.PTE	PTE File	4,960,662	5/26/98 4:54:56 AM
BASE55.PTE	PTE File	5,025,070	5/26/98 5:11:26 AM
BASE56.PTE	PTE File	4,960,662	5/26/98 5:27:40 AM
BASE57.PTE	PTE File	5,089,478	5/26/98 5:44:26 AM
BASE58.PTE	PTE File	5,025,070	5/26/98 6:01:18 AM
BASE59.PTE	PTE File	5,282,702	5/26/98 6:18:34 AM
BASE60.PTE	PTE File	5,411,518	5/26/98 6:35:48 AM
BASE61.PTE	PTE File	4,896,254	5/26/98 6:51:38 AM
BASE62.PTE	PTE File	4,896,254	5/26/98 7:06:58 AM
BASE63.PTE	PTE File	5,025,070	5/26/98 7:23:20 AM
BASE64.PTE	PTE File	4,960,662	5/26/98 7:39:48 AM
BASE65.PTE	PTE File	5,025,070	5/26/98 7:56:24 AM
BASE66.PTE	PTE File	4,896,254	5/26/98 8:12:16 AM
BASE67.PTE	PTE File	5,089,478	5/26/98 8:28:56 AM
BASE68.PTE	PTE File	5,089,478	5/26/98 8:44:48 AM
BASE69.PTE	PTE File	4,960,662	5/26/98 9:00:16 AM
BASE70.PTE	PTE File	5,025,070	5/26/98 9:16:04 AM

APPENDIX E

METEOROLOGICAL DATA

1. METOC FILES

Description :

This Appendix presents the description of METOC1 and METOC2 files. Their recorded parameters are listed and a sample taken directly from the METOC files is shown.

Conditions :

Information provided by NPS-Meteorological Group.

Notes :

None.

STORAGE FORMAT FOR METOC01 (DASC) DATA

The data is stored in a set of files with the names "eopace.*" and "30sec.*". The extension for the file names is the Julian date the file was started on. A new pair of files is started every day at 00:00 GMT. The time data in the files are all GMT. The eopace files have the data averaged over 10 minutes. The 30sec files have the GPS data averaged over 30 seconds and the last set of data from the Campbell. In the 30sec file, the Campbell data are not averaged. The data format for both files is the same. Each file has a header which tells when the file was started. Each file also has a footer that tells when the file was finished. Some files may also have additional start and stop times interspersed with the data, depending on whether data logging was turned off or the program was stopped before the end of the day. The data are arranged in fields separated by spaces across a line of text. A carriage return character and a line feed character are at the end of each line. Each new reading is on a new line. The fields are in the order below. The numbers before the fields are not in the data. They serve to make identifying the fields easier.

- 01 number of readings in this average, nn
- 02 year, yyyy
- 03 Julian date, ddd
- 04 hours & minutes, hhmm
- 05 seconds, ss
- 06 Relative Wind Speed, m/s, mmm
- 07 Relative Wind Direction, degrees, ddd
- 08 Ship Speed, knots, at present always 0
- 09 Ship Direction, degrees, at present always 090
- 10 True Wind Speed, m/s, mmm
- 11 True Wind Direction, degrees, ddd
- 12 T air, degrees C, tt.t
- 13 RH, per cent, pp
- 14 Pressure, millibars, pppp.p
- 15 Sea Surface Temperature, degrees C, tt.t
- 16 GPS time, hhmmss
- 17 GPS Latitude, ddmm.m
- 18 GPS North/South Indicator, either 'N' or 'S'
- 19 GPS Longitude, dddmm.m
- 20 GPS East/West Indicator, either 'E' or 'W'
- 21 GPS Speed Over Ground, knots, kk.k
- 22 GPS Course Over Ground, degrees, ddd.d
- 23 GPS Antenna Height, meters, mm.m

Here is a sample of the data:

```
30 1996 99 1103 28 5 009 0 090 3 323 12.3 91 1013.9
20.3 110838 3306.2 N 11806.0 W 0.0 90.0 189.6
```


STORAGE FORMAT FOR METOC02 DATA

The METOC02 system had two additional temperature sensors and two additional RH sensors. The data are arranged slightly differently than the METOC01 system. The data is stored in a set of files with the names "eopace.*" and "30sec.*". The extension for the file names is the Julian date the file was started on. A new pair of files is started every day at 00:00 GMT. The time data in the files are all GMT. The eopace files have the data averaged over 10 minutes.

The 30sec files have the GPS data averaged over 30 seconds and the last set of data from the Campbell. In the 30sec file, the Campbell data are not averaged. The data format for both files is the same. Each file has a header which tells when the file was started. Each file also has a footer that tells when the file was finished. Some files may also have additional start and stop times interspersed with the data, depending on whether data logging was turned off or the program was stopped before the end of the day. The data are arranged in fields separated by spaces across a line of text. A carriage return character and a line feed character are at the end of each line. Each new reading is on a new line. The fields are in the order below. The numbers before the fields are not in the data. They serve to make identifying the fields easier.

- 01 number of readings in this average, nn
- 02 year, yyyy
- 03 Julian date, ddd
- 04 hours & minutes, hhmm
- 05 seconds, ss
- 06 Relative Wind Speed, m/s, mmm
- 07 Relative Wind Direction, degrees, ddd
- 08 Ship Speed, knots, at present always 0
- 09 Ship Direction, degrees, at present always 090
- 10 True Wind Speed, m/s, mmm
- 11 True Wind Direction, degrees, ddd
- 12 T air, degrees C, tt.t
- 13 RH, per cent, pp
- 14 Pressure, millibars, pppp.p
- 15 Sea Surface Temperature, degrees C, tt.t
- 16 T air A, degrees C, tt.t
- 17 RH A, per cent, pp
- 18 T air B, degrees C, tt.t
- 19 RH B, per cent, pp
- 20 delimiter between Campbell data and GPS data, "****"
- 21 GPS time, hhmmss
- 22 GPS Latitude, ddmm.m
- 23 GPS North/South Indicator, either 'N' or 'S'
- 24 GPS Longitude, dddmm.m
- 25 GPS East/West Indicator, either 'E' or 'W'
- 26 GPS Speed Over Ground, knots, kk.k
- 27 GPS Course Over Ground, degrees, ddd.d
- 28 GPS Antenna Height, meters, mm.m

Here is a sample of the data :

```
18 1996 99 0319 28 2 090 0 090 3 263 12.2 96 1012.3 16.4
12.2 96.9 12.7 95.7*** 031908 3322.3 N 11836.9 W 5.0 126.3 25.7
```

METOC 1 FORMAT

Data logging started at Tue Apr 09 00:00:00 1996

30	1996	99	2355	44	2	156	0	090	6	294	15.4	81	1016.2
21.2	000024	3311.2	N 11728.2	W	6.3	124.3	56.8						
30	1996	99	2355	44	2	156	0	090	6	294	15.4	81	1016.2
21.2	000054	3311.2	N 11728.2	W	6.3	123.9	52.5						
30	1996	99	2355	44	2	156	0	090	6	294	15.4	81	1016.2
21.2	000124	3311.1	N 11728.1	W	6.3	123.5	42.0						
30	1996	99	2355	44	2	156	0	090	6	294	15.4	81	1016.2
21.2	000154	3311.1	N 11728.0	W	6.3	123.0	26.9						
30	1996	99	2355	44	2	156	0	090	6	294	15.4	81	1016.2
21.2	000224	3311.1	N 11728.0	W	6.4	121.6	9.9						
30	1996	99	2355	44	2	156	0	090	6	294	15.4	81	1016.2
21.2	000254	3311.1	N 11727.9	W	6.3	120.5	-4.2						
30	1996	99	2355	44	2	156	0	090	6	294	15.4	81	1016.2
21.2	000324	3311.0	N 11727.9	W	5.9	129.6	-10.7						
30	1996	99	2355	44	2	156	0	090	6	294	15.4	81	1016.2
21.2	000354	3311.0	N 11727.9	W	4.1	185.6	-6.7						
30	1996	99	2355	44	2	156	0	090	6	294	15.4	81	1016.2
21.2	000424	3311.0	N 11727.9	W	4.1	233.5	9.0						

METOC 2 FORMAT

Data logging started at Tue Apr 09 00:00:00 1996

30	1996	99	2352	32	2	138	0	090	5	288	16.5	75	1016.9
16.8	0.0	0.0	0.0	0.0***	000035	3311.2	N 11728.2	W	6.3	124.3	46.3		
30	1996	99	2352	32	2	138	0	090	5	288	16.5	75	1016.9
16.8	0.0	0.0	0.0	0.0***	000105	3311.1	N 11728.1	W	6.3	124.2	40.7		
30	1996	99	2352	32	2	138	0	090	5	288	16.5	75	1016.9
16.8	0.0	0.0	0.0	0.0***	000135	3311.1	N 11728.1	W	6.2	123.6	29.4		
29	1996	99	2352	32	2	138	0	090	5	288	16.5	75	1016.9
16.8	0.0	0.0	0.0	0.0***	000205	3311.1	N 11728.0	W	6.4	122.3	14.0		
30	1996	100	0002	8	2	149	0	090	5	292	16.2	76	1016.9
16.6	0.0	0.0	0.0	0.0***	000235	3311.1	N 11728.0	W	6.3	121.4	-2.1		
30	1996	100	0002	8	2	149	0	090	5	292	16.2	76	1016.9
16.6	0.0	0.0	0.0	0.0***	000305	3311.0	N 11727.9	W	6.2	120.7	-13.8		
30	1996	100	0002	8	2	149	0	090	5	292	16.2	76	1016.9
16.6	0.0	0.0	0.0	0.0***	000335	3311.0	N 11727.9	W	4.6	159.8	-17.5		
30	1996	100	0002	8	2	149	0	090	5	292	16.2	76	1016.9
16.6	0.0	0.0	0.0	0.0***	000405	3311.0	N 11727.9	W	3.7	216.5	-10.2		
30	1996	100	0002	8	2	149	0	090	5	292	16.2	76	1016.9
16.6	0.0	0.0	0.0	0.0***	000435	3311.0	N 11727.9	W	3.8	259.1	8.3		

2. METEOROLOGICAL CONDITIONS

Description :

This Appendix presents the experimental and the calculated conditions for all 70 analyzed files. The data is presented in 2 tables where each column represents a parameter and each line represents a file. File number, date, recording time, GPS data, angular positioning and atmospheric transmittance were added to the METOC data.

Conditions :

Meteorological data presented in this Appendix represent the average value from METOC1 and METOC2 during the record time interval of each file (image sequence). Range and angular information were obtained by calculation using the ship GPS and sensor location information. Atmospheric transmittance was calculated using MODTRAN under conditions described in Chapter III item A.4.c.

Notes :

Day column shows 9 or 10 corresponding to April 9 and April 10, 1996.

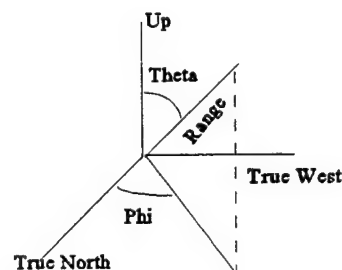
Values in "time" column are elapsed time given in seconds starting at 00h:00min (local) of the corresponding day.

Latitude (Lat) and longitude (Lon) are presented in minutes and the ship GPS antenna height (H) is presented in meters.

Heading and Bearing information are referred to the True North.

The range and angular information (Range, Theta, Phi) are spherical coordinates referred to the camera coordinate system:

- Origin : Camera position
- x axis : Oriented to true North
- y axis : Oriented to true West
- z axis : Up



AVERAGE DATA FROM METOC

File (#)	Day	Time (sec)	Lat (min)	Lon (min)	H (m)	Temp (C)	RH (%)	Press. (mb)	Wind (m/s)	Sea Temp (C)	Range (m)	Theta (rd)	Phi (rd)	Atm Trans
1	9	44018.00	1959.20	7034.80	-27.01	15.30	72.00	1018.25	6.50	18.55	998.52	1.62	2.41	0.82
2	9	44304.80	1959.20	7034.80	-23.98	15.32	71.92	1018.24	6.34	18.58	998.52	1.62	2.41	0.82
3	9	44648.10	1959.20	7034.80	-19.07	15.80	70.50	1018.15	6.00	18.65	998.52	1.62	2.41	0.82
4	9	45681.70	1958.80	7035.10	23.86	15.70	70.50	1018.00	5.50	17.70	1868.07	1.60	2.49	0.71
5	9	45872.10	1958.80	7035.08	18.72	15.50	70.50	1018.00	4.50	16.20	1850.58	1.60	2.50	0.71
6	9	46026.30	1958.80	7035.05	18.50	15.50	70.50	1018.00	4.50	16.20	1820.90	1.60	2.52	0.71
7	9	46279.20	1958.80	7035.00	16.80	15.45	70.00	1018.05	4.00	16.60	1777.28	1.60	2.56	0.72
8	9	47062.80	1958.50	7035.20	26.40	15.75	69.00	1017.95	4.00	17.00	2413.99	1.59	2.58	0.67
9	9	47252.40	1958.50	7035.20	27.43	15.75	69.00	1017.95	4.00	17.00	2413.99	1.59	2.58	0.67
10	9	47451.70	1958.50	7035.20	37.22	15.65	69.20	1017.97	4.00	16.82	2413.99	1.59	2.58	0.67
11	9	47701.20	1958.47	7035.06	-6.40	15.40	69.50	1018.05	6.50	15.80	2361.33	1.59	2.67	0.68
12	9	47990.80	1958.30	7034.90	-11.43	15.40	69.50	1018.05	6.50	15.80	2545.05	1.59	2.81	0.66
13	9	48498.80	1958.00	7035.40	10.79	15.90	67.00	1018.05	6.50	17.30	3370.32	1.59	2.65	0.61
14	9	48669.90	1958.00	7035.40	11.61	15.97	66.73	1018.01	6.77	17.31	3370.32	1.59	2.65	0.61
15	9	48875.40	1958.00	7035.40	7.43	15.80	67.00	1017.80	5.00	17.30	3370.32	1.59	2.65	0.61
16	9	49060.60	1958.00	7035.40	7.23	15.80	67.00	1017.80	5.00	17.30	3370.32	1.59	2.65	0.61
17	9	49236.40	1958.00	7035.35	7.75	15.80	67.00	1017.80	5.00	17.30	3334.01	1.59	2.67	0.63
18	9	49976.30	1957.10	7035.80	49.85	16.00	65.50	1017.75	6.50	17.60	5138.57	1.58	2.69	0.48
19	9	50342.10	1957.10	7035.60	30.82	16.00	65.50	1017.70	5.00	18.75	5008.72	1.58	2.75	0.50
20	9	50552.20	1957.00	7035.50	6.93	15.90	65.83	1017.68	4.67	18.63	5127.45	1.58	2.79	0.48

File (#)	Day	Time (sec)	Lat (min)	Lon (min)	H (m)	Temp (C)	RH (%)	Press. (mb)	Wind (m/s)	Sea Temp (C)	Range (m)	Theta (rd)	Phi (rd)	Atm Trans
21	9	52738.60	1957.60	7032.20	51.22	15.40	68.50	1017.25	5.00	15.45	5016.51	1.58	3.88	0.50
22	9	52905.50	1957.60	7032.20	45.29	15.40	68.50	1017.25	5.00	15.45	5016.51	1.58	3.88	0.50
23	9	53080.20	1957.76	7032.29	2.02	15.35	68.04	1017.12	4.54	15.52	4694.53	1.58	3.90	0.53
24	9	53231.60	1957.70	7032.45	27.14	15.35	68.00	1017.05	4.50	15.65	4623.36	1.58	3.85	0.53
25	9	53385.50	1957.60	7032.54	28.10	15.35	68.00	1017.05	4.50	15.65	4674.57	1.58	3.80	0.53
26	9	53539.00	1957.50	7032.50	-6.61	15.35	68.00	1017.05	4.50	15.65	4861.17	1.58	3.79	0.51
27	9	54281.70	1958.04	7033.60	-64.40	15.50	67.65	1016.84	5.85	16.34	3136.75	1.59	3.53	0.64
28	9	54427.90	1958.10	7033.60	10.35	15.05	68.50	1016.65	6.50	16.50	3026.40	1.59	3.55	0.66
29	9	54609.30	1958.00	7033.73	0.19	15.05	68.50	1016.65	6.50	16.50	3124.74	1.59	3.47	0.64
30	9	55132.70	1957.78	7033.81	34.47	15.60	66.50	1016.70	5.50	17.10	3474.34	1.59	3.39	0.62
31	9	56711.50	1958.80	7033.40	-38.41	15.30	68.50	1016.46	5.43	16.51	2117.26	1.59	3.94	0.72
32	9	57059.90	1958.80	7033.40	-33.04	15.40	68.00	1016.50	5.00	16.05	2117.26	1.59	3.94	0.72
33	9	57250.40	1958.80	7033.40	-31.08	15.40	68.00	1016.50	5.00	16.05	2117.26	1.59	3.94	0.72
34	9	57456.80	1958.80	7033.40	-27.43	15.30	66.50	1016.45	6.00	16.20	2117.26	1.59	3.94	0.72
35	9	57679.90	1958.80	7033.40	-27.65	15.30	66.50	1016.45	6.00	16.20	2117.26	1.59	3.94	0.72
36	9	57838.20	1958.90	7033.31	-11.60	15.30	66.50	1016.45	6.00	16.20	2097.62	1.59	4.05	0.72
37	9	58854.90	1959.10	7033.80	40.00	15.50	66.50	1016.45	5.50	15.50	1284.37	1.61	3.91	0.81
38	9	59009.70	1959.10	7033.80	37.80	15.50	66.50	1016.45	5.50	15.50	1284.37	1.61	3.91	0.81
39	9	59178.50	1959.10	7033.80	35.15	15.44	66.50	1016.41	5.77	15.83	1284.37	1.61	3.91	0.81
40	9	59301.30	1959.18	7033.77	1.38	15.45	66.50	1016.40	6.00	15.90	1211.72	1.61	4.01	0.82
41	9	59489.20	1959.20	7033.70	-20.76	15.45	66.50	1016.40	6.00	15.90	1280.12	1.61	4.10	0.81

File (#)	Day	Time (sec)	Lat (min)	Lon (min)	H (m)	Temp (C)	RH (%)	Press. (mb)	Wind (m/s)	Sea Temp (C)	Range (m)	Theta (rd)	Phi (rd)	Atm Trans
42	9	59615.70	1959.20	7033.70	-19.80	15.45	66.50	1016.40	6.00	15.90	1280.12	1.61	4.10	0.81
43	9	60679.60	1959.60	7034.10	2.59	15.30	67.50	1016.25	7.00	15.45	421.01	1.69	3.71	0.91
44	9	60826.10	1959.60	7034.10	2.51	15.30	67.50	1016.25	7.00	15.45	421.01	1.69	3.71	0.91
45	9	60963.30	1959.67	7034.10	5.87	15.35	68.00	1016.35	6.00	16.25	444.74	1.68	2.25	0.91
46	9	61087.40	1959.80	7033.99	9.33	15.45	69.00	1016.40	6.00	16.60	694.26	1.64	2.01	0.87
47	9	61253.60	1959.80	7033.90	14.08	15.45	69.00	1016.40	6.00	16.60	821.55	1.63	2.10	0.85
48	9	62045.90	1959.45	7034.30	-18.80	15.60	67.00	1016.50	5.00	15.60	299.18	1.74	3.52	0.93
49	9	62187.50	1959.45	7034.30	-14.58	15.45	68.50	1016.35	5.50	16.50	299.18	1.74	3.52	0.93
50	9	63068.30	1959.40	7034.40	-19.44	15.30	69.00	1016.40	4.00	16.60	373.21	1.71	3.02	0.92
51	9	63235.40	1959.40	7034.40	-22.65	15.30	69.00	1016.40	4.00	16.60	373.21	1.71	3.02	0.92
52	9	63812.20	1959.20	7034.80	-5.37	15.45	68.00	1016.45	4.50	17.45	998.52	1.62	2.41	0.83
53	9	63956.50	1959.20	7034.80	-4.48	15.40	68.93	1016.45	4.03	17.50	998.52	1.62	2.41	0.83
54	9	64134.10	1959.20	7034.80	-5.31	15.35	70.00	1016.45	5.00	17.65	998.52	1.62	2.41	0.83
55	9	64282.70	1959.20	7034.80	4.06	15.35	70.00	1016.45	5.00	17.65	998.52	1.62	2.41	0.83
56	9	64421.40	1959.20	7034.80	-2.23	15.35	70.00	1016.45	5.00	17.65	998.52	1.62	2.41	0.83
57	9	64541.90	1959.20	7034.80	-0.71	15.35	69.91	1016.47	5.00	17.67	998.52	1.62	2.41	0.83
58	10	29421.60	1959.50	7034.14	7.11	14.60	82.50	1015.35	2.00	16.85	408.31	1.69	4.24	0.89
59	10	29849.20	1959.50	7034.20	7.15	15.14	77.14	1015.39	2.89	18.08	322.60	1.73	4.10	0.91
60	10	29998.00	1959.50	7034.20	6.88	15.20	76.50	1015.40	3.00	18.30	322.60	1.73	4.10	0.91
61	10	30118.20	1959.50	7034.20	6.18	15.20	76.50	1015.40	3.00	18.30	322.60	1.73	4.10	0.91
62	10	30271.30	1959.50	7034.20	6.13	15.20	76.50	1015.40	3.00	18.30	322.60	1.73	4.10	0.91

File (#)	Day	Time (sec)	Lat (min)	Lon (min)	H (m)	Temp (C)	RH (%)	Press. (mb)	Wind (m/s)	Sea Temp (C)	Range (m)	Theta (rd)	Phi (rd)	Atm Trans
63	10	30445.80	1959.50	7034.20	7.25	15.40	76.00	1015.40	2.86	18.03	322.60	1.73	4.10	0.91
64	10	30609.90	1959.50	7034.18	6.61	15.40	76.00	1015.40	2.50	17.85	344.76	1.72	4.15	0.90
65	10	30884.00	1959.50	7034.11	5.28	15.40	76.00	1015.40	2.50	17.85	441.88	1.68	4.28	0.89
66	10	31002.80	1959.50	7034.10	5.99	15.43	75.70	1015.43	2.20	18.45	459.93	1.68	4.30	0.89
67	10	31143.20	1959.50	7034.10	5.90	15.50	74.50	1015.55	1.50	19.75	459.93	1.68	4.30	0.89
68	10	31265.40	1959.50	7034.10	6.04	15.50	74.50	1015.55	1.50	19.75	459.93	1.68	4.30	0.89
69	10	31777.30	1959.10	7033.70	5.29	15.95	74.00	1015.60	2.00	21.05	1395.36	1.61	3.99	0.75
70	10	31905.30	1959.10	7033.70	-4.36	15.95	74.00	1015.60	2.00	21.05	1395.36	1.61	3.99	0.75

POSITIONING DATA

File (#)	Day ¹	Time ² Hour	Time Min	Time Sec	Ship Latitude (min)	Ship Longitude (min)	Ship Height (m)	Ship Heading (Degrees)	Ship Bearing (Degrees)	Range (m)	Theta (rd)	Phi (rd)
1	9	12	13	37.90	1959.20	7034.80	-27.01	99	221.85	998.52	1.62	2.41
2	9	12	18	24.80	1959.20	7034.80	-23.98	122	221.85	998.52	1.62	2.41
3	9	12	24	8.10	1959.20	7034.80	-19.07	205	221.85	998.52	1.62	2.41
4	9	12	41	21.70	1958.80	7035.10	23.86	67	217.26	1868.07	1.60	2.49
5	9	12	44	32.10	1958.80	7035.08	18.72	93	216.69	1850.58	1.60	2.50
6	9	12	47	6.30	1958.80	7035.05	18.50	107	215.54	1820.9	1.60	2.52
7	9	12	51	19.10	1958.80	7035.00	16.80	198	213.25	1777.28	1.60	2.56
8	9	13	4	22.80	1958.50	7035.20	26.40	42	212.10	2413.99	1.59	2.58
9	9	13	7	32.40	1958.50	7035.20	27.43	65	212.10	2413.99	1.59	2.58
10	9	13	10	51.70	1958.50	7035.20	37.22	87	212.10	2413.99	1.59	2.58
11	9	13	15	1.20	1958.47	7035.06	-6.40	116	206.94	2361.33	1.59	2.67
12	9	13	19	50.80	1958.30	7034.90	-11.43	189	198.92	2545.05	1.59	2.81
13	9	13	28	18.80	1958.00	7035.40	10.79	39	208.09	3370.32	1.59	2.65
14	9	13	31	9.90	1958.00	7035.40	11.61	60	208.09	3370.32	1.59	2.65
15	9	13	34	35.40	1958.00	7035.40	7.43	79	208.09	3370.32	1.59	2.65
16	9	13	37	40.60	1958.00	7035.40	7.23	100	208.09	3370.32	1.59	2.65
17	9	13	40	36.40	1958.00	7035.35	7.75	189	206.94	3334.01	1.59	2.67
18	9	13	52	56.30	1957.10	7035.80	49.85	49	215.80	5138.57	1.58	2.69
19	9	13	59	2.10	1957.10	7035.60	30.82	117	215.36	5008.72	1.58	2.75
20	9	14	2	32.20	1957.00	7035.50	6.93	197	215.06	5127.45	1.58	2.79

File (#)	Day ¹	Time ² Hour	Time Min	Time Sec	Ship Latitude (min)	Ship Longitude (min)	Ship Height (m)	Ship Heading (Degrees)	Ship Bearing (Degrees)	Range (m)	Theta (rd)	Phi (rd)
21	9	14	38	58.60	1957.60	7032.20	51.22	347	137.58	5016.51	1.58	3.88
22	9	14	41	45.50	1957.60	7032.20	45.29	307	137.58	5016.51	1.58	3.88
23	9	14	44	40.20	1957.76	7032.29	2.02	289	136.43	4694.53	1.58	3.90
24	9	14	47	11.60	1957.70	7032.45	27.14	265	139.30	4623.36	1.58	3.85
25	9	14	49	45.50	1957.60	7032.54	28.10	214	142.17	4674.57	1.58	3.80
26	9	14	52	18.90	1957.50	7032.50	-6.61	142	142.74	4861.17	1.58	3.79
27	9	15	4	41.70	1958.04	7033.60	-64.40	323	157.64	3136.75	1.59	3.53
28	9	15	7	7.80	1958.10	7033.60	10.35	299	156.50	3026.4	1.59	3.55
29	9	15	10	9.30	1958.00	7033.73	0.19	275	161.08	3124.74	1.59	3.47
30	9	15	18	52.70	1957.78	7033.81	34.47	156	165.67	3474.34	1.59	3.39
31	9	15	45	11.50	1958.80	7033.40	-38.41	292	134.14	2117.26	1.59	3.94
32	9	15	50	59.90	1958.80	7033.40	-33.04	286	134.14	2117.26	1.59	3.94
33	9	15	54	10.40	1958.80	7033.40	-31.08	331	134.14	2117.26	1.59	3.94
34	9	15	57	36.80	1958.80	7033.40	-27.43	348	134.14	2117.26	1.59	3.94
35	9	16	1	19.90	1958.80	7033.40	-27.65	14	134.14	2117.26	1.59	3.94
36	9	16	3	58.20	1958.90	7033.31	-11.60	62	127.83	2097.62	1.59	4.05
37	9	16	20	54.90	1959.10	7033.80	40.00	297	135.86	1284.37	1.61	3.91
38	9	16	23	29.70	1959.10	7033.80	37.80	335	135.86	1284.37	1.61	3.91
39	9	16	26	18.50	1959.10	7033.80	35.15	349	135.86	1284.37	1.61	3.91
40	9	16	28	21.30	1959.18	7033.77	1.38	5	130.13	1211.72	1.61	4.01
41	9	16	31	29.20	1959.20	7033.70	-20.76	56	124.97	1280.12	1.61	4.10

File (#)	Day ¹	Time ² Hour	Time Min	Time Sec	Ship Latitude (min)	Ship Longitude (min)	Ship Height (m)	Ship Heading (Degrees)	Ship Bearing (Degrees)	Range (m)	Theta (rd)	Phi (rd)
42	9	16	33	35.70	1959.20	7033.70	-19.80	98	124.97	1280.12	1.61	4.10
43	9	16	51	19.50	1959.60	7034.10	2.59	354	147.32	421.01	1.69	3.71
44	9	16	53	46.10	1959.60	7034.10	2.51	17	147.32	421.01	1.69	3.71
45	9	16	56	3.30	1959.67	7034.10	5.87	128	228.02	444.74	1.68	2.25
46	9	16	58	7.40	1959.80	7033.99	9.33	176	244.78	694.26	1.64	2.01
47	9	17	0	53.60	1959.80	7033.90	14.08	228	239.62	821.55	1.63	2.10
48	9	17	14	5.90	1959.45	7034.30	-18.80	98	158.22	299.18	1.74	3.52
49	9	17	16	27.50	1959.45	7034.30	-14.58	106	158.22	299.18	1.74	3.52
50	9	17	31	8.30	1959.40	7034.40	-19.44	68	186.88	373.21	1.71	3.02
51	9	17	33	55.40	1959.40	7034.40	-22.65	114	186.88	373.21	1.71	3.02
52	9	17	43	32.20	1959.20	7034.80	-5.37	26	221.85	998.52	1.62	2.41
53	9	17	45	56.50	1959.20	7034.80	-4.48	44	221.85	998.52	1.62	2.41
54	9	17	48	54.10	1959.20	7034.80	-5.31	52	221.85	998.52	1.62	2.41
55	9	17	51	22.70	1959.20	7034.80	4.06	86	221.85	998.52	1.62	2.41
56	9	17	53	41.40	1959.20	7034.80	-2.23	115	229.13	998.52	1.62	2.41
57	9	17	55	41.90	1959.20	7034.80	-0.71	148	221.85	998.52	1.62	2.41
58	10	8	10	21.60	1959.50	7034.14	7.11	262	116.94	408.31	1.69	4.24
59	10	8	17	29.20	1959.50	7034.20	7.15	284	124.97	322.6	1.73	4.10
60	10	8	19	58.00	1959.50	7034.20	6.88	306	124.97	322.6	1.73	4.10
61	10	8	21	58.20	1959.50	7034.20	6.18	320	124.97	322.6	1.73	4.10
62	10	8	24	31.30	1959.50	7034.20	6.13	342	124.97	322.6	1.73	4.10

File (#)	Day ¹	Time ² Hour	Time Min	Time Sec	Ship Latitude (min)	Ship Longitude (min)	Ship Height (m)	Ship Heading (Degrees)	Ship Bearing (Degrees)	Range (m)	Theta (rd)	Phi (rd)
63	10	8	27	25.80	1959.50	7034.20	7.25	352	124.97	322.6	1.73	4.10
64	10	8	30	9.90	1959.50	7034.18	6.61	5	122.10	344.76	1.72	4.15
65	10	8	34	44.00	1959.50	7034.11	5.28	35	114.65	441.88	1.68	4.28
66	10	8	36	42.80	1959.50	7034.10	5.99	48	113.50	459.93	1.68	4.30
67	10	8	39	3.20	1959.50	7034.10	5.90	77	113.50	459.93	1.68	4.30
68	10	8	41	5.40	1959.50	7034.10	6.04	94	113.50	459.93	1.68	4.30
69	10	8	49	37.30	1959.10	7033.70	5.29	327	131.27	1395.36	1.61	3.99
70	10	8	51	45.30	1959.10	7033.70	-4.36	8	131.27	1395.36	1.61	3.99

1 April 1996

2 Local time

APPENDIX F

SHIP SKIN TEMPERATURE

Description :

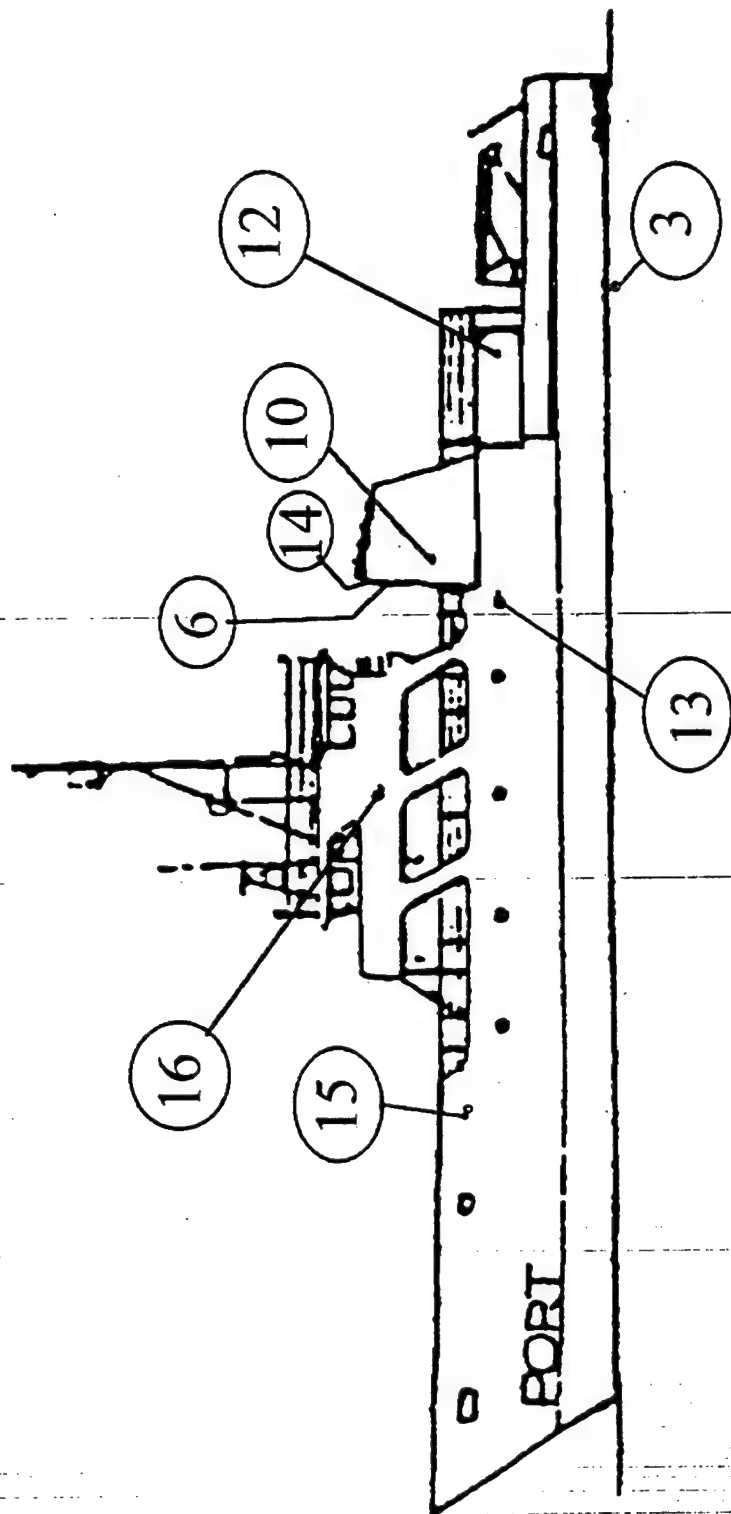
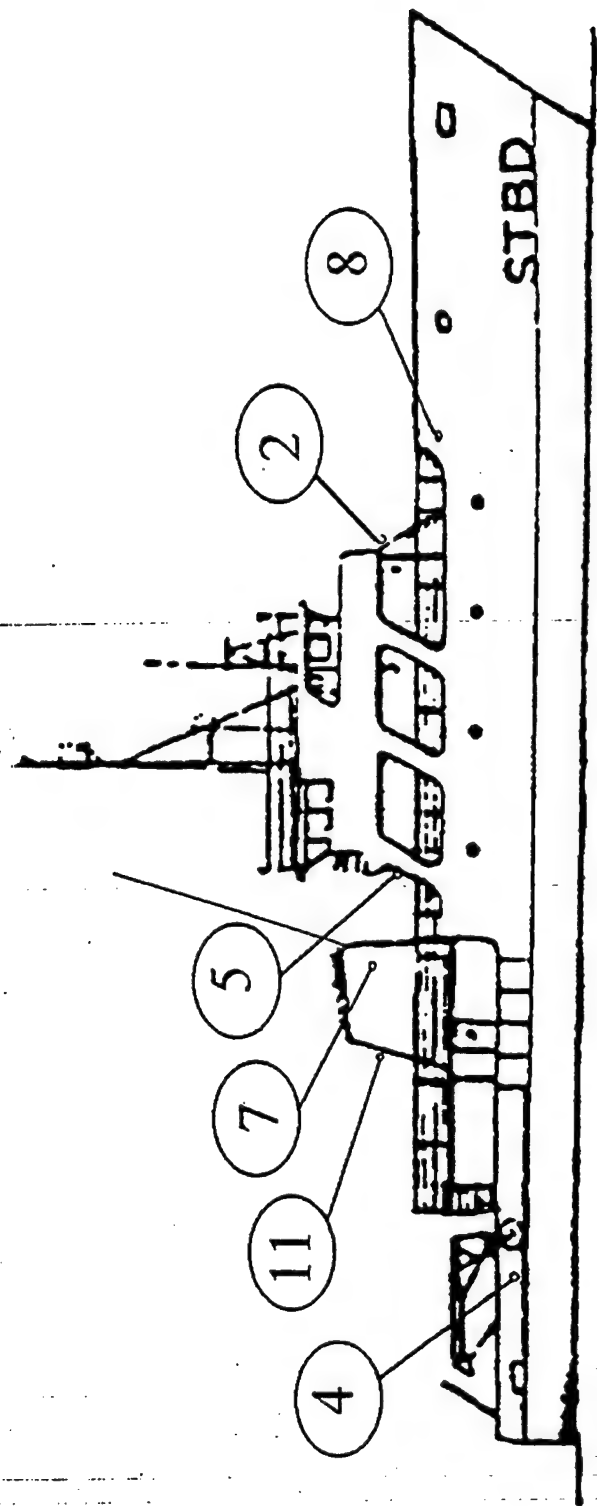
This Appendix presents the position of the thermistors used to measure the ship skin temperature during the experiment. It also presents the format used to store the skin temperature data.

Conditions :

The data was collected by the NPS-NACIT group using 16 thermistors in different positions on the ship surfaces.

Notes :

The first column of the skin temperature data is the elapsed time in seconds from the initial recording time. This initial time is recorded at the top of the file.



SKIN TEMPERATURE DATA FORMAT

april9.1

Mon,Day,Year= 4 9 1996

Hour,Min,Sec= 20 8 27

volts,istart,istop,nsam,iref 1.49939 1 16 100 1

763707 25.001 14.458 17.209 13.710 14.943 16.570 13.946 14.468 25.001 15.562 14.130

31.901 15.310 27.986 15.783 15.153

763727 25.001 14.451 17.108 13.704 14.938 16.585 13.948 14.457 25.001 15.561 14.115

31.826 15.315 27.927 15.780 15.149

763747 25.001 14.448 17.189 13.692 14.928 16.573 13.952 14.463 25.001 15.553 14.110

31.801 15.299 27.878 15.776 15.148

763767 25.001 14.435 17.225 13.679 14.922 16.579 13.944 14.450 25.001 15.547 14.099

31.789 15.295 27.852 15.771 15.141

763787 25.001 14.424 17.226 13.666 14.916 16.584 13.927 14.436 25.001 15.539 14.089

31.769 15.311 27.839 15.769 15.148

763807 25.001 14.422 17.225 13.660 14.911 16.591 13.922 14.425 25.001 15.546 14.084

31.744 15.308 27.816 15.769 15.134

763827 25.001 14.420 17.226 13.649 14.908 16.599 13.922 14.411 25.001 15.537 14.071

31.701 15.285 27.814 15.766 15.135

763847 25.001 14.420 17.221 13.650 14.907 16.608 13.922 14.405 25.001 15.550 14.066

31.628 15.266 27.744 15.764 15.129

763867 = ELAPSED TIME IN SECONDS FROM INITIAL TIME

25.001 14.417 17.224 13.648 14.905 16.610 13.920 14.412 25.001 15.562 14.070 31.528

15.233 27.655 15.757 15.129 = TEMPERATURE FROM EACH THERMISTOR IN C

APPENDIX G

AGA 780 LABORATORY CALIBRATION CURVES

Description :

This Appendix presents the laboratory calibration of the camera.

Conditions :

The calibration was done in MAR/21/96 by E.C. Crittenden for the NOSC LW Head with internal polarizers.

Notes :

Constant conversion for use in CEDIP or CATS software is provided.

Refer to the AGA780 manual [Ref. 8] for further information.

The calibrations is done for each filter setting by recording the thermal level measured of a blackbody for a set of different temperatures.

The calibration curve is then obtained by a curve fitting process. The equation used for the curve fitting has a set of constants. Depending on the acquisition software (AGEMA-CATS or CEDIP PTRWIN), a different set of constants is determined by the curve fitting process. In this Appendix are presented both sets of constants as well as the conversion equations.

Calibration of the NOSC LW Head with internal polarizers.

3/21/96, by E.C. Crittenden.

Using CATS calibration constants.

The curves and data are in "Split Field" notebook (green hardback)

Copies are included with this.

CATS constants are A, B, OS and C, with C always = 1.

CEDIP constants are R, B, V, e, and F with F always = 1.

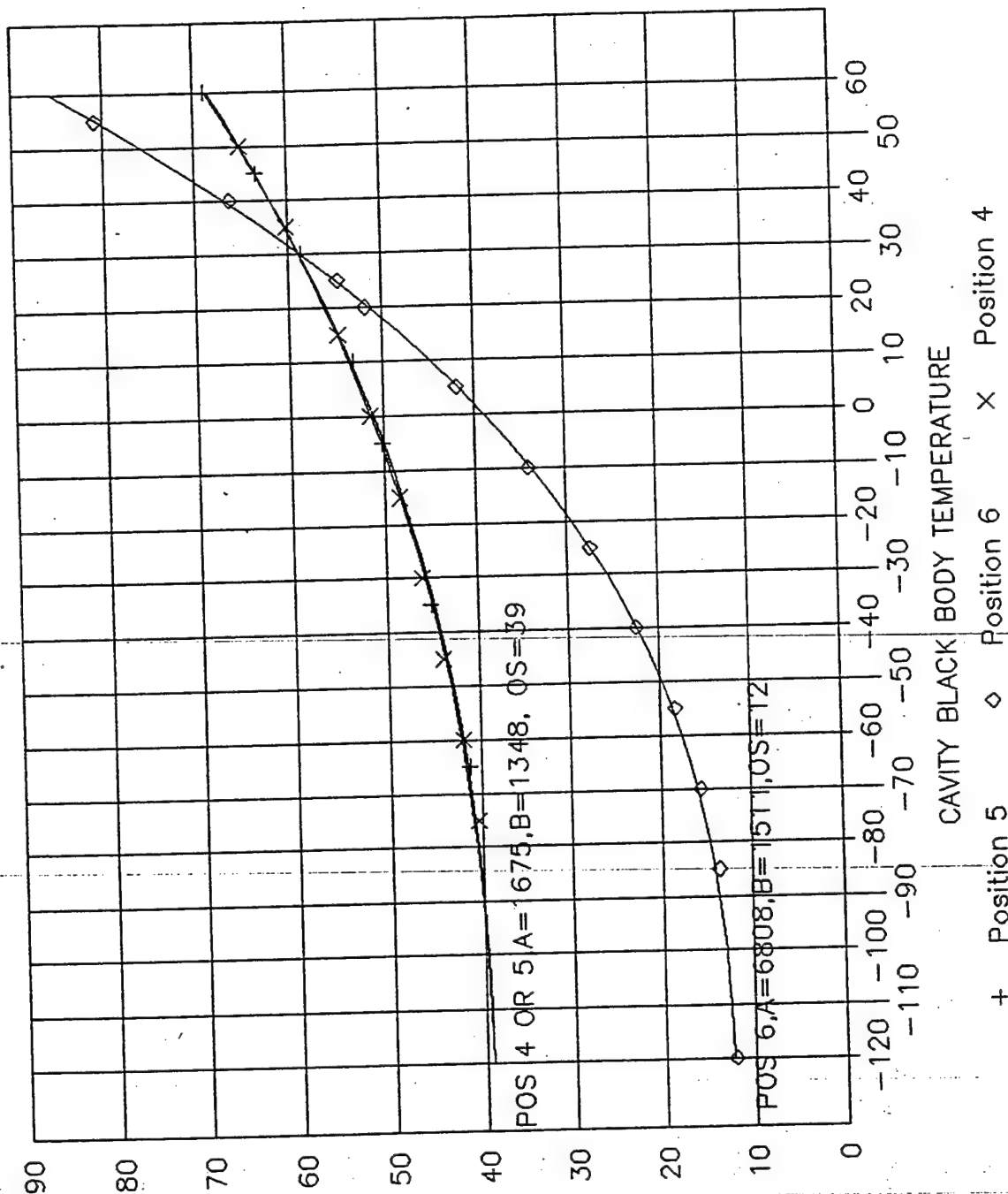
The constants obtained are;

Pos	A	B	OS
4	1675	1348	39
5	1675	1348	39
6	6808	1511	12

The corresponding values for the CEDIP constants are obtained
from the equations on the following page.

NRAD (NOSC) Head. LW

Internal Polarizers, 3/21/96



SUMMARY OF VALUES TO ENTER IN CEDIP:

Numerical values below are examples:

A = 5708 From AGEMA calibration curve fit

B = 1447 CEDIP B = AGEMA B

F = 1 Almost always

V = 293 Called "Background Temp". This can be arbitrarily chosen, but will change e and hence R. Set V to 273 + the temp in C. most important in the image.

OS = 10.4 OS from AGEMA calibration

e = 0.80 Calc. from formula at right →
[Two decimal places can be entered in CEDIP]

R = 7149 R = A/e

OS = 10.4 Calc. as a check, with formula at right →

AGEMA Thermal Level (TL):

[C= 1 usually]

$$[TL] = \frac{A}{C \cdot \exp(B/T) - 1} + (OS)$$

CEDIP Thermal Level (UI):

[F = 1 usually]

$$[UI] = e \cdot \frac{R}{\exp(B/T) - F} + (1-e) \cdot \frac{R}{\exp(B/V) - F}$$

$$e = \frac{A}{OS \cdot [\exp(B/V) - F] + A} = 0.7884$$

$$OS = \frac{1 - e}{e} \cdot \frac{A}{\exp(B/V) - F} = 10.40$$

ENTERING CALIBRATION CONSTANTS:

R, B, and F are set in CEDIP under "Measure, Calibration, New, (or Open)"

F should normally be left at unity.

e is set in CEDIP under "Measure, Emissivity"

V is set in CEDIP, under "Measure, Background"

VERIFYING AND CORRECTING THE OFFSET:

To verify the offset, measure the temperature of a black body at the temperature chosen for V.

If an incorrect T is obtained, increasing V increases the offset (slides the whole curve uniformly upward)

Increasing V will lower the observed temperature.

VERIFYING AND CORRECTING THE CALIBRATION CURVE SLOPE:

This correction should be rarely needed.

Verify a temperature above, or below, the temperature chosen for V.

If that T is incorrect, increasing e increases the calibration curve slope, rotating about the T = V value.

Increasing e also lowers the offset, corresponding to rotation of the curve about T = V. This offset

lowers the curve to compensate for the new slope, so the curve still passes through the point at T = V.

APPENDIX H

ANALYSIS PROGRAMS

1. LIST OF THE ANALYSIS PROGRAMS

Description :

This Appendix presents a table describing the type and the objective of all analysis programs written in IDL.

Conditions :

None.

Notes :

None.

TABLE H.1
ANALYSIS PROGRAMS

Name	Type	Objective
Ache	Auxiliary	Calculate the sum or maximum or minimum or average values of a matrix elements by column, line and general
Angular	Executive	Calculate aspect angle results for the ship and the model's main planes
Areagen	Executive	Find the edges of the analysis "box" for each frame
Aspect	Executive	Estimate ship aspect angle
Basegen	Data Manager	Convert *.PTW files to *.PTE files
Basemet	Data Manager	Convert original metoc data to metdata.pte format
Calcule	Data Manager	Prepare data and call executive programs to get analysis results
Calibre	Auxiliary	Calibrate the imagee
Compare	Auxiliary	Compare model and ship image statistics
Contraste	Executive	Calculate contrast results
Deltat	Auxiliary	Calculate elapsed time
Desenhe	Auxiliary	Show a picture with a given size and window numbers
Diff	Auxiliary	Calculate the differences between elements of a vector
Draw_md1	Auxiliary	Draw the ship model
Elements	Auxiliary	Generate "mask matrices" (1 for the object pixels and 0 otherwise) for : ship, sea, sky, ship above horizon and ship below horizon.
Escreva	Data Manager	Write data into basic files
Get_box	Auxiliary	Create a image submatrix based on its edges
Horizonte	Executive	Find the horizon line equation for each frame
Hotspot	Executive	Find the hotspot thermal value and its position for each frame
Inclua	Data Manager	Include data into the result matrix
Leia_pte	Auxiliary	Read variables from basic files
Linespace	Auxiliary	Create a vector of n numbers linearly spaced between two given values
Meteoro	Data Manager	Interpolate meteorological data to each frame time
Modele	Auxiliary	Show a scaled ship model as surfaces or wireframe. Shows a ship model demonstration . Optionally the model can be drawn over a given image.
Norma	Auxiliary	Normalize the image
Pontes	Data Manager	Run analysis programs in correct sequence

Name	Type	Objective
Position	Executive	Calculate the ship position in the camera coordinate system.
Rectang ¹	Auxiliary	Draw a rectangle given the center and the sides in device coordinates
Sel_box	Auxiliary	Select a box interactively from an image using the mouse
Skintemp	Data Manager	Interpolate skin temp data to each frame time
Statist	Auxiliary	Calculate statistics of an image
Tau	Data Manager	Generate a venet.pte matrix
Thermal	Auxiliary	Calculate calibrated thermal level
Threshold	Auxiliary	Find the threshold value for the ship in a normalized image
Timedata	Data Manager	Find initial recording time for each basic file
Translat	Auxiliary	Translate the reference point to draw the ship model

1. This program is based on "draw_box.pro" program created by Mr. Jerry Lentz - Physics Department / 1994.

2. HOTSPOT TRACKING

Description :

This Appendix presents figures showing the hotspot program tracking feature.

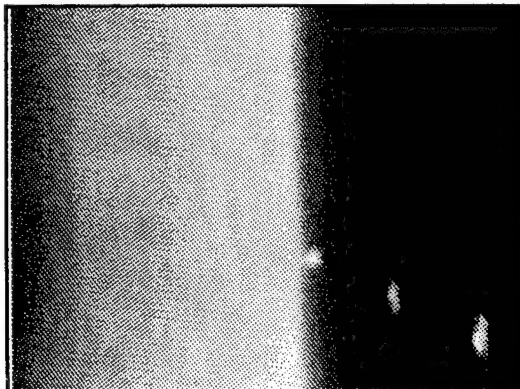
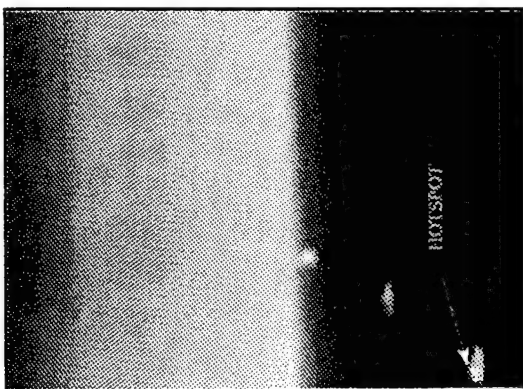
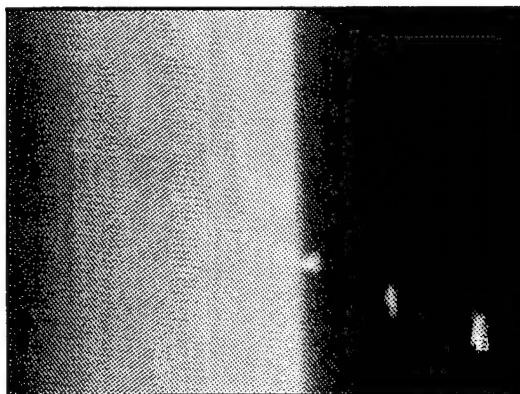
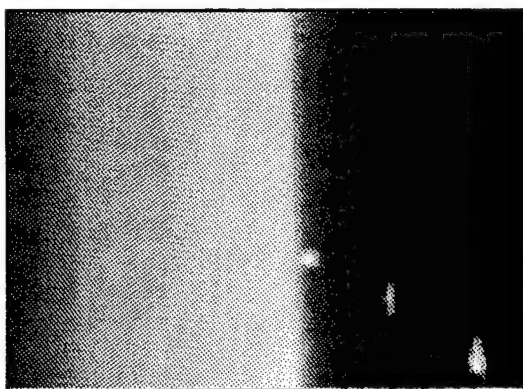
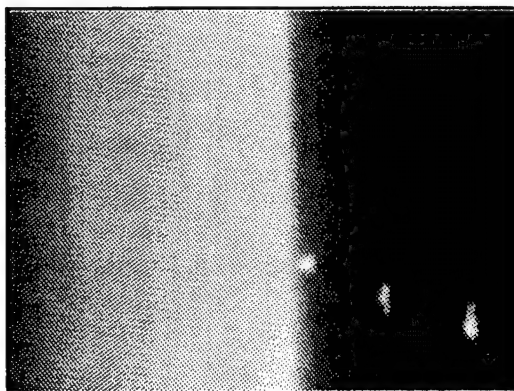
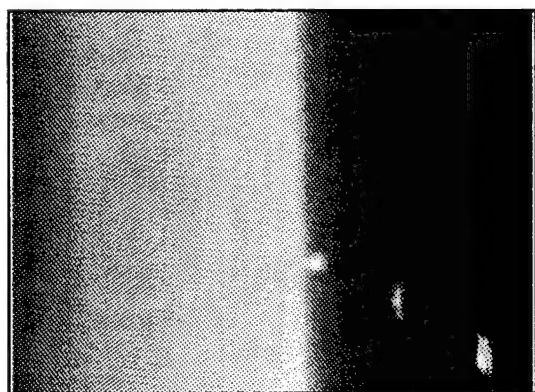
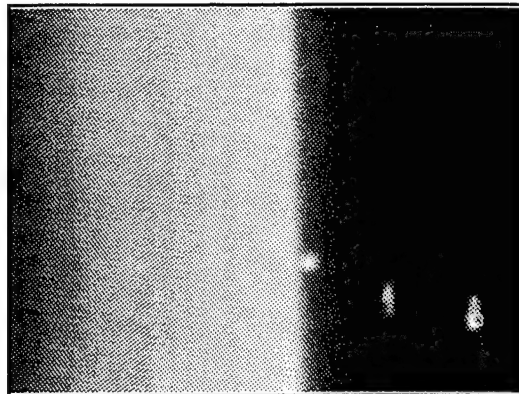
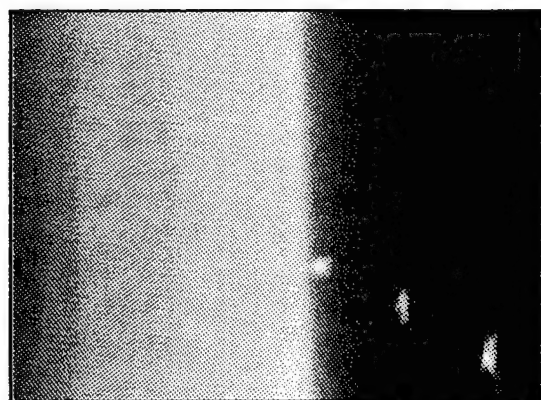
Conditions :

Sample extracted from BASE18.PTE unpolarized case. The R/V POINT SUR in this file is at range 5,134m, motionless near to the horizon line. However, in order to show the hotspot tracking capability in a cluttered scene (3 targets in this case), a small boat was chosen to be tracked on its hotspot. Therefore, in this Appendix, a sequence of 8 images is presented showing the tracking of a small boat moving from left to right at the bottom of the images.

Notes :

The hotspot position is indicated by a small square superimposed to the target image. The image sequence shows the hotspot tracking capability of the program HOTSPOT.PRO and possibility of using a cluttered image for analysis without losing the hotspot correctness.

HOTSPOT TRACKING IN A CLUTTERED SCENE (BASE18.PTE)



3. BOX POSITIONING

Description :

This Appendix presents figures showing the analysis box positioning.

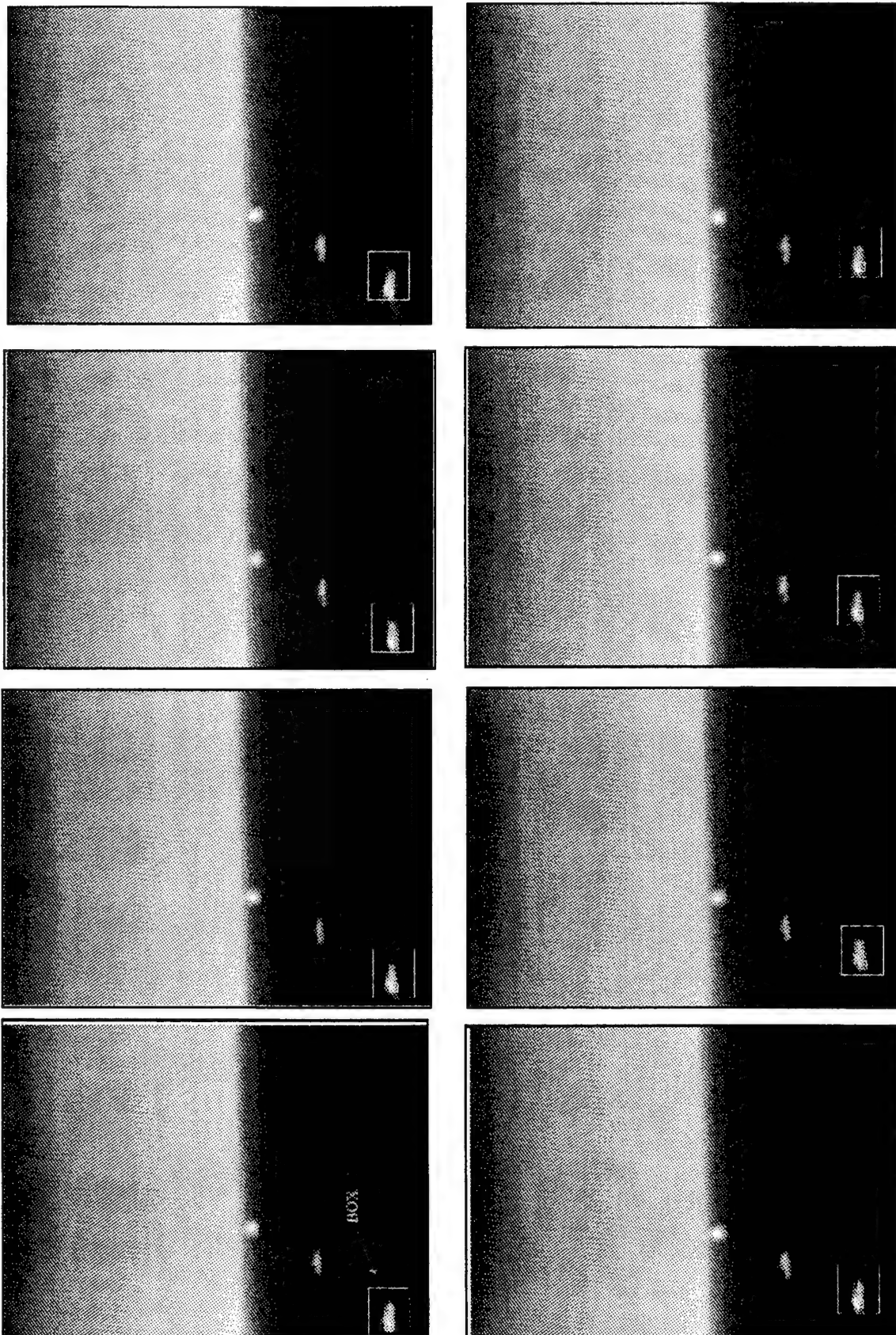
Conditions :

Sample extracted from BASE18.PTE unpolarized case. The R/V POINT SUR in this file is at range 5,134m, motionless near to the horizon line. However, in order to show the box positioning capability in a cluttered scene (3 targets in this case), a small moving boat was chosen to be the target. Therefore, in this Appendix, a sequence of 8 images is presented showing the box positioning around a small boat moving from left to right at the bottom of the images.

Notes :

The analysis box is indicated by a square around the target image. The box positioning uses the hotspot position as its reference.

BOX POSITIONING



4. IMAGE SAMPLE

Description :

This Appendix presents one of the 5,508 analysed images. This is the frame #0 from the unpolarized case in BASE01.PTE file (file #01).

Conditions :

From tables in Appendix E.2:

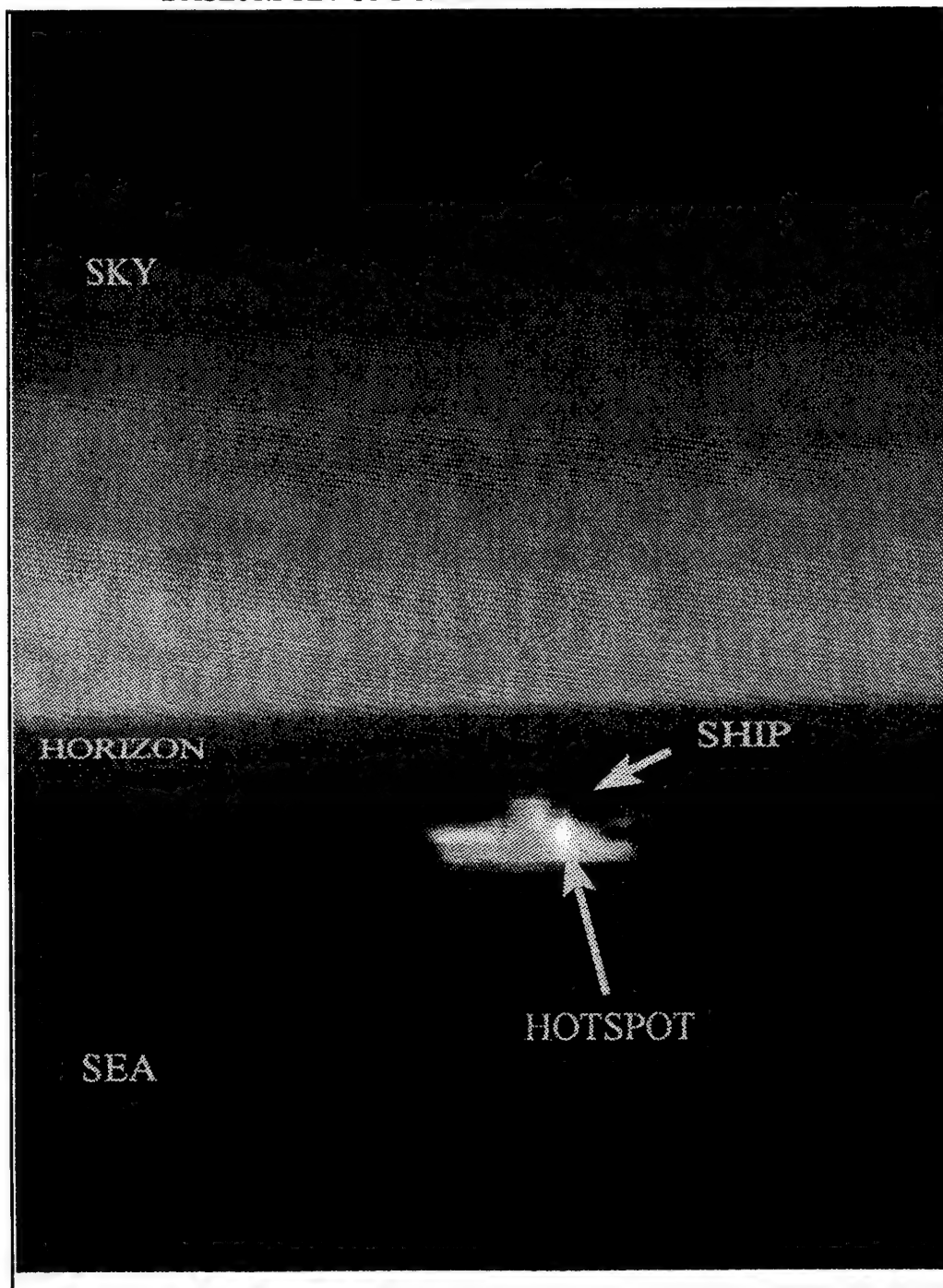
File #01 :

Day : April 9 1996
Time : 44,018 seconds (elapsed time from 00h:00min local time = 12h13min38sec)
Latitude : 1959.20 minutes
Longitude : 7034.80 minutes
Ship GPS Antenna Height : -27.01 m
Air Temperature : 15.30 C
Relative Humidity : 72 %
Air Pressure : 1018.25 mb
Wind Speed : 6.5 m/s
Sea Surface Temperature : 18.55 C
Range : 998.52 m
Theta : 1.62 rad
Phi : 2.41 rad
Heading : 99 degrees
Bearing : 221.85 degrees
Atmospheric Transmittance : 0.82

Notes :

Conditions defined in Appendix E.2.

BASE01.PTE / UNPOLARIZED CASE / FRAME #0



5. COMBINED IMAGE / SURFACE / CONTOUR PLOT

Description :

This Appendix presents one of the 5,508 analysed images. This is the frame #0 from the unpolarized case in BASE01.PTE file (file #01). The figure is in "show3" IDL format. This format shows a combined picture with image, surface and contour plots.

Conditions :

From tables in Appendix E.2:

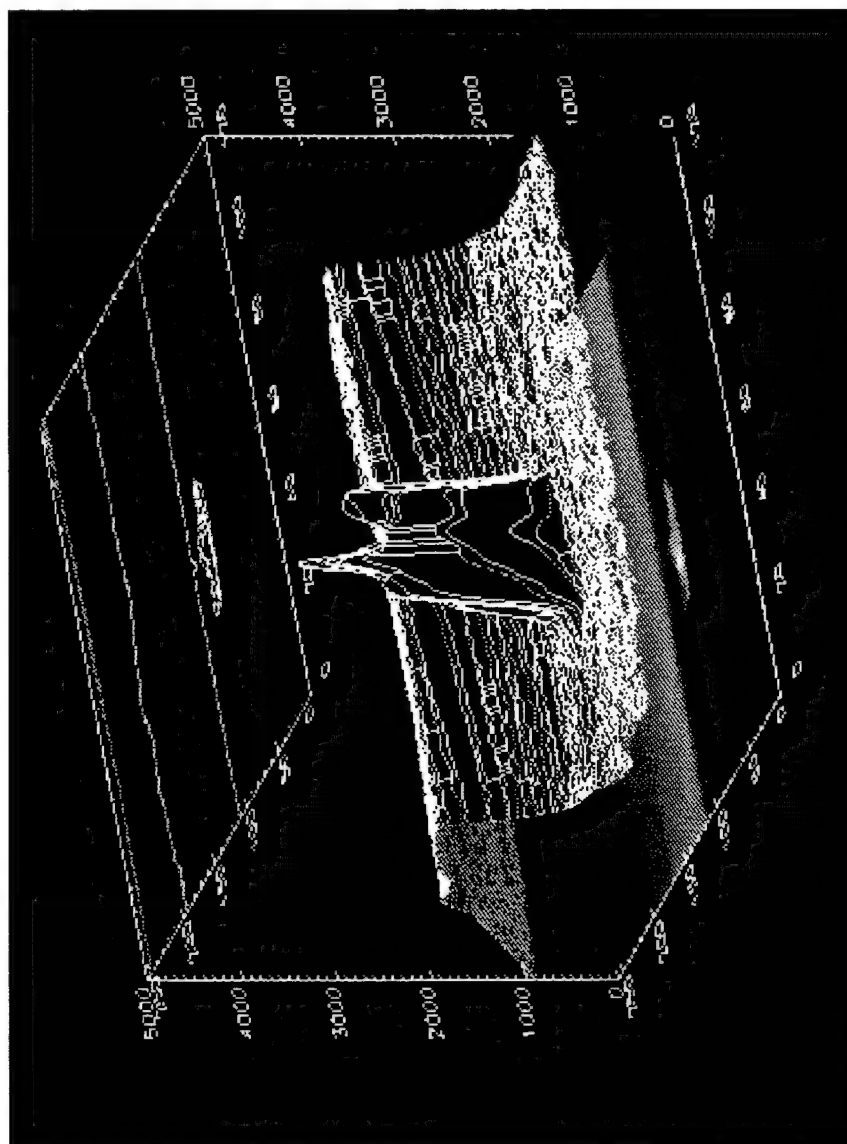
File #01 :

Day : April 9 1996
Time : 44,018 seconds (elapsed time from 00h:00min local time = 12h13min38sec)
Latitude : 1959.20 minutes
Longitude : 7034.80 minutes
Ship GPS Antenna Height : -27.01 m
Air Temperature : 15.30 C
Relative Humidity : 72 %
Air Pressure : 1018.25 mb
Wind Speed : 6.5 m/s
Sea Surface Temperature : 18.55 C
Range : 998.52 m
Theta : 1.62 rad
Phi : 2.41 rad
Heading : 99 degrees
Bearing : 221.85 degrees
Atmospheric Transmittance : 0.82

Notes :

Conditions defined in Appendix E.2.

BASE01.PTE / UNPOLARIZED CASE / FRAME #0



6. SURFACE PLOT

Description :

This Appendix presents one of the 5,508 analysed images. This is the frame #0 from the unpolarized case in BASE01.PTE file (file #01). The image is shown in surface plot.

Conditions :

From tables in Appendix E.2:

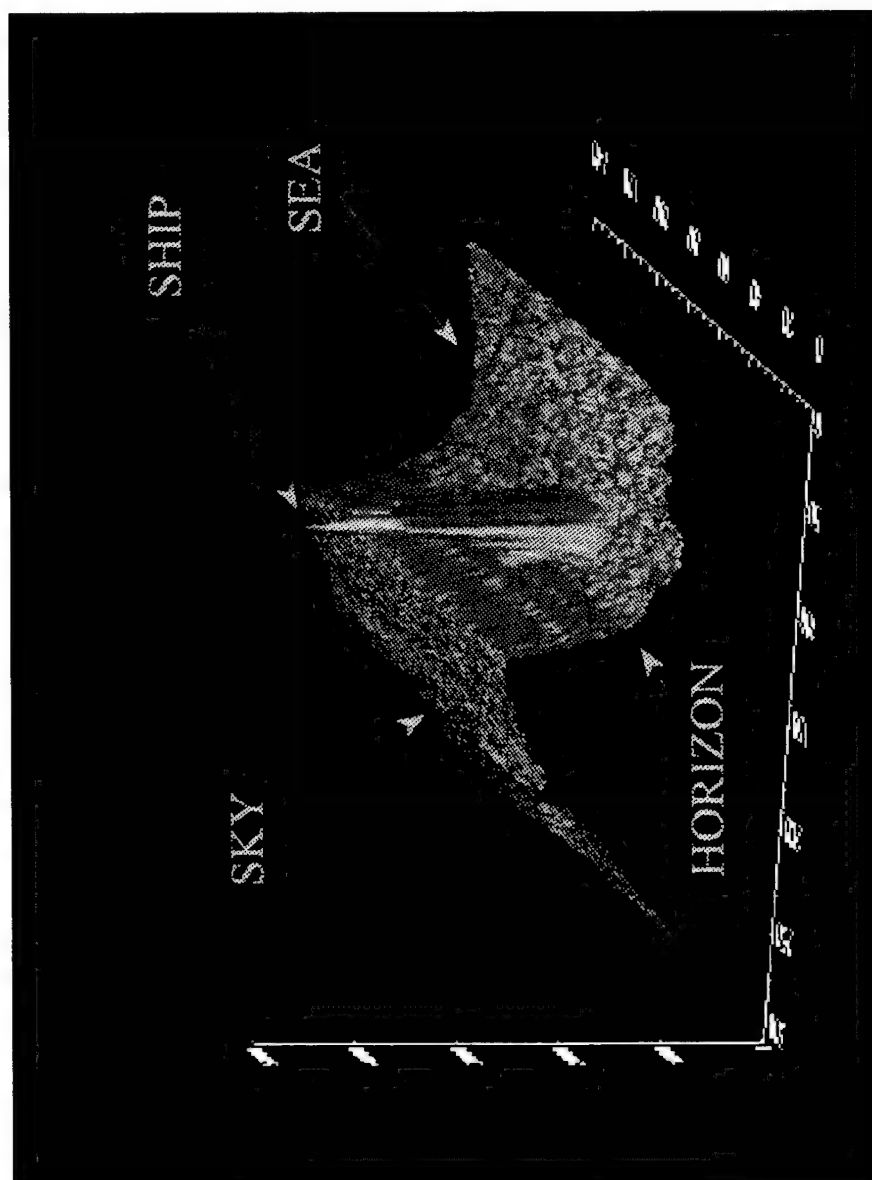
File #01 :

Day : April 9 1996
Time : 44,018 seconds (elapsed time from 00h:00min local time = 12h13min38sec)
Latitude : 1959.20 minutes
Longitude : 7034.80 minutes
Ship GPS Antenna Height : -27.01 m
Air Temperature : 15.30 C
Relative Humidity : 72 %
Air Pressure : 1018.25 mb
Wind Speed : 6.5 m/s
Sea Surface Temperature : 18.55 C
Range : 998.52 m
Theta : 1.62 rad
Phi : 2.41 rad
Heading : 99 degrees
Bearing : 221.85 degrees
Atmospheric Transmittance : 0.82

Notes :

Conditions defined in Appendix E.2.

Main image elements are indicated in the picture. Observe the characteristic "wall shape" at the horizon line.



7. NORMALIZATION : PHASE 1

Description :

This Appendix presents one of the 5,508 analysed images during the normalization process used by the THRESHOLD.PRO program. This is the frame #0 from the unpolarized case in BASE01.PTE file (file #01). The image is shown in surface plot.

Conditions :

From tables in Appendix E.2:

File #01 :

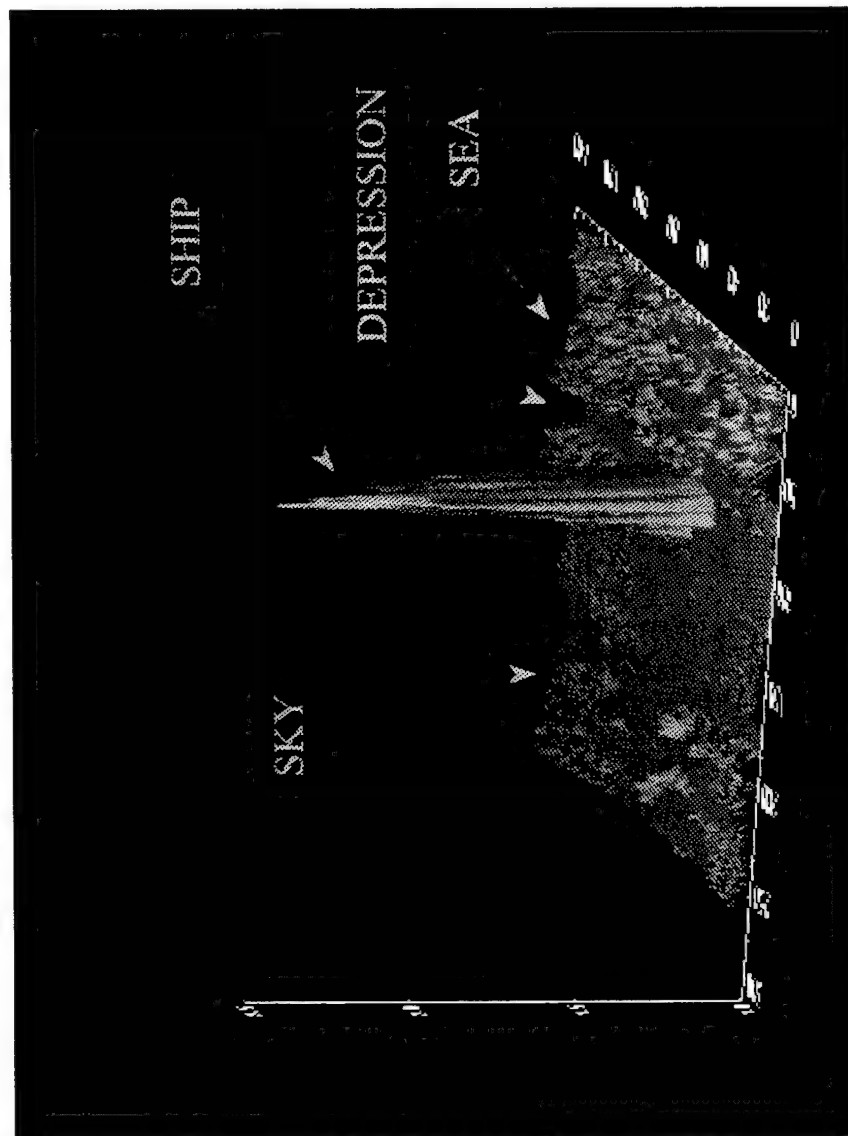
Day : April 9 1996
Time : 44,018 seconds (elapsed time from 00h:00min local time = 12h13min38sec)
Latitude : 1959.20 minutes
Longitude : 7034.80 minutes
Ship GPS Antenna Height : -27.01 m
Air Temperature : 15.30 C
Relative Humidity : 72 %
Air Pressure : 1018.25 mb
Wind Speed : 6.5 m/s
Sea Surface Temperature : 18.55 C
Range : 998.52 m
Theta : 1.62 rad
Phi : 2.41 rad
Heading : 99 degrees
Bearing : 221.85 degrees
Atmospheric Transmittance : 0.82

Notes :

Conditions defined in Appendix E.2.

The main elements of the image are indicated. Compare with the surface plot of the same image before the normalization (Appendix H.6). After normalization (phase 1) the characteristic "elevation" seen in the sky thermal level surface plot disappeared. The depression caused by the target presence is visible. "Noise" level at the sky and sea image components are still significant.

BASE01.PTE / UNPOLARIZED CASE / FRAME #0 / NORMALIZATION : PHASE 1



8. NORMALIZATION : PHASE 2

Description :

This Appendix presents one of the 5,508 analysed images during the normalization process (phase 2) used by the THRESHOLD.PRO program. This is the frame #0 from the unpolarized case in BASE01.PTE file (file #01). The image is shown in surface plot.

Conditions :

From tables in Appendix E.2:

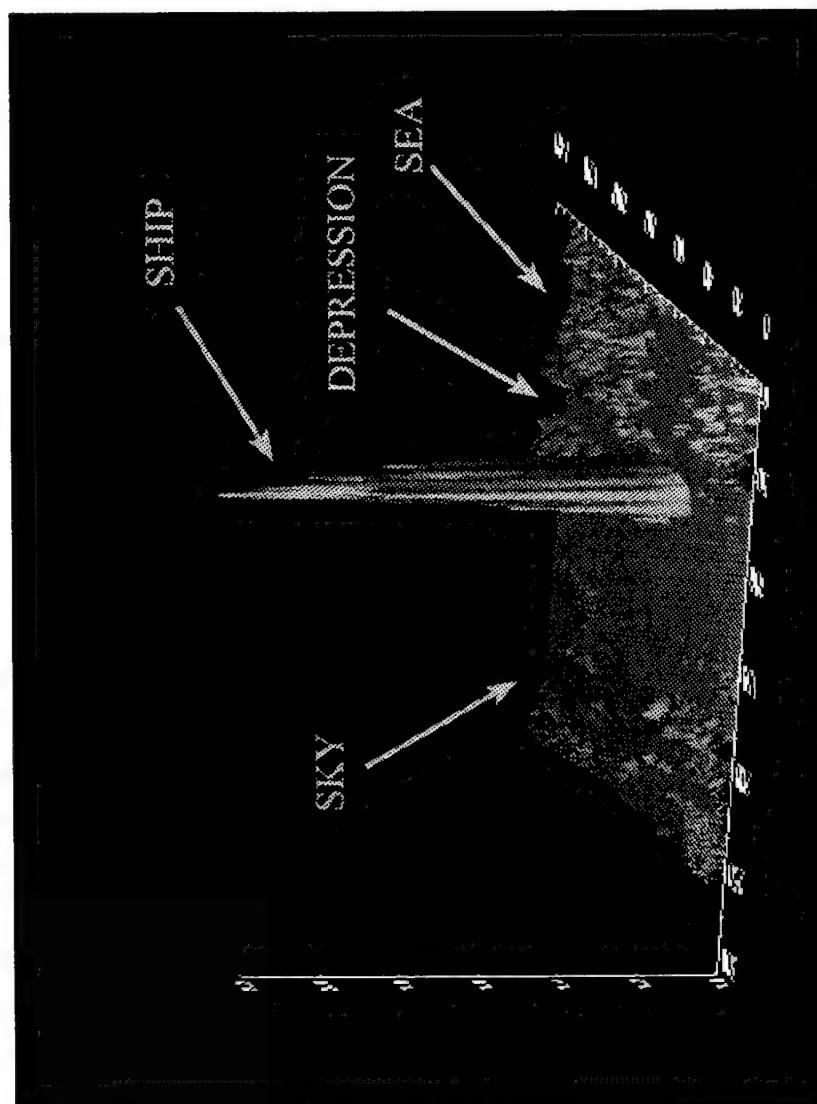
File #01 :

Day : April 9 1996
Time : 44,018 seconds (elapsed time from 00h:00min local time = 12h13min38sec)
Latitude : 1959.20 minutes
Longitude : 7034.80 minutes
Ship GPS Antenna Height : -27.01 m
Air Temperature : 15.30 C
Relative Humidity : 72 %
Air Pressure : 1018.25 mb
Wind Speed : 6.5 m/s
Sea Surface Temperature : 18.55 C
Range : 998.52 m
Theta : 1.62 rad
Phi : 2.41 rad
Heading : 99 degrees
Bearing : 221.85 degrees
Atmospheric Transmittance : 0.82

Notes :

Conditions defined in Appendix E.2.

The main elements of the image are indicated. Compare with the surface plot of the normalization phase 1 (Appendix H.7). After normalization (phase 2) the "noise" level at the sky and sea image components are reduced and the background surface is basically flat. The depression caused by the target presence is still visible. The ship is now easily identified and there is no alteration in his shape.



9. IMAGE ELEMENTS

Description :

This Appendix presents one of the 5,508 analysed images during the image elements identification process done by the ELEMENTS.PRO program. This is the frame #0 from the unpolarized case in BASE50.PTE file (file #50). The image is shown in its full version with the hotspot and the analysis box indicated. Below the full image, the analysis box and the main element masks (ship, sea and sky) are shown.

Conditions :

From tables in Appendix E.2:

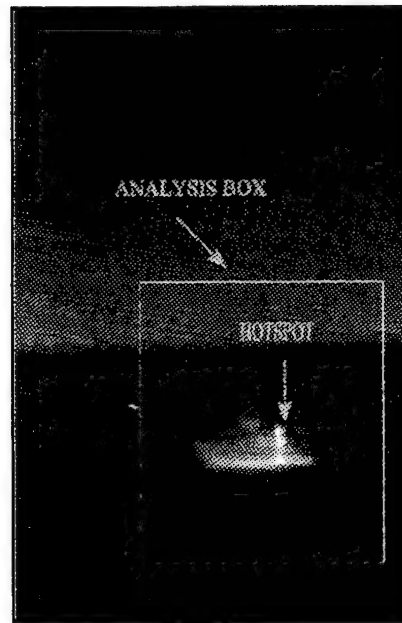
File #50 :

Day : April 9 1996
Time : 62,187.5 seconds (elapsed time from 00h:00min local time = 17h31min8sec)
Latitude : 1959.40 minutes
Longitude : 7034.40 minutes
Ship GPS Antenna Height : -19.44 m
Air Temperature : 15.30 C
Relative Humidity : 69 %
Air Pressure : 1016.40 mb
Wind Speed : 4.0 m/s
Sea Surface Temperature : 16.60 C
Range : 373.21 m
Theta : 1.71 rad
Phi : 3.02 rad
Heading : 68 degrees
Bearing : 186.9 degrees
Atmospheric Transmittance : 0.92

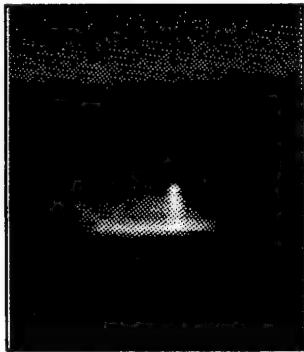
Notes :

The white color in the mask figures (ship, sea and sky) represents pixels with values of 1. The black color means pixel value of zero.

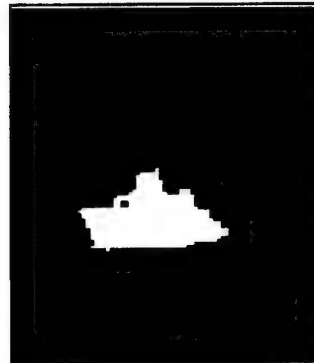
IMAGE ELEMENTS (MASKS)



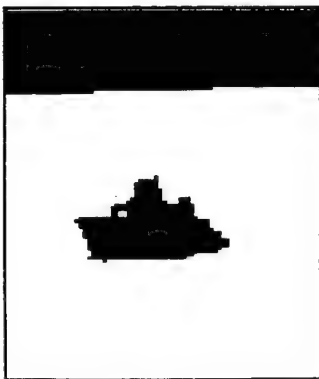
Full Image



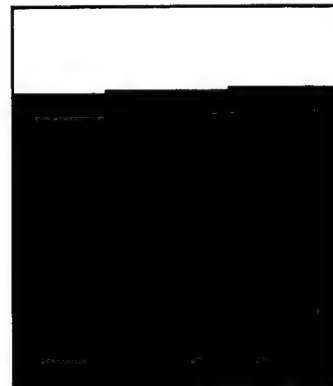
Analysis Box



Ship



Sea



Sky

10. SHIP MODEL

Description :

This Appendix presents the ship model viewed from different angles.

Conditions :

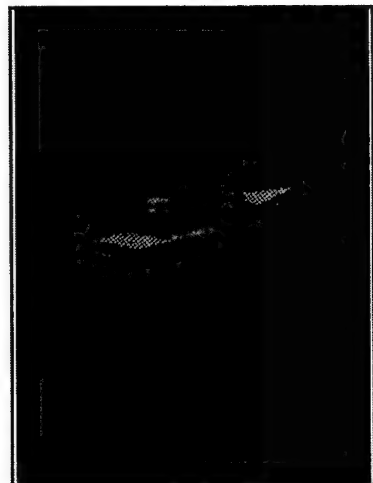
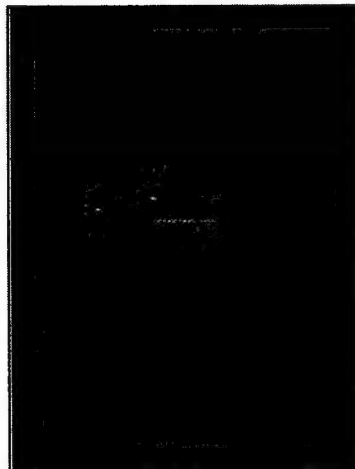
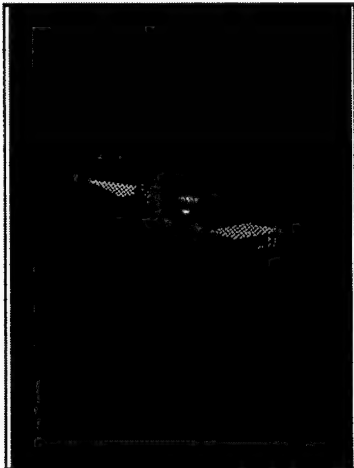
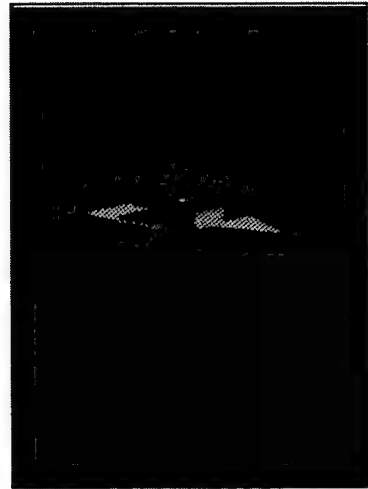
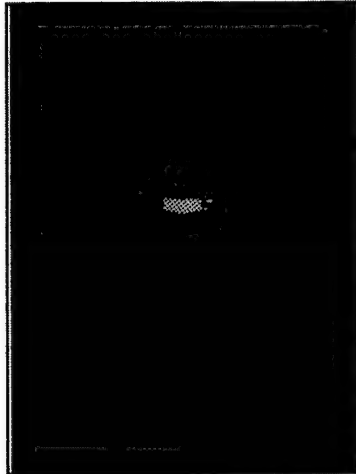
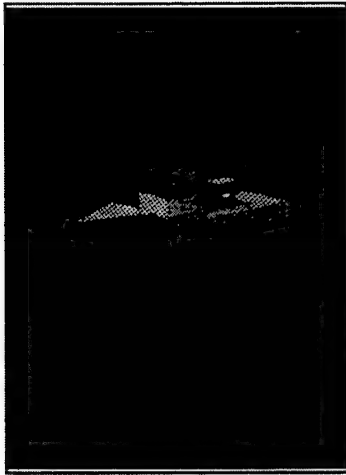
Elevation angle for all picture is 2 degrees.

Starting from the upper left picture, the azimuth angles are: 45, 0, 315, 135, 180 and 225 degrees.

Notes :

None.

SHIP MODEL



11. SHIP MODEL : WIREFRAME MODE

Description :

This Appendix presents the ship model in wireframe mode superimposed to analysis box corresponding to the frame #0 of the unpolarized case of the BASE50.PTE file.

Conditions :

Model elevation and azimuth angle are 2 and 70 degrees respectively.
For the Image, from tables in Appendix E.2:

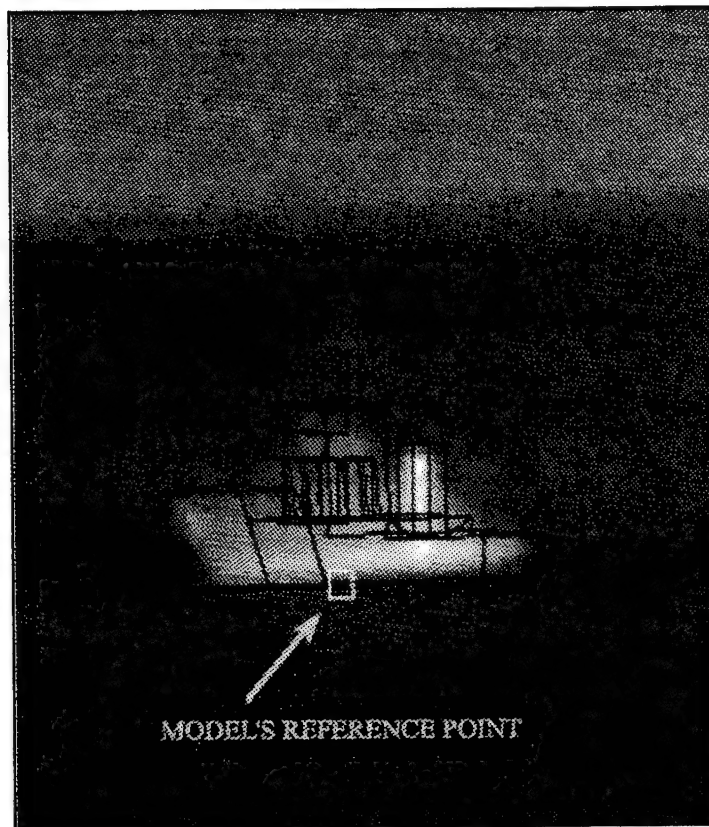
File #50 :

Day : April 9 1996
Time : 62,187.5 seconds (elapsed time from 00h:00min local time = 17h31min8sec)
Latitude : 1959.40 minutes
Longitude : 7034.40 minutes
Ship GPS Antenna Height : -19.44 m
Air Temperature : 15.30 C
Relative Humidity : 69 %
Air Pressure : 1016.40 mb
Wind Speed : 4.0 m/s
Sea Surface Temperature : 16.60 C
Range : 373.21 m
Theta : 1.71 rad
Phi : 3.02 rad
Heading : 68 degrees
Bearing : 186.9 degrees
Atmospheric Transmittance : 0.92

Notes :

Model's reference point is shown in the picture. This point is used to anchor the model to the ship image. It is located in x coordinate of the ship image area centroid and at the average y coordinate of the ship image's bottom line.

WIREFRAME MODE



12. SHIP MODEL'S MAIN PLANES

Description :

This Appendix presents the position of the ship model's main planes.

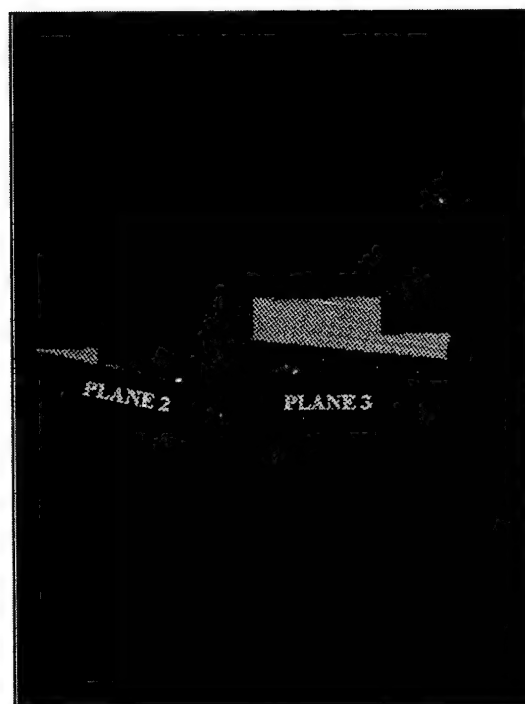
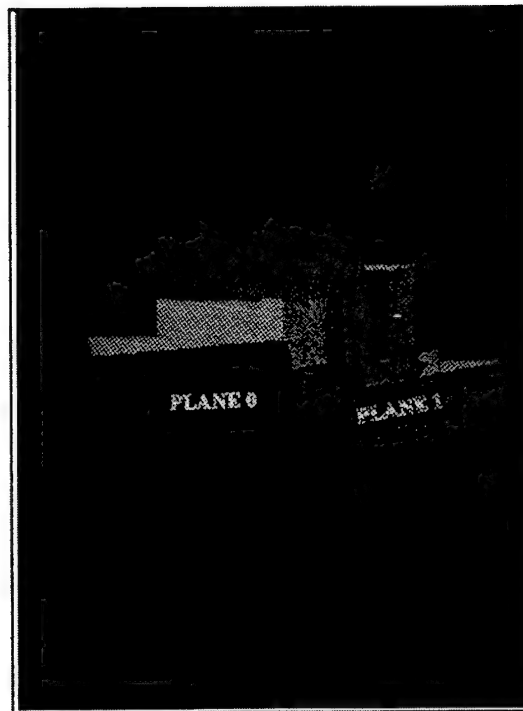
Conditions :

Model elevation angles are 1.5 degree. The azimuth angles are 20 and 340 for the upper and lower pictures respectively.

Notes :

There are 4 main planes considered in the ship model. They are numbered from 0 to 3 and comprise the sides of the hull of the ship model.

MODEL'S MAIN PLANES



13. MASK APPLICATION EXAMPLE

Description :

This Appendix presents an example of the mask application process corresponding to the plane 0 in the analysis box of the frame #0 of the unpolarized case of the BASE50.PTE file. There are 2 pictures in this Appendix.

Conditions :

Model elevation and azimuth angle are 2 and 70 degrees respectively.
For the Image, from tables in Appendix E.2:

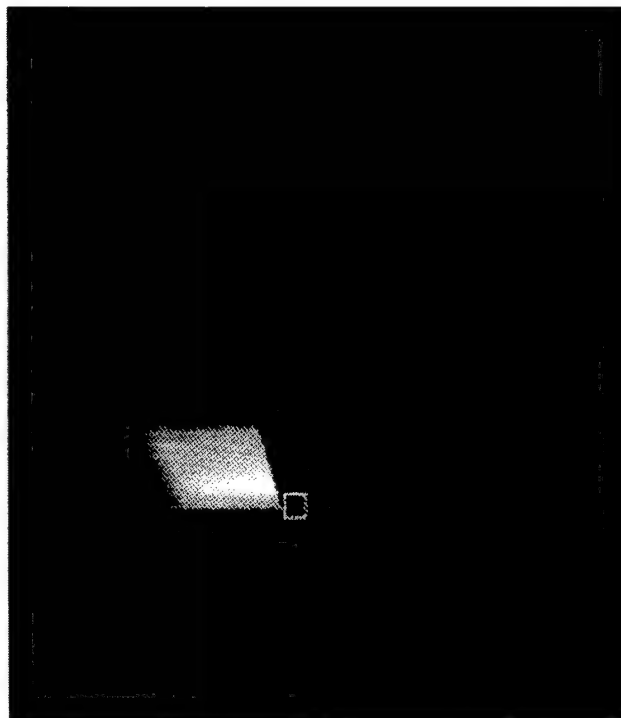
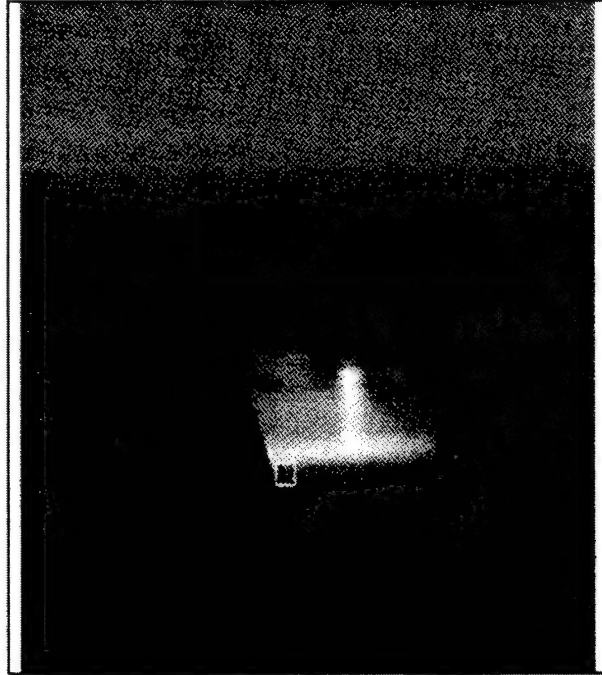
File #50 :

Day : April 9 1996
Time : 62,187.5 seconds (elapsed time from 00h:00min local time = 17h31min8sec)
Latitude : 1959.40 minutes
Longitude : 7034.40 minutes
Ship GPS Antenna Height : -19.44 m
Air Temperature : 15.30 C
Relative Humidity : 69 %
Air Pressure : 1016.40 mb
Wind Speed : 4.0 m/s
Sea Surface Temperature : 16.60 C
Range : 373.21 m
Theta : 1.71 rad
Phi : 3.02 rad
Heading : 68 degrees
Bearing : 186.9 degrees
Atmospheric Transmittance : 0.92

Notes :

The upper picture is plotted just to show the position of the plane 0 in the image. The lower picture shows the real effect of the mask application in extracting the plane 0 corresponding pixels from the ship image. The small square in the picture is the reference point. It is shown in the pictures for better localization. The irregular left edge observed in the lower picture is the consequence of the ship mask application over the plane 0 mask. This application is necessary to avoid computation of the background part in the model plane 0 as if it was part of the ship for contrast calculation. Therefore, only the ship pixels inside the superimposed model's plane 0 are considered for contrast calculation.

MASK APPLICATION



APPENDIX I

RESULT TABLES

1. RESULT MATRIX DESCRIPTION

Description :

Table describing the columns of the result matrices.

Conditions :

None.

Notes :

None

RESULT MATRIX

COLUMN	DESCRIPTION
0	DT : Elapsed Time
1	Hotspot : Thermal Value
2	Hotspot : x Position (data coordinates)
3	Hotspot : y Position (data coordinates)
4	Analysis "Box" : Down Left Corner x Position (data coordinates)
5	Analysis "Box" : Down Left Corner y Position (data coordinates)
6	Analysis "Box" : Up Right Corner x Position (data coordinates)
7	Analysis "Box" : Up Right Corner y Position (data coordinates)
8	Horizon Equation : Linear Coefficient (data coordinates)
9	Horizon Equation : Angular Coefficient (data coordinates)
10	Empty
11	Empty
12	Empty
13	Empty
14	Empty
15	Empty
16	Empty
17	Empty
18	Empty
19	Empty
20	Ship G.P.S. Position : Latitude (minutes)
21	Ship G.P.S. Position : Longitude (minutes)
22	Ship G.P.S. Position : Height (m)
23	Air Temperature (C)
24	Relative Humidity (%)
25	Air Pressure (mb)
26	Wind Speed (m/s)
27	Sea Surface Temperature(C)
28	Camera Position : Latitude (minutes)

COLUMN	DESCRIPTION
29	Camera Position : Longitude (minutes)
30	Camera Position : Height (m)
31	Distance Camera - Ship (m) - Camera Referential
32	Phi : Azimuth Angle (rd) - Camera Referential
33	Theta : Elevation Angle (rd) - Camera Referential
34	Average Atmospheric Transmission
35	Ship Horizontal Aspect Angle (degrees) - as seen from camera position
36	Ship Vertical Aspect Angle (degrees) - as seen from camera position
37	Ship True Heading (degrees)
38	Ship Modeling Reference Point : x Position (device coordinates)
39	Ship Modeling Reference Point : y Position (device coordinates)
40	Average Ship Stack Temperature (C)
41	Ship Skin Temperature : point 1 (C)
42	Ship Skin Temperature : point 2 (C)
43	Ship Skin Temperature : point 3 (C)
44	Ship Skin Temperature : point 4 (C)
45	Ship Skin Temperature : point 5 (C)
46	Ship Skin Temperature : point 6 (C)
47	Ship Skin Temperature : point 7 (C)
48	Ship Skin Temperature : point 8 (C)
49	Ship Skin Temperature : point 9 (C)
50	Ship Skin Temperature : point 10 (C)
51	Ship Skin Temperature : point 11 (C)
52	Ship Skin Temperature : point 12 (C)
53	Ship Skin Temperature : point 13 (C)
54	Ship Skin Temperature : point 14 (C)
55	Ship Skin Temperature : point 15 (C)
56	Ship Skin Temperature : point 16 (C)
57	Empty
58	Empty

COLUMN	DESCRIPTION
60	Contrast Ship x Background
61	Ship : Average Thermal Level
62	Ship : Number of Pixels
63	Background : Average Thermal Level
64	Background : Number of Pixels
65	Contrast Ship Above (above horizon line) x Sky
66	Ship Above : Average Thermal Level
67	Ship Above : Number of Pixels
68	Sky : Average Thermal Level
69	Sky : Number of Pixels
70	Contrast Ship Below (below horizon line) x Sea
71	Ship Below : Average Thermal Level
72	Ship Below : Number of Pixels
73	Sea : Average Thermal Level
74	Sea : Number of Pixels
75	Contrast Plane 0 x Background
76	Plane 0 : Average Thermal level
77	Plane 0 : Number of Pixels
78	Plane 0 : Aspect Angle (degrees)
79	Contrast Plane10 x Background
80	Plane 1 : Average Thermal level
81	Plane 1 : Number of Pixels
82	Plane 1 : Aspect Angle (degrees)
83	Contrast Plane 2 x Background
84	Plane 2 : Average Thermal level
85	Plane 2 : Number of Pixels
86	Plane 2 : Aspect Angle (degrees)
87	Contrast Plane 3 x Background
88	Plane 3 : Average Thermal level
89	Plane 3 : Number of Pixels

COLUMN	DESCRIPTION
90	Plane 3 : Aspect Angle (degrees)
91	Empty
92	Empty
93	Empty
94	Empty
95	Empty
96	Empty
97	Empty
98	Empty
99	Empty

NOTES:

1 . There is one Result Matrix for each polarization case. Therefore, since there are 3 polarization cases (Horizontal, Vertical and Unpolarized) in each BASEN.PTE file, there are 3 Result Matrices in each BASEN.PTE file as well.

2 . The number of lines in each Result Matrix equals the number of frames of the correspondent polarization case. Therefore, each line corresponds to one frame data and thus, each Result Matrix is 100 columns by "number of frames" lines .

3 . Camera Referential is defined as follow:

Origin : Camera
x axis : True North
y axis : True West
z axis : Upward

4 . Contrast Values equal " -1 " means null average thermal level of the correspondent "target" part. Contrast Values equal "77" means null average thermal level of the correspondent "background" part.

5 . Plane Aspect Angle is the angle between the plane normal vector and the line connecting the plane center and the camera.

2. SUMMARY MATRIX DESCRIPTION

Description :

Table describing the columns of the “summary matrix”.

Conditions :

None.

Notes :

None

SUMMARY MATRIX

COLUMN	DESCRIPTION
0	File Number ("N" in BASE"N".PTE file)
1	Average Ship Aspect Angle (degrees)
2	Average Plane 0 Aspect Angle (degrees)
3	Average Plane 1 Aspect Angle (degrees)
4	Average Plane 2 Aspect Angle (degrees)
5	Average Plane 3 Aspect Angle (degrees)
6	Average Distance Ship - Camera (m)
7	Ship Contrast Improvement : Horizontal Polarization
8	Ship Contrast Improvement : Vertical Polarization
9	Plane 0 Contrast Improvement : Horizontal Polarization
10	Plane 0 Contrast Improvement : Vertical Polarization
11	Plane 1 Contrast Improvement : Horizontal Polarization
12	Plane 1 Contrast Improvement : Vertical Polarization
13	Plane 2 Contrast Improvement : Horizontal Polarization
14	Plane 2 Contrast Improvement : Vertical Polarization
15	Plane 3 Contrast Improvement : Horizontal Polarization
16	Plane 3 Contrast Improvement : Vertical Polarization
17	Empty
18	Empty
19	Empty
20	Hor. Polarization : Number of Frames
21	Hor. Polarization : Average Ship Contrast
22	Hor. Polarization : Linear Coefficient for Ship Contrast Variation in Time
23	Hor. Polarization : Angular Coefficient for Ship Contrast Variation in Time
24	Hor. Polarization : Linear Correlation for Ship Contrast Variation in Time
25	Hor. Polarization : Standard Deviation for Ship Contrast Variation in Time
26	Hor. Polarization : Average Plane 0 Contrast
27	Hor. Polarization : Linear Coefficient for Plane 0 Contrast Variation in Time
28	Hor. Polarization : Angular Coefficient for Plane 0 Contrast Variation in Time

COLUMN	DESCRIPTION
29	Hor. Polarization : Linear Correlation for Plane 0 Contrast Variation in Time
30	Hor. Polarization : Standard Deviation for Plane 0 Contrast Variation in Time
31	Hor. Polarization : Average Plane 1 Contrast
32	Hor. Polarization : Linear Coefficient for Plane 1 Contrast Variation in Time
33	Hor. Polarization : Angular Coefficient for Plane 1 Contrast Variation in Time
34	Hor. Polarization : Linear Correlation for Plane 1 Contrast Variation in Time
35	Hor. Polarization : Standard Deviation for Plane 1 Contrast Variation in Time
36	Hor. Polarization : Average Plane 2 Contrast
37	Hor. Polarization : Linear Coefficient for Plane 2 Contrast Variation in Time
38	Hor. Polarization : Angular Coefficient for Plane 2 Contrast Variation in Time
39	Hor. Polarization : Linear Correlation for Plane 2 Contrast Variation in Time
40	Hor. Polarization : Standard Deviation for Plane 2 Contrast Variation in Time
41	Hor. Polarization : Average Plane 3 Contrast
42	Hor. Polarization : Linear Coefficient for Plane 3 Contrast Variation in Time
43	Hor. Polarization : Angular Coefficient for Plane 3 Contrast Variation in Time
44	Hor. Polarization : Linear Correlation for Plane 3 Contrast Variation in Time
45	Hor. Polarization : Standard Deviation for Plane 3 Contrast Variation in Time
46	Ver. Polarization : Number of Frames
47	Ver. Polarization : Average Ship Contrast
48	Ver. Polarization : Linear Coefficient for Ship Contrast Variation in Time
49	Ver. Polarization : Angular Coefficient for Ship Contrast Variation in Time
50	Ver. Polarization : Linear Correlation for Ship Contrast Variation in Time
51	Ver. Polarization : Standard Deviation for Ship Contrast Variation in Time
52	Ver. Polarization : Average Plane 0 Contrast
53	Ver. Polarization : Linear Coefficient for Plane 0 Contrast Variation in Time
54	Ver. Polarization : Angular Coefficient for Plane 0 Contrast Variation in Time
55	Ver. Polarization : Linear Correlation for Plane 0 Contrast Variation in Time
56	Ver. Polarization : Standard Deviation for Plane 0 Contrast Variation in Time
57	Ver. Polarization : Average Plane 1 Contrast
58	Ver. Polarization : Linear Coefficient for Plane 1 Contrast Variation in Time

COLUMN	DESCRIPTION
59	Ver. Polarization : Angular Coefficient for Plane 1 Contrast Variation in Time
60	Ver. Polarization : Linear Correlation for Plane 1 Contrast Variation in Time
61	Ver. Polarization : Standard Deviation for Plane 1 Contrast Variation in Time
62	Ver. Polarization : Average Plane 2 Contrast
63	Ver. Polarization : Linear Coefficient for Plane 2 Contrast Variation in Time
64	Ver. Polarization : Angular Coefficient for Plane 2 Contrast Variation in Time
65	Ver. Polarization : Linear Correlation for Plane 2 Contrast Variation in Time
66	Ver. Polarization : Standard Deviation for Plane 2 Contrast Variation in Time
67	Ver. Polarization : Average Plane 3 Contrast
68	Ver. Polarization : Linear Coefficient for Plane 3 Contrast Variation in Time
69	Ver. Polarization : Angular Coefficient for Plane 3 Contrast Variation in Time
70	Ver. Polarization : Linear Correlation for Plane 3 Contrast Variation in Time
71	Ver. Polarization : Standard Deviation for Plane 3 Contrast Variation in Time
72	Unpolarized : Number of Frames
73	Unpolarized : Average Ship Contrast
74	Unpolarized : Linear Coefficient for Ship Contrast Variation in Time
75	Unpolarized : Angular Coefficient for Ship Contrast Variation in Time
76	Unpolarized : Linear Correlation for Ship Contrast Variation in Time
77	Unpolarized : Standard Deviation for Ship Contrast Variation in Time
78	Unpolarized : Average Plane 0 Contrast
79	Unpolarized : Linear Coefficient for Plane 0 Contrast Variation in Time
80	Unpolarized : Angular Coefficient for Plane 0 Contrast Variation in Time
81	Unpolarized : Linear Correlation for Plane 0 Contrast Variation in Time
82	Unpolarized : Standard Deviation for Plane 0 Contrast Variation in Time
83	Unpolarized : Average Plane 1 Contrast
84	Unpolarized : Linear Coefficient for Plane 1 Contrast Variation in Time
85	Unpolarized : Angular Coefficient for Plane 1 Contrast Variation in Time
86	Unpolarized : Linear Correlation for Plane 1 Contrast Variation in Time
87	Unpolarized : Standard Deviation for Plane 1 Contrast Variation in Time
88	Unpolarized : Average Plane 2 Contrast

COLUMN	DESCRIPTION
89	Unpolarized : Linear Coefficient for Plane 2 Contrast Variation in Time
90	Unpolarized : Angular Coefficient for Plane 2 Contrast Variation in Time
91	Unpolarized : Linear Correlation for Plane 2 Contrast Variation in Time
92	Unpolarized : Standard Deviation for Plane 2 Contrast Variation in Time
93	Unpolarized : Average Plane 3 Contrast
94	Unpolarized : Linear Coefficient for Plane 3 Contrast Variation in Time
95	Unpolarized : Angular Coefficient for Plane 3 Contrast Variation in Time
96	Unpolarized : Linear Correlation for Plane 3 Contrast Variation in Time
97	Unpolarized : Standard Deviation for Plane 3 Contrast Variation in Time
98	Ship : Degree of Polarization
99	Plane 0: Degree of Polarization
100	Plane 1: Degree of Polarization
101	Plane 2: Degree of Polarization
102	Plane 3: Degree of Polarization
103	Ship / Horizontal Polarization : Average Thermal Level
104	Ship / Vertical Polarization : Average Thermal Level
105	Ship / Unpolarized : Average Thermal Level
106	Plane 0 / Horizontal Polarization : Average Thermal Level
107	Plane 0 / Vertical Polarization : Average Thermal Level
108	Plane 0 / Unpolarized : Average Thermal Level
109	Plane 1 / Horizontal Polarization : Average Thermal Level
110	Plane 1 / Vertical Polarization : Average Thermal Level
111	Plane 1 / Unpolarized : Average Thermal Level
112	Plane 2 / Horizontal Polarization : Average Thermal Level
113	Plane 2 / Vertical Polarization : Average Thermal Level
114	Plane 2 / Unpolarized : Average Thermal Level
115	Plane 3 / Horizontal Polarization : Average Thermal Level
116	Plane 3 / Vertical Polarization : Average Thermal Level
117	Plane 3 / Unpolarized : Average Thermal Level
118	Sea : Degree of Polarization

COLUMN	DESCRIPTION
119	Sky : Degree of Polarization
120	Sea / Horizontal Polarization : Average Thermal Level
121	Sea / Vertical Polarization : Average Thermal Level
122	Sea / Unpolarized : Average Thermal Level
123	Sky / Horizontal Polarization : Average Thermal Level
124	Sky / Vertical Polarization : Average Thermal Level
125	Sky / Unpolarized : Average Thermal Level
126	Empty
127	Empty
128	Empty
129	Empty

NOTES:

1 . Dimensions of Summary Matrix:

130 columns(summary parameters) by 70 lines (BASEN.PTE files)

3. CONTRAST VARIATION IN TIME

Description :

This Appendix presents 3 tables with numerical results from the curve fitting process for the ship contrast variation in time for each of the 70 analyzed files. Each table corresponds to one polarization case (horizontal, vertical and unpolarized). The tables' columns represent the calculated parameters and their lines represent the data files.

Conditions :

Appendix E.2 presents the conditions for each one of the 70 analyzed data files.

Notes :

None

**SHIP CONTRAST VARIATION IN TIME
CURVE FITTING DATA
HORIZONTAL POLARIZATION CASE**

File	Average Contrast	Linear Coefficient	Angular Coefficient	Correlation Coefficient	Standard Deviation
1	2.80165	2.85781	-0.0143103	0.668752	0.203140
2	2.80883	2.81643	-0.00170590	0.528814	0.160196
3	3.65163	3.51321	0.0301833	0.796223	0.287902
4	2.17118	2.31451	-0.0369719	0.928972	0.206059
5	1.94353	2.07550	-0.0322707	0.867610	0.218043
6	1.27496	1.43855	-0.0418325	0.978913	0.174972
7	1.53642	1.54735	-0.00305780	0.540394	0.167734
8	1.63538	1.61315	0.00563710	0.573669	0.184521
9	2.17445	2.09851	0.0194168	0.762126	0.178305
10	1.55079	1.68258	-0.0335488	0.978913	0.151809
11	1.83582	1.97652	-0.0320644	0.858977	0.241668
12	1.84789	1.91962	-0.0175047	0.766276	0.163482
13	1.10643	1.23842	-0.0311132	0.891780	0.205079
14	1.25555	1.31311	-0.0107580	0.717171	0.159973
15	1.42046	1.47126	-0.0129936	0.682429	0.170873
16	1.11659	1.11855	-0.000370000	0.511226	0.102462
17	2.15119	2.23562	-0.0214278	0.666799	0.307376
18	0.661015	0.630466	0.00755910	0.636610	0.137544
19	0.773015	0.745295	0.00588670	0.706657	0.0813143
20	0.634380	0.695613	-0.00402900	0.714679	0.0771875
21	1.31758	1.15618	0.0428472	0.719358	0.434080
22	0.769486	0.789252	-0.00466500	0.534465	0.345064
23	1.28167	1.28111	0.000143000	0.501193	0.284283
24	1.50233	1.27581	0.0575093	0.771774	0.506715
25	0.633017	0.634451	-0.000318100	0.507058	0.120337
26	1.08100	0.987104	0.0260545	0.959757	0.120780
27	1.74491	1.66732	0.0165698	0.582347	0.573178
28	2.12856	2.12218	0.00156960	0.514481	0.265728
29	1.42869	1.52246	-0.0231520	0.761684	0.212018
30	2.68013	2.58043	0.0245254	0.675362	0.346031
31	1.49569	1.64148	-0.0368720	0.802147	0.293751
32	1.11322	1.23294	-0.0305141	0.670331	0.428686
33	1.71059	1.70843	0.000445600	0.502961	0.441944
34	2.10271	2.15569	-0.0141800	0.604514	0.312333
35	2.07356	2.05961	0.00357060	0.554649	0.156133
36	2.03846	2.05987	-0.00548300	0.533086	0.396091
37	2.23930	2.15457	0.0226713	0.599584	0.522287
38	3.34082	3.28529	0.0153200	0.685720	0.185431
39	2.58644	3.72767	-0.281168	0.978913	0.757946
40	1.90422	3.08502	-0.359358	0.978913	0.820252

File	Average Contrast	Linear Coefficient	Angular Coefficient	Correlation Coefficient	Standard Deviation
41	4.30706	4.24591	0.0162531	0.596834	0.386256
42	2.81381	3.04393	-0.0588096	0.978913	0.225648
43	5.17213	4.48191	0.169080	0.821299	1.30717
44	9.50296	10.0436	-0.133343	0.978913	0.654553
45	9.12538	9.60646	-0.120213	0.938590	0.667210
46	8.74781	9.16930	-0.107082	0.877180	0.679866
47	8.52847	8.57558	-0.0119631	0.569198	0.413992
48	4.03500	4.31024	-0.0704433	0.844654	0.488401
49	4.84643	4.63820	0.0555559	0.950588	0.284294
50	5.00610	5.15838	-0.0391236	0.742347	0.385789
51	4.05197	4.04206	0.00291050	0.515773	0.390803
52	2.98657	2.96867	0.00438850	0.530429	0.357792
53	5.06469	4.67272	0.105268	0.821022	0.753541
54	4.27813	4.25102	0.00755260	0.542883	0.388482
55	5.04765	4.88280	0.0437411	0.721393	0.454511
56	3.24872	3.34633	-0.0251006	0.803891	0.197450
57	3.98802	4.01190	-0.00696730	0.552126	0.282903
58	4.90922	4.78759	0.0321090	0.647594	0.503450
59	5.48694	5.26906	0.0555288	0.890188	0.341674
60	4.29067	4.10611	0.0337203	0.805949	0.364256
61	4.59787	3.91598	0.196924	0.978913	0.728621
62	4.75310	4.77335	-0.00518570	0.509585	1.29376
63	4.95280	4.60385	0.0798857	0.964189	0.458330
64	5.56581	4.89260	0.165547	0.978913	0.758760
65	3.90502	4.06693	-0.0382276	0.725763	0.435940
66	3.52566	3.52932	-0.000940500	0.503029	0.741582
67	4.18790	4.33764	-0.0380327	0.811837	0.291695
68	4.15409	4.04489	0.0258802	0.775146	0.241804
69	3.28224	3.03942	0.0594761	0.790860	0.510322
70	3.56515	3.65409	-0.0225826	0.616673	0.464753

**SHIP CONTRAST VARIATION IN TIME
CURVE FITTING DATA
VERTICAL POLARIZATION CASE**

File	Average Contrast	Linear Coefficient	Angular Coefficient	Correlation Coefficient	Standard Deviation
1	2.07926	2.16238	-0.0220855	0.917904	0.121681
2	2.20152	2.29522	-0.0226768	0.856538	0.170310
3	2.35063	2.53705	-0.0448562	0.981560	0.202534
4	1.72437	1.70750	0.00352470	0.588868	0.121922
5	1.14064	1.19479	-0.0118561	0.891219	0.0835699
6	0.875345	0.966203	-0.0152129	0.927931	0.139760
7	1.39069	1.38529	0.00113050	0.521495	0.156799
8	1.45242	1.54902	-0.0244514	0.822164	0.183349
9	1.70469	1.24071	0.125553	0.942385	0.648509
10	1.45817	1.40472	0.0145767	0.770545	0.126642
11	1.26608	1.42338	-0.0297845	0.981560	0.147410
12	1.97564	1.93624	0.0114744	0.595973	0.253321
13	0.640966	0.630764	0.00274090	0.542522	0.151011
14	0.870467	0.866022	0.00107620	0.517420	0.158740
15	0.955703	0.979517	-0.00552270	0.646425	0.100803
16	1.08764	1.04499	0.00927520	0.733827	0.109460
17	1.36986	1.50222	-0.0371935	0.856415	0.234837
18	0.873683	0.704838	0.0347649	0.839374	0.330412
19	0.434872	0.434136	0.000235200	0.505499	0.0844069
20	0.667986	0.673790	-0.00107170	0.546010	0.0771668
21	0.966984	0.648565	0.0597602	0.981560	0.364847
22	0.871381	0.865531	0.000961600	0.510191	0.351386
23	0.754552	0.716056	0.00608100	0.579543	0.294911
24	1.48194	1.52886	-0.00804800	0.582448	0.350090
25	1.52314	1.51820	0.000842000	0.505707	0.528090
26	0.887348	0.877089	0.00137810	0.534275	0.186258
27	1.58146	1.49273	0.0164316	0.669073	0.321954
28	1.68657	1.74299	-0.00926230	0.703519	0.169178
29	2.12061	1.96205	0.0295708	0.944763	0.220237
30	1.62637	1.62605	8.48000e-005	0.501086	0.185154
31	0.941800	0.871198	0.0179436	0.685193	0.232333
32	0.292536	0.322877	-0.00751330	0.595391	0.195788
33	0.830968	1.00356	-0.0424596	0.834020	0.315640
34	1.77094	1.76876	0.000498700	0.508327	0.159653
35	1.85003	1.91174	-0.0157777	0.718975	0.172170
36	2.24780	1.97066	0.0739158	0.998733	0.340360
37	1.85654	1.94024	-0.0213637	0.722923	0.228740
38	1.53497	1.96652	-0.113340	0.981560	0.438001
39	3.06921	2.97788	0.0240404	0.725269	0.252612
40	3.87009	3.65755	0.0466593	0.918586	0.306329

File	Average Contrast	Linear Coefficient	Angular Coefficient	Correlation Coefficient	Standard Deviation
41	3.18932	3.35162	-0.0403319	0.836592	0.296846
42	2.26884	2.23032	0.00950500	0.591319	0.257858
43	3.97425	3.65866	0.0883503	0.953594	0.431382
44	6.15951	6.08536	0.0182694	0.643296	0.316965
45	6.03524	5.94822	0.0230765	0.659352	0.334339
46	5.91096	5.81108	0.0278836	0.675407	0.351712
47	5.72501	5.66645	0.0150379	0.579280	0.454030
48	2.33569	2.46773	-0.0337294	0.857354	0.225624
49	3.58970	3.55011	0.00896870	0.599042	0.241228
50	3.73979	4.04736	-0.0744561	0.864258	0.520242
51	3.99233	3.64039	0.0780609	0.907372	0.526952
52	1.49792	1.46151	0.00880420	0.528776	0.780617
53	2.20792	2.11717	0.0253324	0.747329	0.226389
54	2.35592	2.34389	0.00305740	0.535242	0.208144
55	3.20514	3.11943	0.0220728	0.693853	0.271772
56	2.59301	2.47996	0.0290683	0.931283	0.161123
57	2.45601	2.47127	-0.00337190	0.521288	0.434999
58	2.62831	2.45404	0.0440237	0.865161	0.290336
59	3.00441	2.97265	0.00685390	0.598069	0.197976
60	2.00306	2.00704	-0.00120140	0.507623	0.321723
61	2.72136	2.76990	-0.0119253	0.615147	0.257311
62	1.66571	1.35568	0.0819600	0.656237	1.20995
63	2.96395	3.17864	-0.0597305	0.869689	0.356761
64	3.12323	3.38279	-0.0689185	0.847562	0.463380
65	2.25382	2.27012	-0.00432070	0.530210	0.330781
66	2.30594	1.78201	0.145194	0.772691	1.17811
67	3.20938	3.10377	0.0268534	0.712197	0.302517
68	3.80472	3.73376	0.0180840	0.659679	0.271108
69	1.82662	1.90984	-0.0222314	0.777947	0.189958
70	2.85635	2.94964	-0.0230254	0.640179	0.409128

**SHIP CONTRAST VARIATION IN TIME
CURVE FITTING DATA
UNPOLARIZED CASE**

File	Average Contrast	Linear Coefficient	Angular Coefficient	Correlation Coefficient	Standard Deviation
1	2.44503	2.56108	-0.0273893	0.645378	0.491036
2	1.87756	2.97718	-0.291580	0.985270	0.719778
3	3.80018	3.89635	-0.0237633	0.668011	0.351763
4	2.41747	2.49466	-0.0189573	0.783558	0.166026
5	1.90084	2.07089	-0.0418907	0.847198	0.293129
6	2.17321	2.14588	0.00645190	0.591816	0.180736
7	2.09211	2.10896	-0.00415600	0.568276	0.151017
8	2.25859	2.25560	0.000764200	0.507833	0.234531
9	2.27140	2.32928	-0.0147498	0.868770	0.0960177
10	2.16845	2.27764	-0.0280011	0.831049	0.202325
11	1.61733	2.06662	-0.115439	0.985270	0.317676
12	2.36995	2.34869	0.00543110	0.537170	0.349842
13	1.28792	1.30946	-0.00531980	0.572425	0.182244
14	0.894373	1.00664	-0.0273881	0.946165	0.153021
15	1.25899	1.30047	-0.00919030	0.755034	0.0983402
16	1.08740	1.23251	-0.0372685	0.985270	0.139264
17	2.23541	2.24308	-0.00189400	0.520996	0.224606
18	0.798607	0.703851	0.0233120	0.784167	0.203517
19	0.430845	0.457457	-0.00656680	0.777433	0.0586804
20	0.783297	0.830262	-0.0112016	0.798389	0.0935049
21	2.75984	2.89649	-0.0324545	0.666823	0.484444
22	0.561443	0.501921	0.0153830	0.883827	0.0926017
23	0.920205	0.833486	0.0231828	0.821444	0.166006
24	1.04728	1.11684	-0.0165255	0.603384	0.397960
25	0.723845	0.749914	-0.00636820	0.565320	0.241938
26	1.08585	1.08812	-0.000535100	0.511226	0.122833
27	1.70568	1.69448	0.00288710	0.533842	0.203789
28	1.94770	1.96670	-0.00489800	0.642421	0.0793498
29	1.18129	1.04583	0.0319996	0.985270	0.145001
30	1.90163	1.93110	-0.00752370	0.573738	0.243779
31	1.94532	2.21659	-0.0665101	0.871735	0.446330
32	1.04401	1.01975	0.00598750	0.572873	0.203862
33	1.54639	1.78945	-0.0597028	0.881841	0.388249
34	2.41976	2.02443	0.100896	0.985270	0.333965
35	1.71758	1.74794	-0.00777160	0.590384	0.205454
36	2.20933	2.08123	0.0302740	0.759005	0.300383
37	3.41596	3.45110	-0.00863250	0.551374	0.416165

File	Average Contrast	Linear Coefficient	Angular Coefficient	Correlation Coefficient	Standard Deviation
38	3.29090	3.23744	0.0132749	0.587260	0.376591
39	4.02375	4.47304	-0.115943	0.985270	0.419761
40	4.27124	4.07288	0.0508010	0.736309	0.512874
41	3.71359	3.61383	0.0255371	0.712148	0.286700
42	3.40036	3.22261	0.0441578	0.806296	0.357087
43	3.81383	6.65601	-0.728271	0.985270	2.29030
44	5.97115	3.60097	0.564396	0.992504	2.94987
45	7.62334	6.87450	0.166625	0.996252	1.82244
46	9.27553	10.1480	-0.231147	0.985270	0.695002
47	7.08689	7.04096	0.0112610	0.566316	0.421557
48	4.20959	3.90683	0.0760477	0.957367	0.408378
49	4.23986	4.05581	0.0474109	0.885936	0.294119
50	5.69474	5.95606	-0.0668053	0.719573	0.727363
51	4.51901	4.43862	0.0213169	0.654616	0.317270
52	4.33459	3.95464	0.0694421	0.985270	0.417945
53	3.63039	3.45443	0.0468858	0.794029	0.366772
54	2.79752	2.93889	-0.0337853	0.586607	1.00575
55	6.06979	6.67215	-0.148401	0.985270	0.665069
56	3.48617	3.11986	0.0981665	0.985270	0.292365
57	4.35625	4.52443	-0.0433923	0.757143	0.402943
58	4.35927	4.13440	0.0552550	0.827964	0.420804
59	4.79361	4.73197	0.0158066	0.623328	0.307652
60	4.14555	4.34462	-0.0506845	0.873456	0.326072
61	4.55138	4.55110	7.01000e-005	0.500457	0.496433
62	1.25162	2.86944	-0.432698	0.985270	1.26721
63	4.65793	4.08372	0.152722	0.985270	0.538072
64	5.79477	5.97091	-0.0470827	0.720392	0.493814
65	3.25656	3.35040	-0.0249026	0.614950	0.499481
66	4.66856	4.79119	-0.0314910	0.784775	0.265526
67	4.81142	4.61471	0.0484001	0.997844	0.241617
68	5.51555	5.72753	-0.0565878	0.838031	0.385874
69	2.94610	2.77539	0.0436237	0.771418	0.386373
70	3.86046	3.81139	0.0129772	0.612273	0.266740

4. CONTRAST IMPROVEMENT AND DEGREE OF POLARIZATION

Description :

This Appendix presents a table with numerical results for ship to background contrast improvement and degree of polarization for each of the 70 analyzed files. The tables' columns represent the calculated parameters and their lines represent the corresponding data files.

Conditions :

Appendix E.2 presents the conditions for each one of the 70 analyzed data files.

Notes :

None

**SHIP CONTRAST IMPROVEMENT
AND
DEGREE OF POLARIZATION**

File	Range (m)	Aspect Angle (degree)	Horizontal Contrast Improvement	Vertical Contrast Improvement	Degree of Polarization
1	998.864	57.6053	1.14586	0.850403	-0.0184325
2	998.755	80.6053	1.49600	1.17254	-0.0108805
3	998.758	163.231	0.960909	0.618558	-0.0185840
4	1868.39	29.9880	0.898121	0.713293	-0.000145900
5	1848.48	56.2289	1.02246	0.600072	-0.000952700
6	1821.53	72.0000	0.586672	0.402789	0.0203949
7	1777.48	164.696	0.734391	0.664730	0.00307000
8	2413.58	9.96000	0.724070	0.643067	-0.00829560
9	2413.58	33.2800	0.957318	0.750500	-0.0255484
10	2413.58	54.4324	0.715161	0.672450	-0.0122041
11	2362.17	89.2105	1.13509	0.782822	-0.00415830
12	2545.18	169.842	0.779719	0.833621	-0.0169203
13	3370.32	10.3924	0.859083	0.497677	-0.000783500
14	3370.32	31.7857	1.40384	0.973271	-0.0134057
15	3370.07	50.7867	1.12826	0.759106	-0.00516510
16	3369.22	72.1818	1.02684	1.00022	-0.00250100
17	3334.13	162.434	0.962323	0.612800	-0.0192313
18	5138.79	13.2436	0.827710	1.09401	0.0364165
19	5007.12	82.2564	1.79418	1.00935	-0.0139722
20	5127.45	162.899	0.809884	0.852787	0.00317430
21	5016.86	29.5132	0.477412	0.350376	0.0461341
22	5017.02	349.709	1.37055	1.55204	0.0311796
23	4681.39	332.848	1.39281	0.819983	0.0292522
24	4611.97	306.038	1.43451	1.41504	-0.0119148
25	4670.11	252.366	0.874520	2.10423	-0.00423360
26	4862.18	180.435	0.995534	0.817190	0.00229850
27	3126.46	345.086	1.02300	0.927175	0.0250924
28	3026.37	322.885	1.09286	0.865929	-0.0134405
29	3122.15	294.312	1.20943	1.79517	-7.2200e-005
30	3479.73	172.103	1.40939	0.855251	-0.0147440
31	2117.77	337.911	0.768865	0.484136	0.0166958
32	2117.59	332.450	1.06629	0.280203	0.0462036
33	2117.41	17.3721	1.10618	0.537359	0.0247786
34	2117.59	34.1125	0.868975	0.731868	-0.0134935
35	2117.85	60.1282	1.20725	1.07711	-0.00790860
36	2104.50	114.430	0.922658	1.01741	0.0164684
37	1283.90	341.833	0.655539	0.543490	-0.0295535
38	1284.01	19.2368	1.01517	0.466429	0.0211658
39	1283.90	33.3077	0.642793	0.762775	-0.0144630
40	1208.65	55.1282	0.445823	0.906080	-0.0596533
41	1280.61	110.885	1.15981	0.858824	-0.00545070
42	1280.61	152.563	0.827502	0.667234	-0.0166726
43	420.751	26.9870	1.35615	1.04206	-0.00913290
44	421.008	49.4756	1.59148	1.03154	-0.0314955
45	560.438	80.3111	1.26729	0.834405	-0.0242675
46	699.869	111.147	0.943106	0.637264	-0.0170394
47	821.898	168.848	1.20341	0.807831	-0.0314977
48	298.692	120.192	0.958524	0.554849	0.00372340

File	Range (m)	Aspect Angle (degree)	Horizontal Contrast Improvement	Vertical Contrast Improvement	Degree of Polarization
49	298.692	28.0500	1.14306	0.846655	-0.0296597
50	373.001	60.5570	0.879074	0.656709	-0.0136805
51	373.210	106.833	0.896651	0.883453	-0.0684252
52	998.931	343.611	0.689009	0.345574	0.125752
53	998.753	362.122	1.39508	0.608178	0.00218570
54	998.757	9.51948	1.52926	0.842146	0.00657230
55	998.864	44.3846	0.831603	0.528048	0.000936200
56	998.864	65.1429	0.931888	0.743799	-0.0146519
57	998.864	106.215	0.915470	0.563788	0.0109230
58	402.338	325.474	1.12616	0.602925	0.0221615
59	323.227	339.293	1.14463	0.626752	-0.0447613
60	323.227	361.143	1.03501	0.483183	0.00741130
61	323.227	15.2632	1.01021	0.597920	-0.0128527
62	323.227	37.1974	3.79755	1.33084	-0.0562200
63	323.035	46.8205	1.06331	0.636324	0.0147427
64	344.938	63.3117	0.960490	0.538975	0.00380640
65	447.752	101.141	1.19913	0.692086	-0.0108047
66	459.450	115.750	0.755192	0.493930	0.0876210
67	459.469	144.506	0.870409	0.667034	-0.0268323
68	459.698	161.190	0.753160	0.689817	-0.0214548
69	1395.80	16.2987	1.11410	0.620011	-0.0571002
70	1395.98	33.7051	0.923504	0.739900	-0.0189662

APPENDIX J

RESULT GRAPHICS

1. CONTRAST VARIATION IN TIME : DATA FILE SAMPLE

Description :

This Appendix presents a sample of the curve fitting process applied to the ship contrast variation in time. The 3 polarization cases are represented by corresponding plots. A comparative plot (with the 3 cases) is also presented. The data file used to generate this example was the BASE01.PTE (file #01).

Conditions :

From the first line of the table in Appendix E.2:

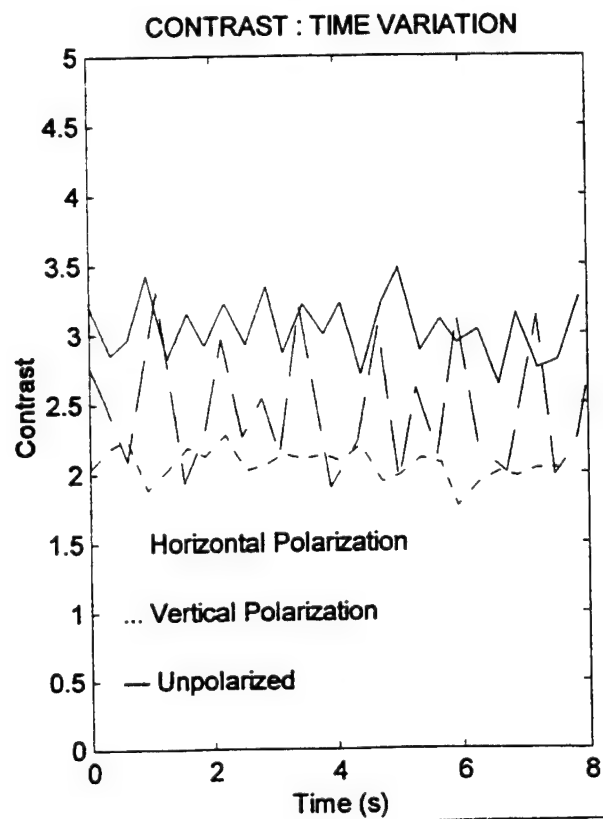
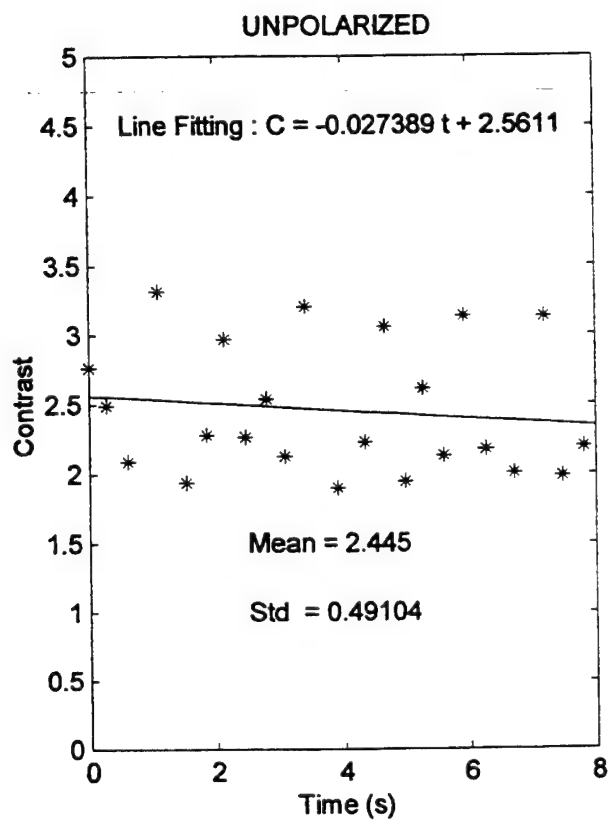
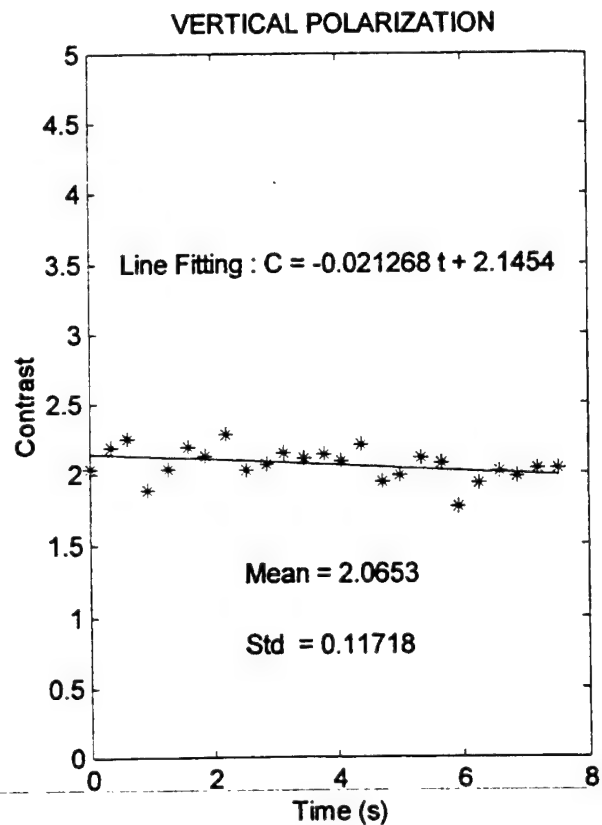
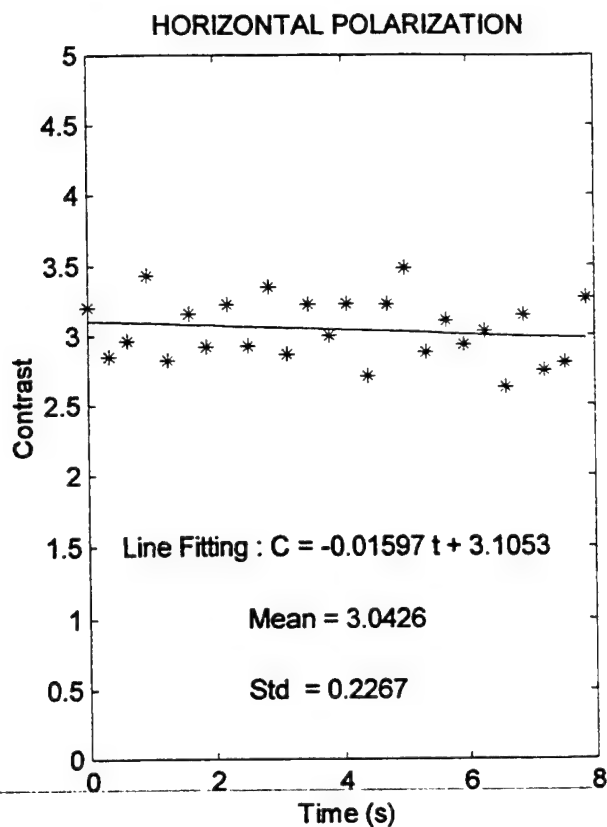
File #01

Day : April 9
Time: 44,018.0 seconds (elapsed time from 00h:00:min of April 9)
Latitude : 1959.20 minutes
Longitude : 7034.80 minutes
Ship GPS Antenna height : -27.01 m
Air Temperature : 15.30 C
Relative Humidity : 72 %
Air Pressure : 1018.25 mb
Wind Speed : 6.5 m/s
Sea Surface Temperature : 18.55 C
Range : 998.52 m
Theta : 1.62 rad
Fi : 2.41 rad
Atmospheric Transmittance : 0.82

Notes :

None

SHIP CONTRAST VARIATION IN TIME : FILE SAMPLE (BASE01.PTE)



2. CONTRAST VARIATION IN TIME : STATISTICAL DISTRIBUTION

Description :

This Appendix presents the statistical distribution (histograms) for the curve fitting parameters of the ship contrast variation in time. The 3 polarization cases are presented separately. All 70 data files were used to generate the plots in this Appendix.

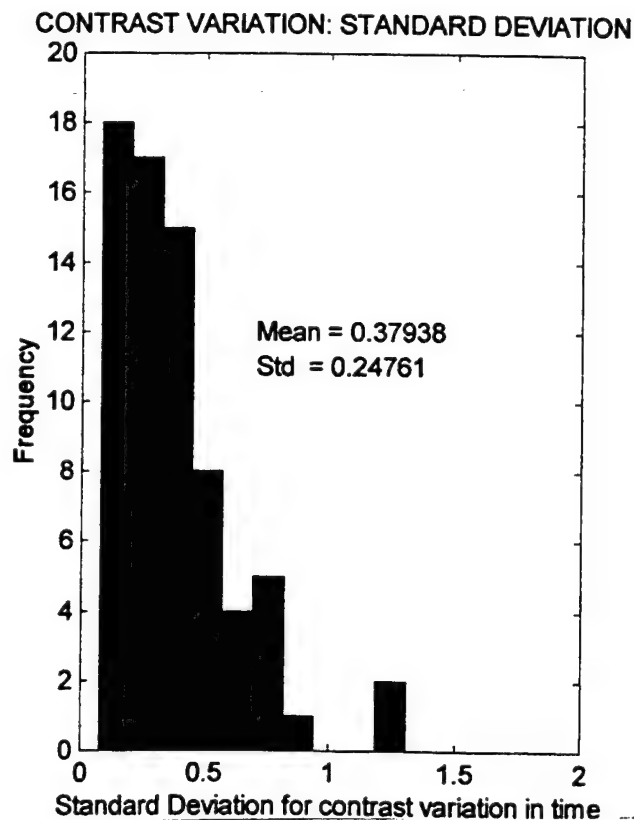
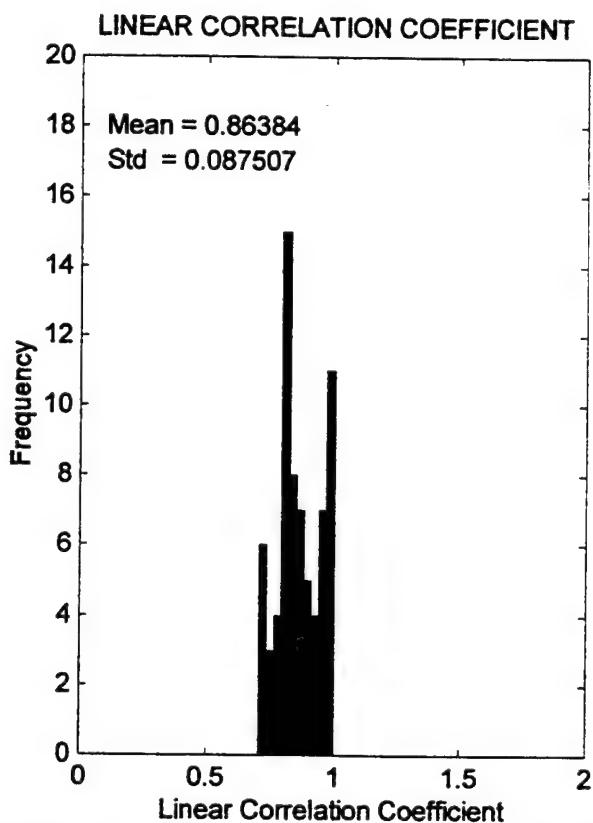
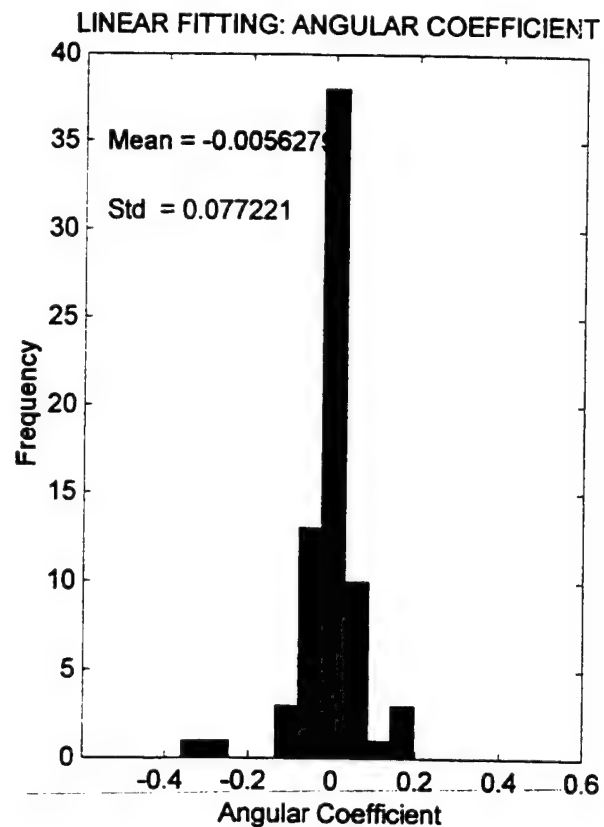
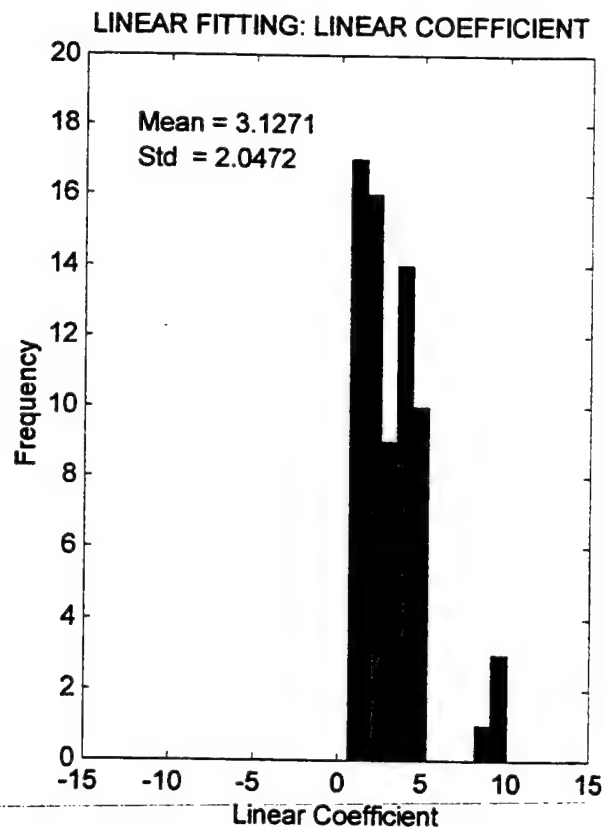
Conditions :

Appendix E.2 presents the conditions for each one of the 70 files used in this Appendix.

Notes :

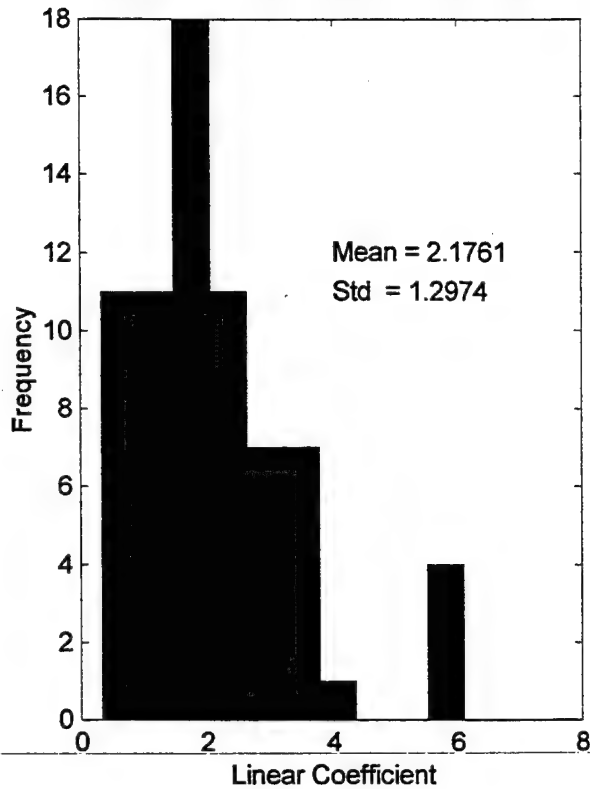
It can be observed by these histograms that the linear fitting parameters have a narrow distribution for all polarization cases. Therefore, they can be very well represented by their mean values.

SHIP CONTRAST VARIATION IN TIME : HORIZONTAL POLARIZATION

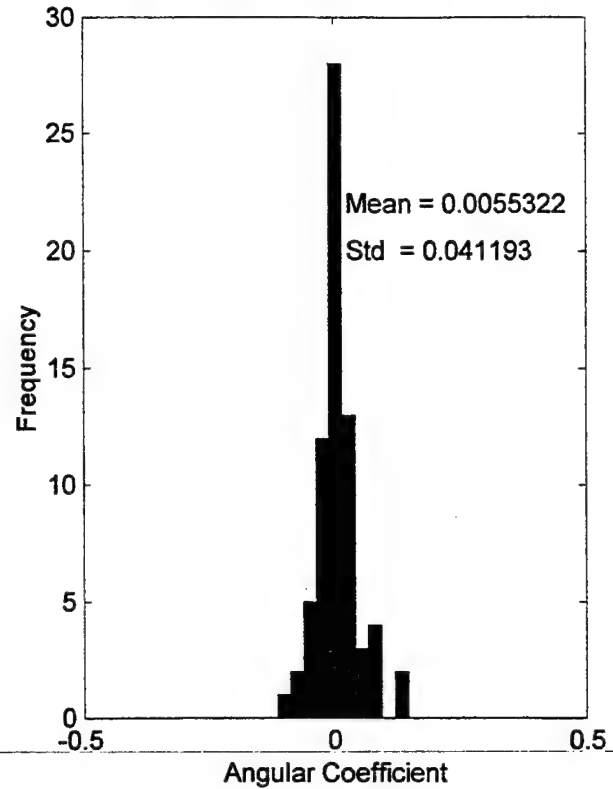


SHIP CONTRAST VARIATION IN TIME : VERTICAL POLARIZATION

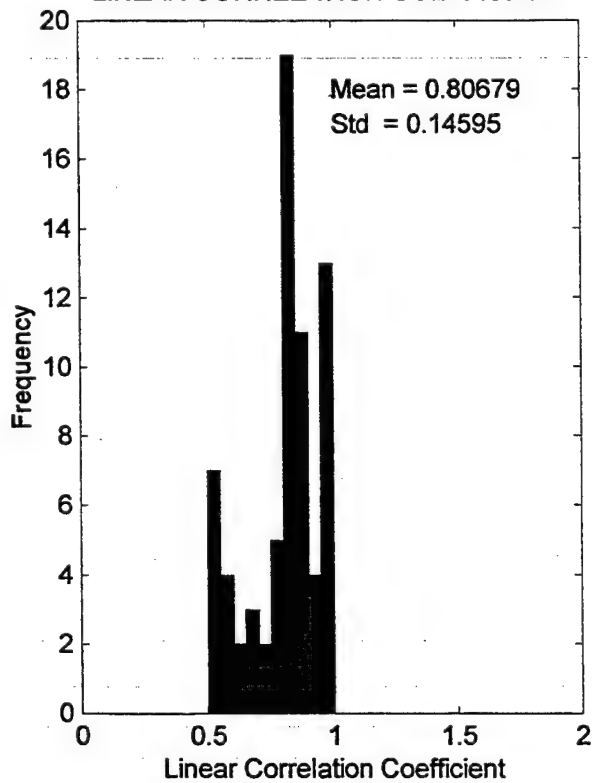
LINEAR FITTING: LINEAR COEFFICIENT



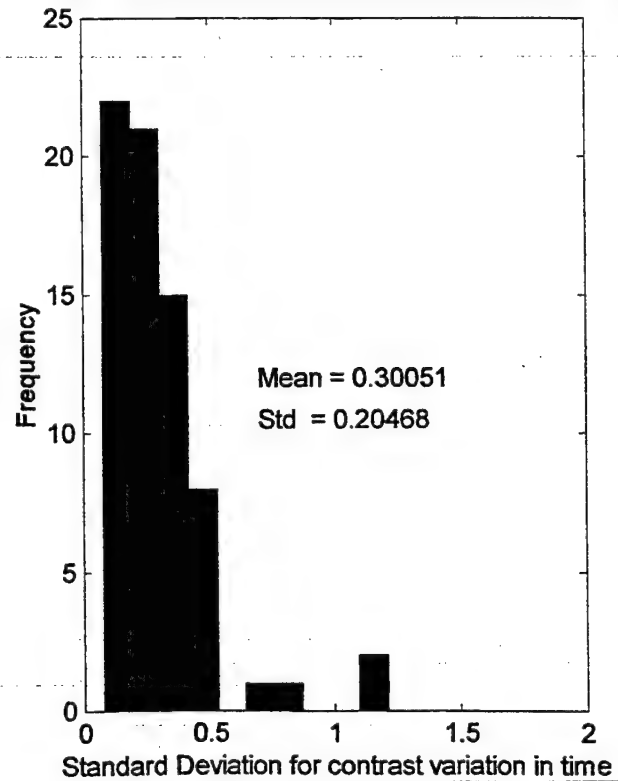
LINEAR FITTING: ANGULAR COEFFICIENT



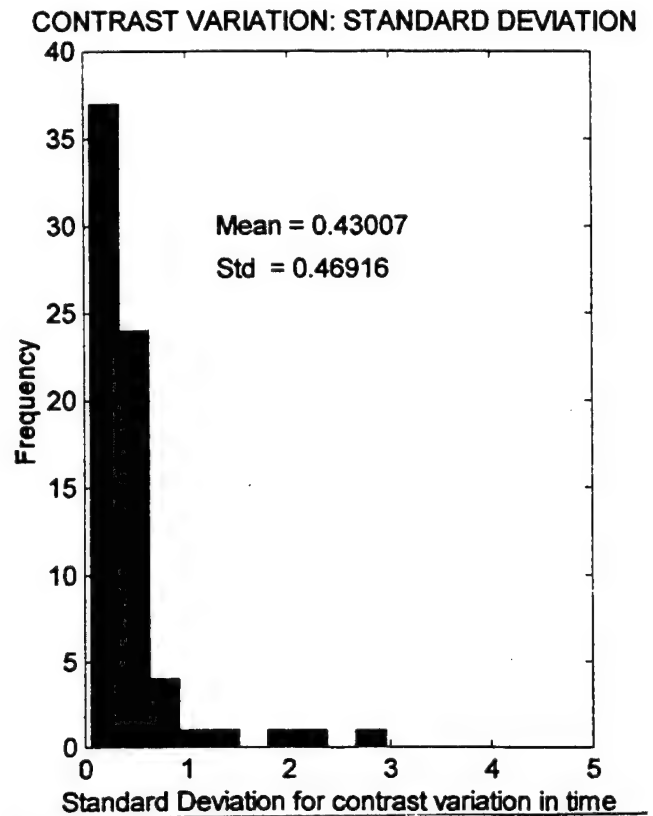
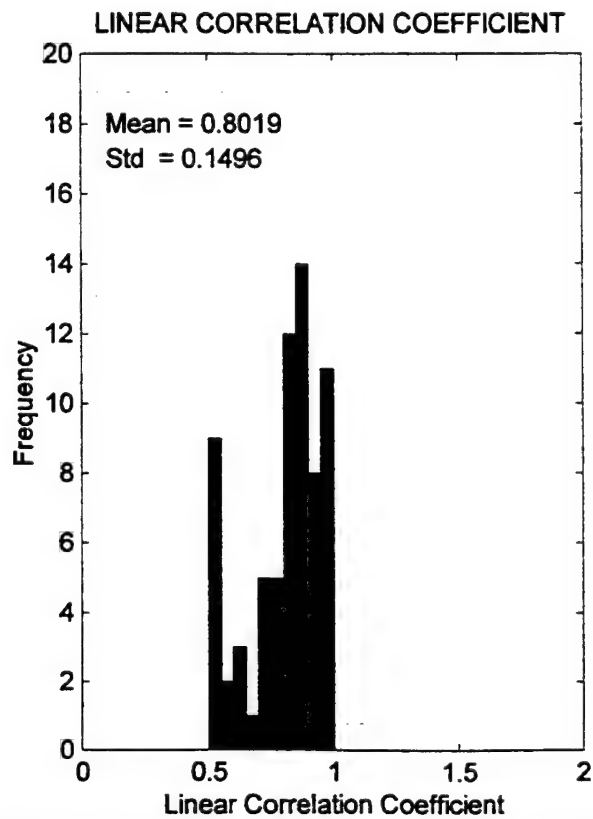
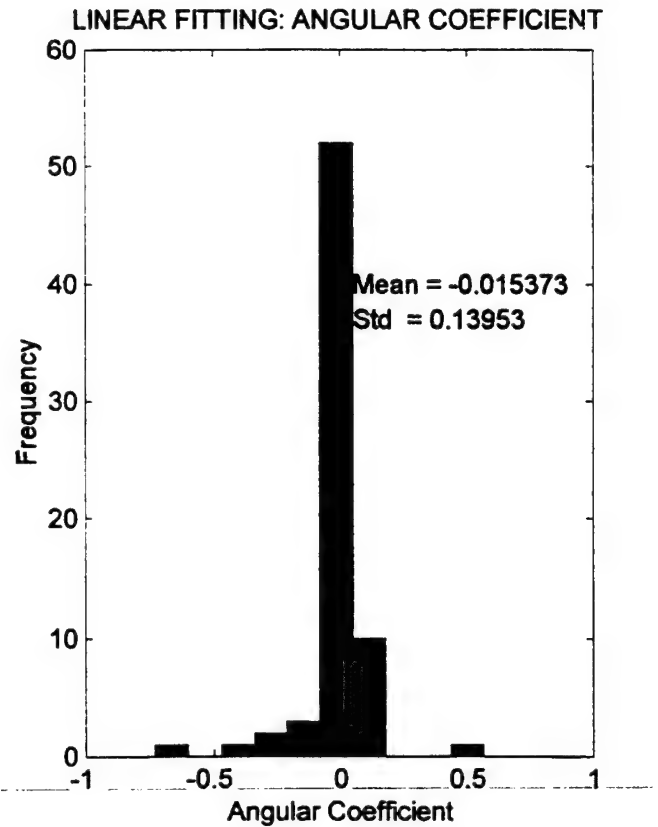
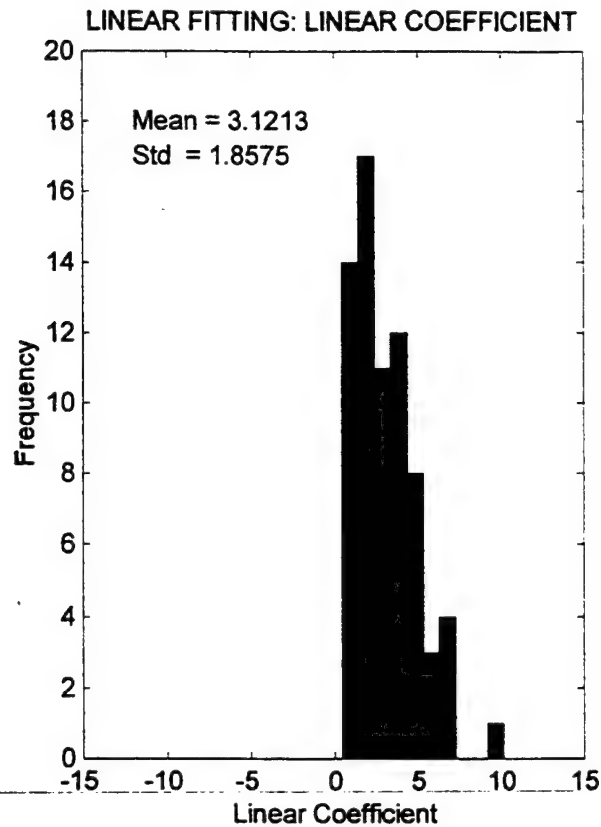
LINEAR CORRELATION COEFFICIENT



CONTRAST VARIATION: STANDARD DEVIATION



SHIP CONTRAST VARIATION IN TIME : UNPOLARIZED



3. CONTRAST IMPROVEMENT AND DEGREE OF POLARIZATION

Description :

This Appendix presents a the statistical distribution (histograms) for the ship contrast improvement and the image elements (ship, sea, sky) degree of polarization. The ship contrast improvement for horizontal and vertical polarization cases are presented in the same scale to permit easy comparison. The degree of polarization histograms for the image elements are also presented using the same scale to permit easy comparison. All 70 files data were used to generate the plots in this Appendix.

Conditions :

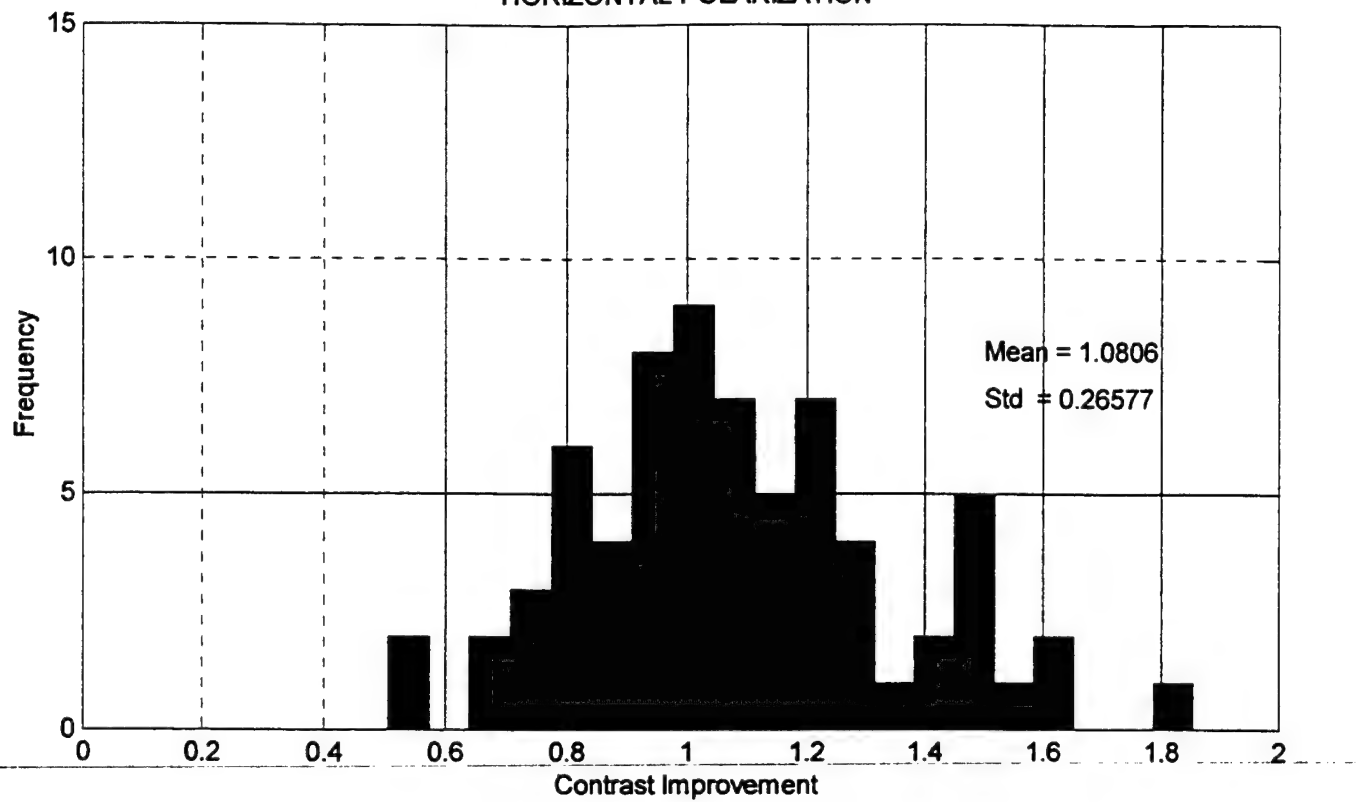
Appendix E.2 presents the conditions for each one of the 70 files used in this Appendix.

Notes :

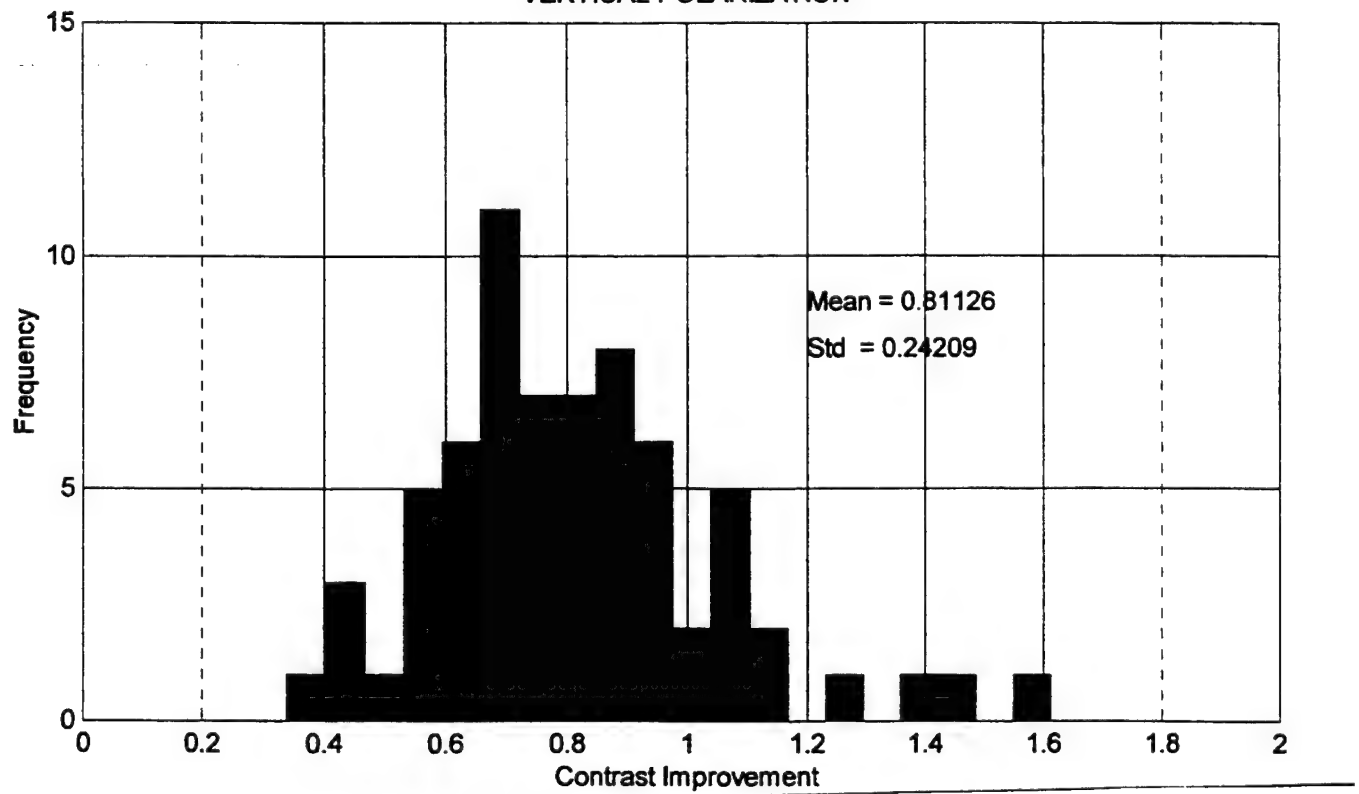
The ship contrast improvement histograms show that in average, there is an advantage in using the horizontal filter for the scenario analyzed. On the other hand, the vertical filter results an average loss in contrast. The ship degree of polarization has a very narrow distribution when compared with the sea and the sky distributions. The sea exhibits predominance of vertical polarization. The ship degree of polarization is effectively zero and the sky shows a random behavior.

SHIP CONTRAST IMPROVEMENT

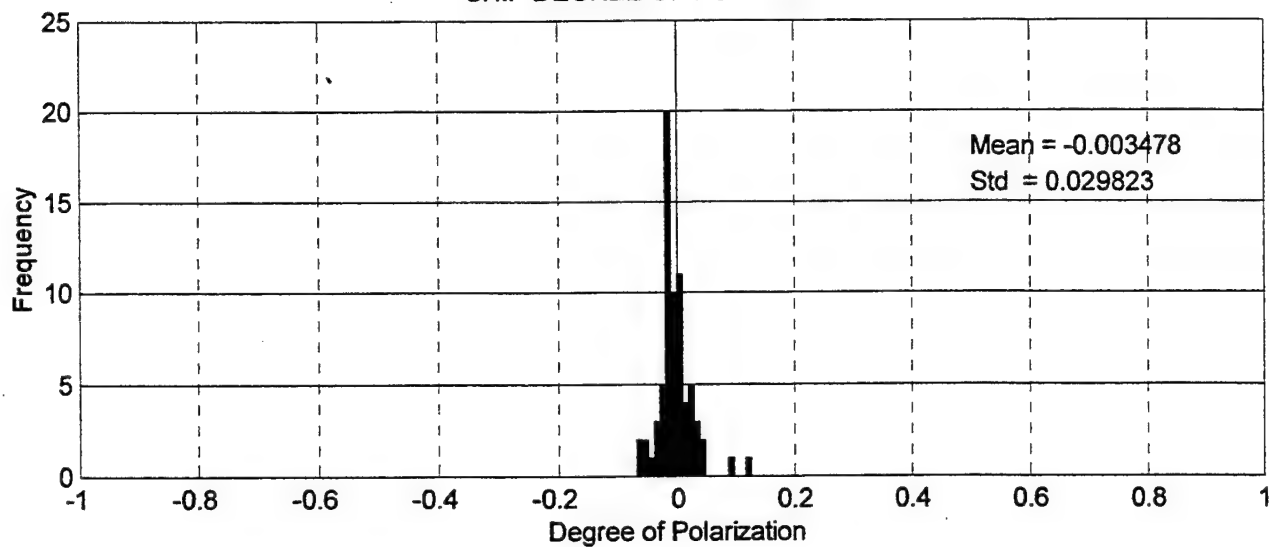
HORIZONTAL POLARIZATION



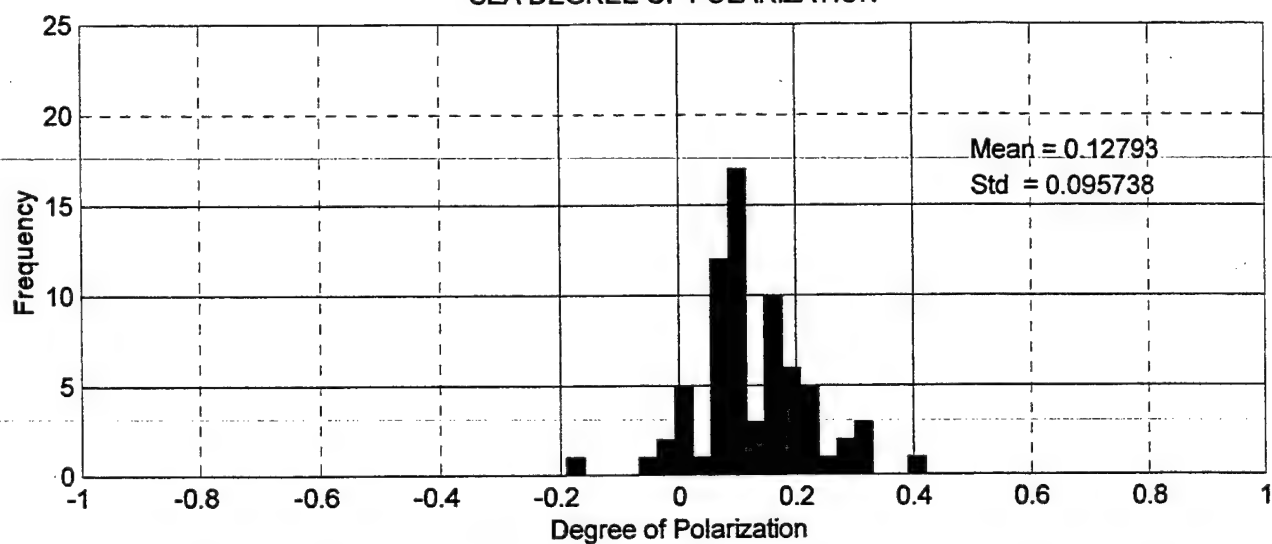
VERTICAL POLARIZATION



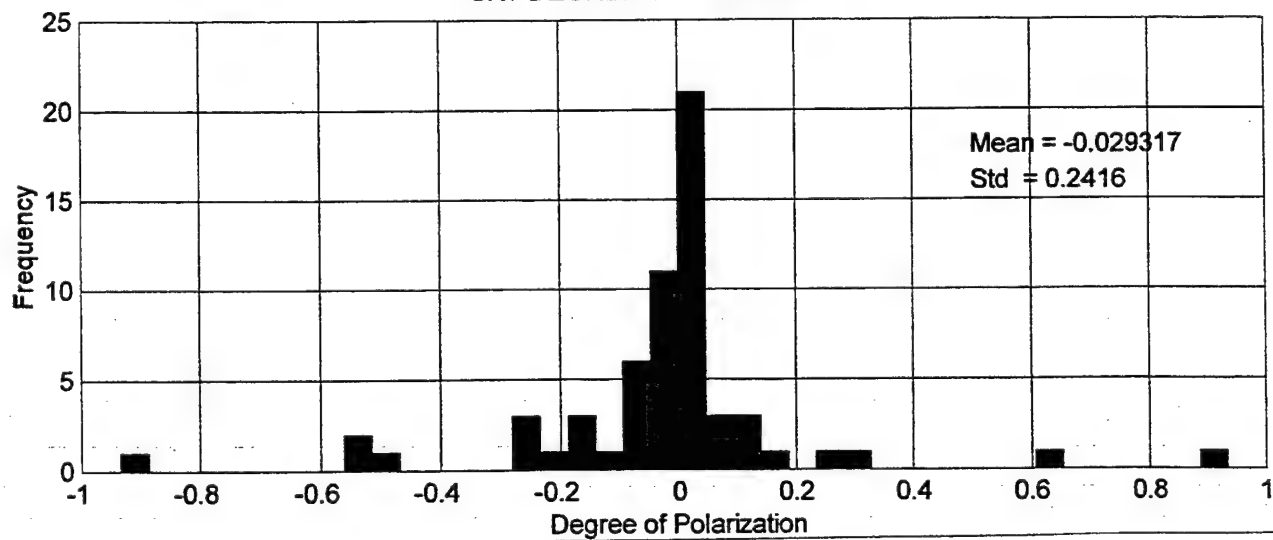
SHIP DEGREE OF POLARIZATION



SEA DEGREE OF POLARIZATION



SKY DEGREE OF POLARIZATION



4. GENERATION OF UNPOLARIZED IMAGES

Description :

This Appendix presents the analysis plots for verifying the assumption of generating unpolarized images by averaging horizontally and vertically polarized images. There are three figures corresponding to the image's main elements: ship, sea and sky. In each picture, there are two plots: line fitting process and difference histogram. All 70 files data were used to generate the plots in this Appendix.

Conditions :

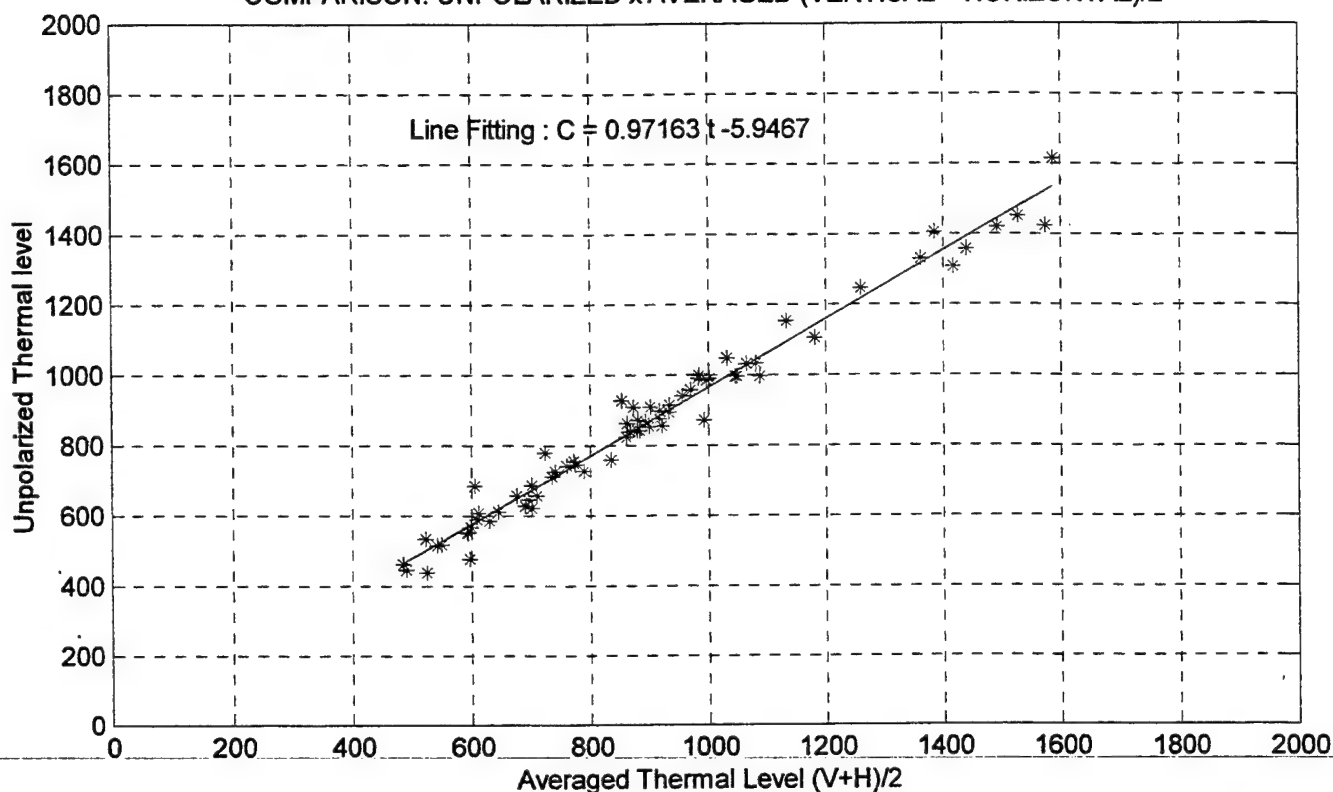
Appendix E.2 presents the conditions for each one of the 70 files used in this Appendix.

Notes :

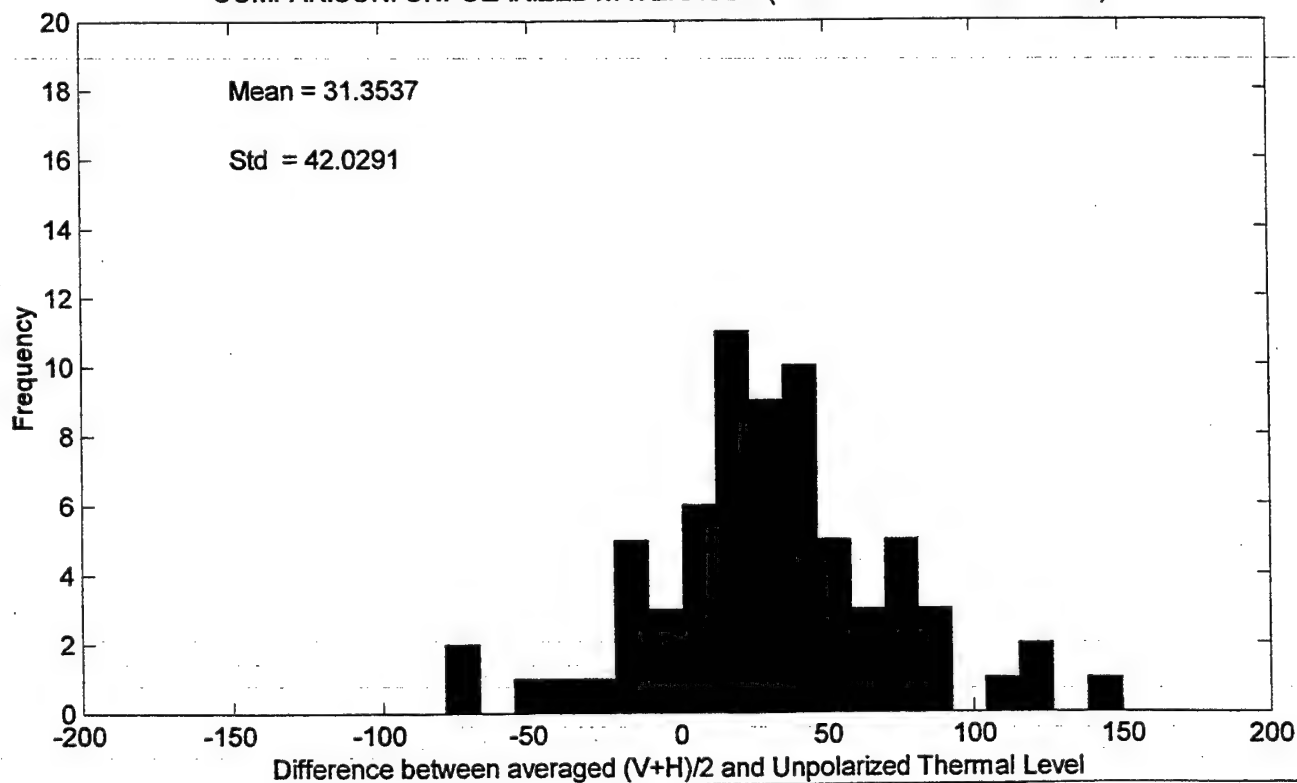
None

SHIP THERMAL LEVEL : COMPARISON UNPOLARIZED x AVERAGED “(V+H)/2”

COMPARISON: UNPOLARIZED x AVERAGED (VERTICAL + HORIZONTAL)/2

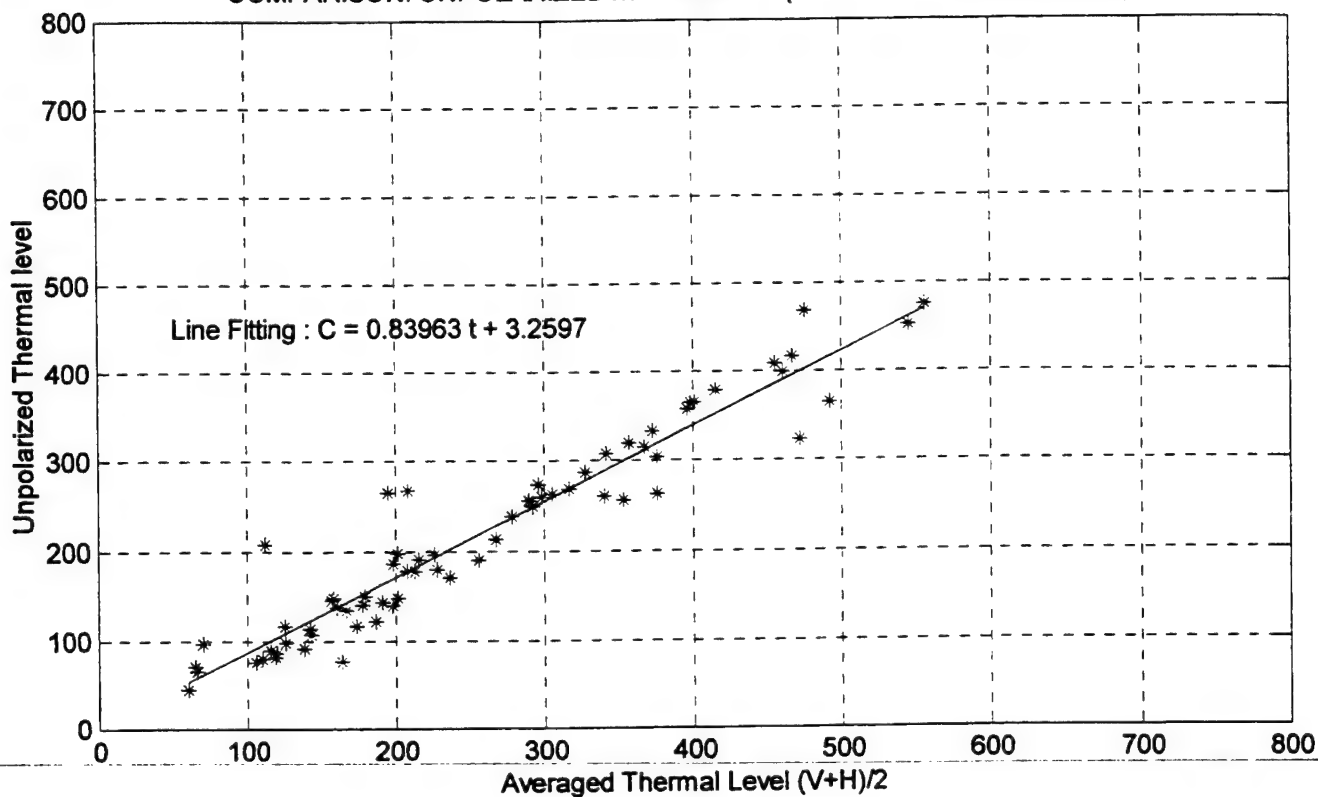


COMPARISON: UNPOLARIZED x AVERAGED (VERTICAL + HORIZONTAL)/2

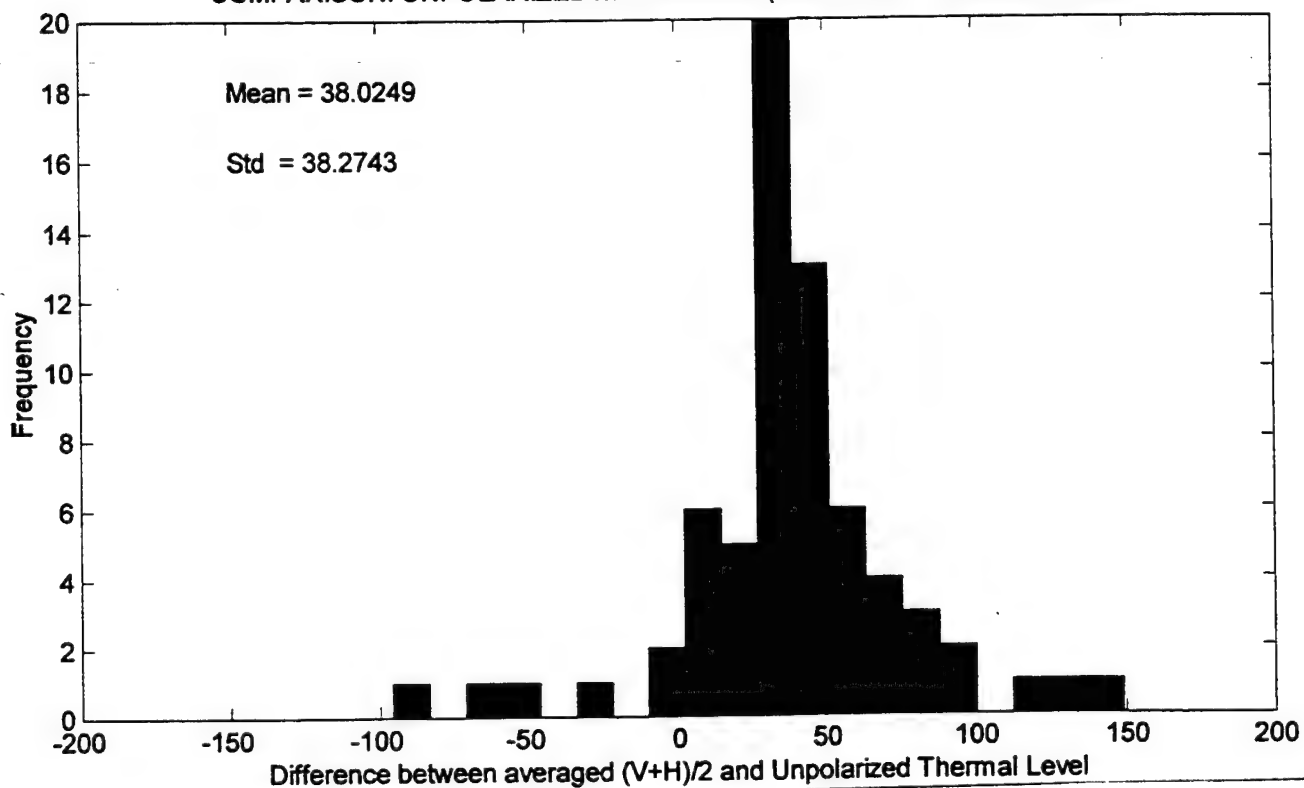


SEA THERMAL LEVEL : COMPARISON UNPOLARIZED x AVERAGED “(V+H)/2”

COMPARISON: UNPOLARIZED x AVERAGED (VERTICAL + HORIZONTAL)/2

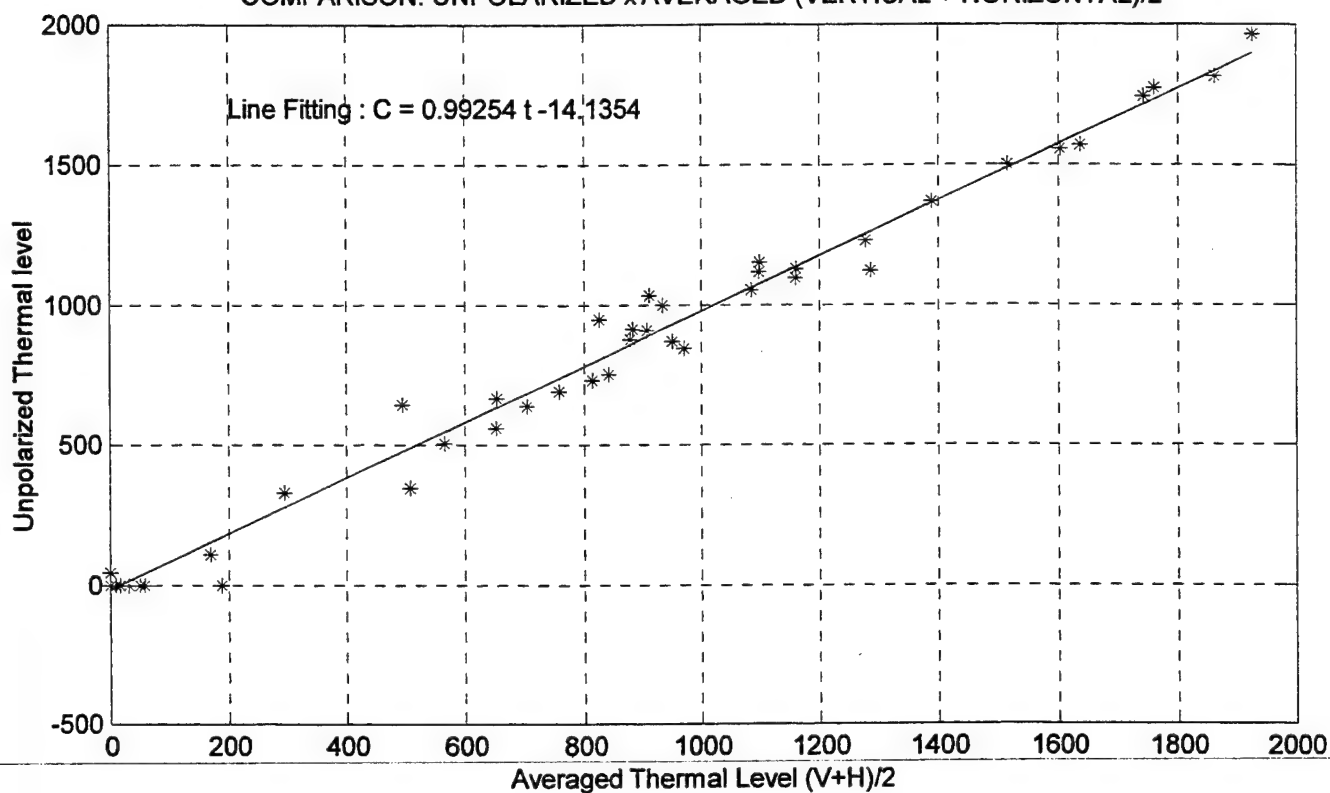


COMPARISON: UNPOLARIZED x AVERAGED (VERTICAL + HORIZONTAL)/2

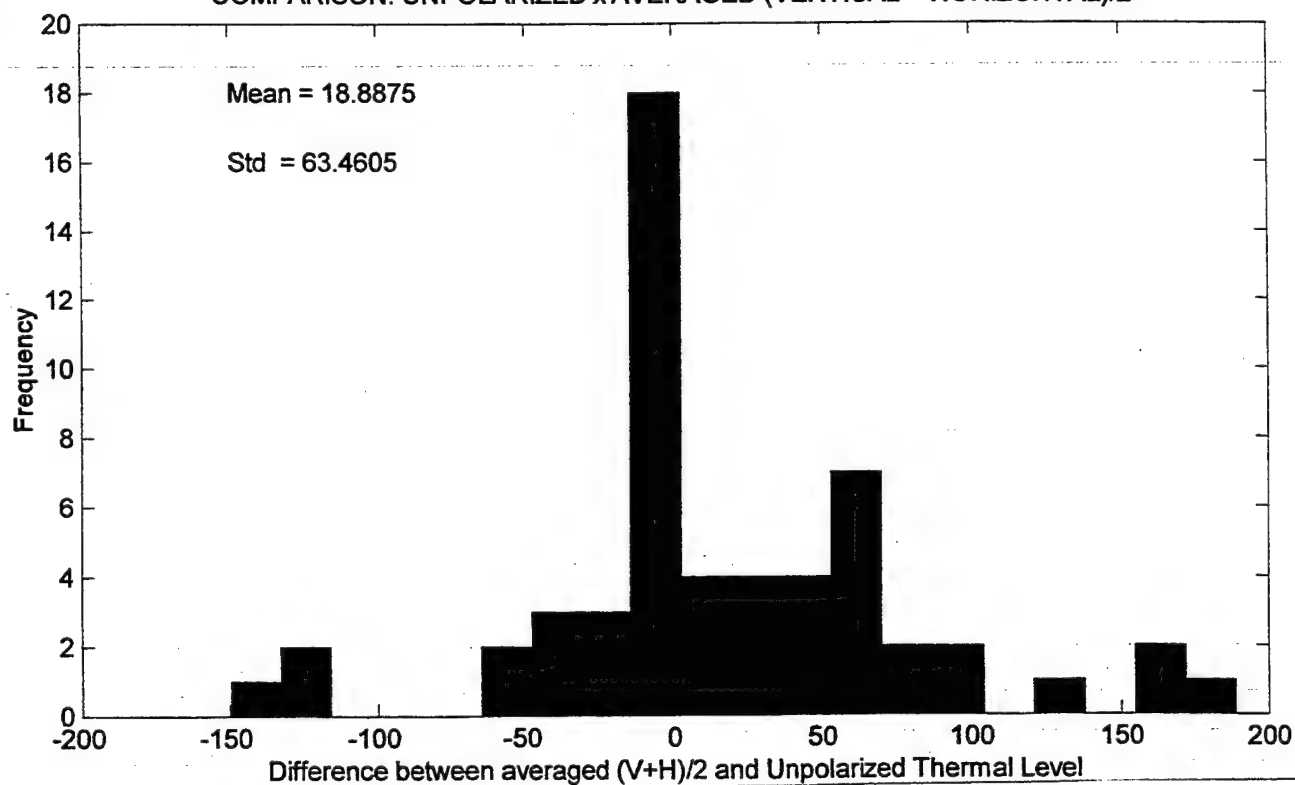


SKY THERMAL LEVEL : COMPARISON UNPOLARIZED x AVERAGED "(V+H)/2"

COMPARISON: UNPOLARIZED x AVERAGED (VERTICAL + HORIZONTAL)/2



COMPARISON: UNPOLARIZED x AVERAGED (VERTICAL + HORIZONTAL)/2



5. TARGET ASPECT ANGLE EFFECTS

Description :

This Appendix presents the analysis plots for verifying the effect of the target aspect angle on its degree of polarization. There are six figures showing the degree of polarization of the ship and its main planes against the aspect angle at different ranges (distance sensor to target) For each plot, the data range information is indicated in its title. When “all ranges” is indicated, that means that all 70 files data were used to generate the plot. For the other plots (where a range interval is indicated) only the corresponding files were used.

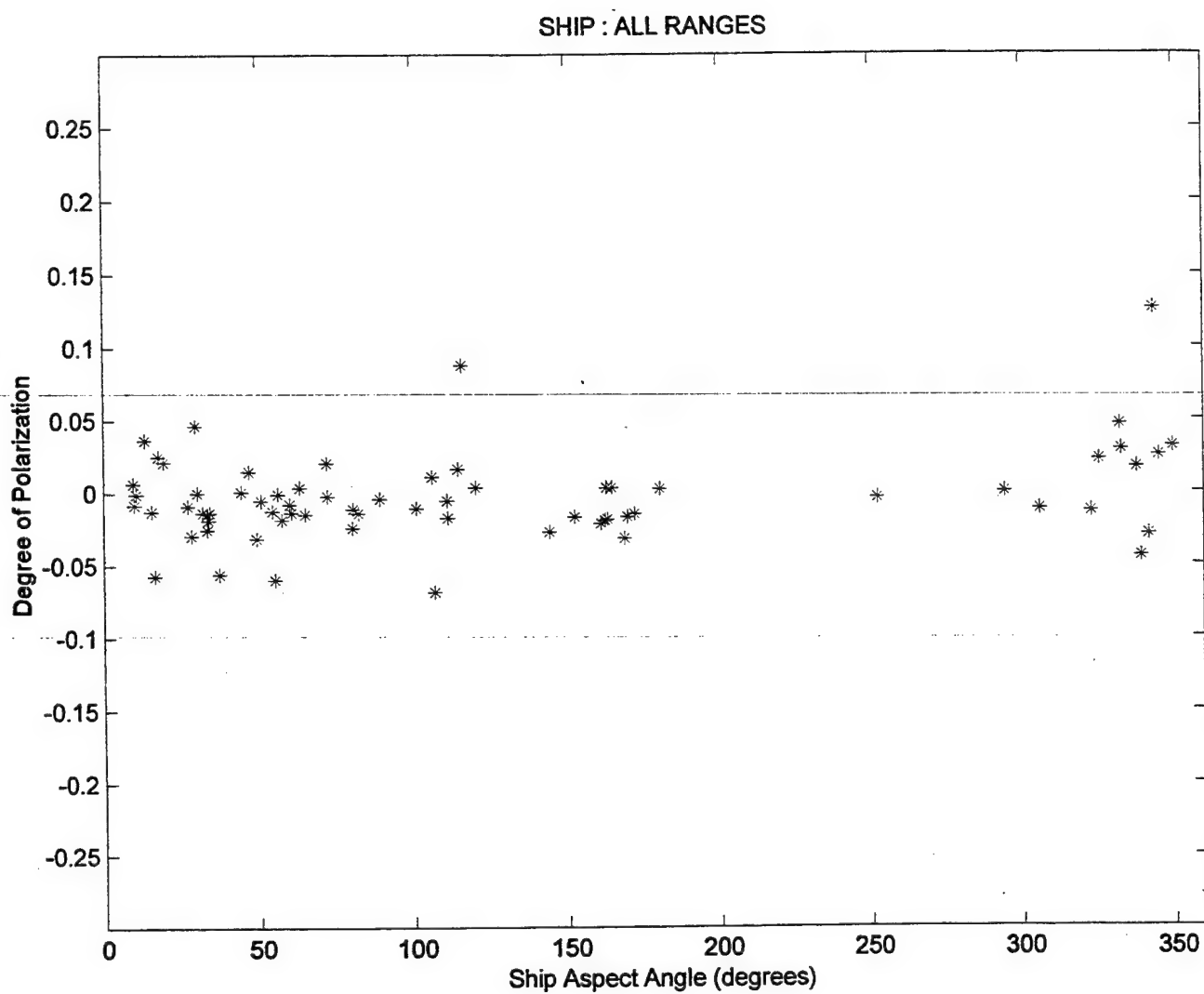
Conditions :

Appendix E.2 presents the conditions for each one of the 70 files used in this Appendix.

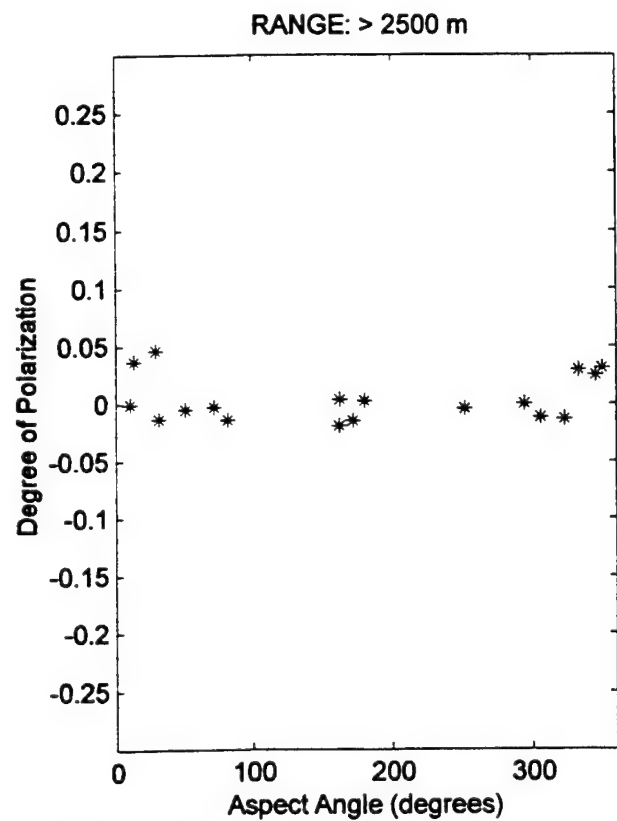
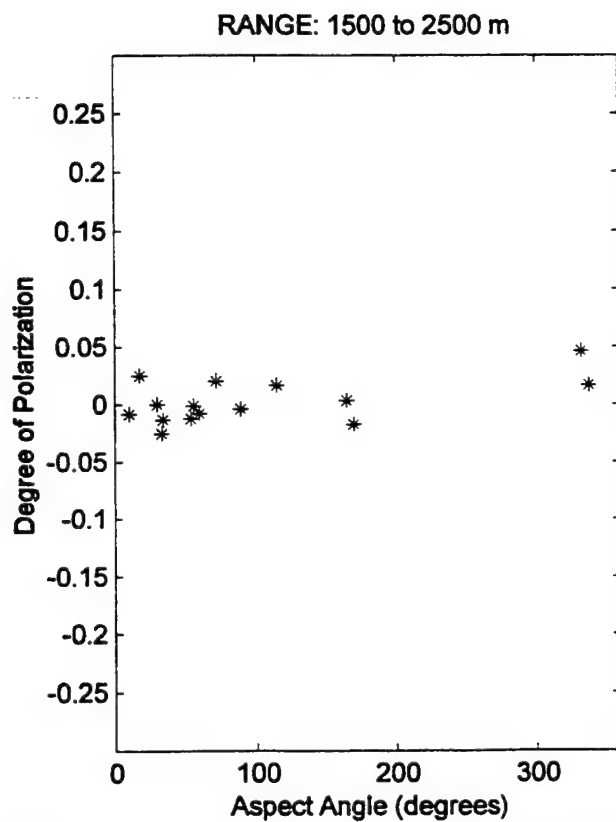
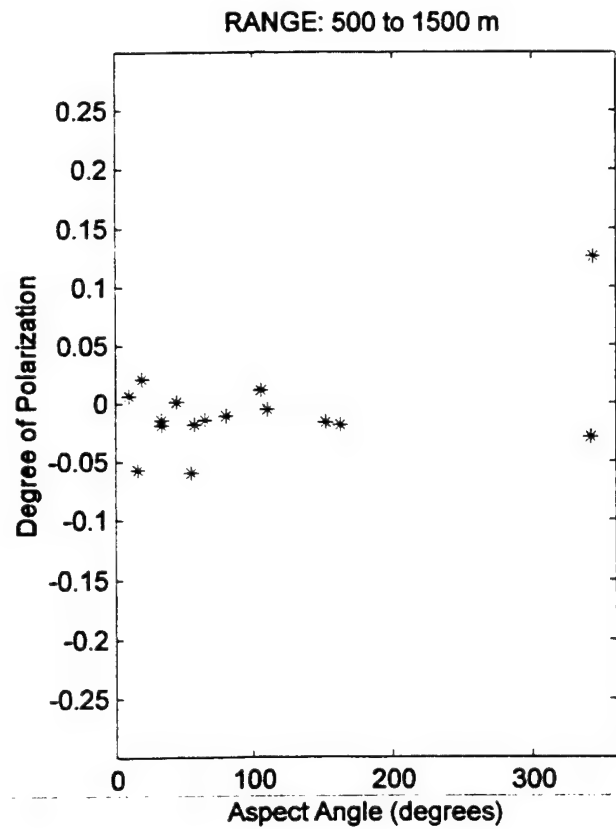
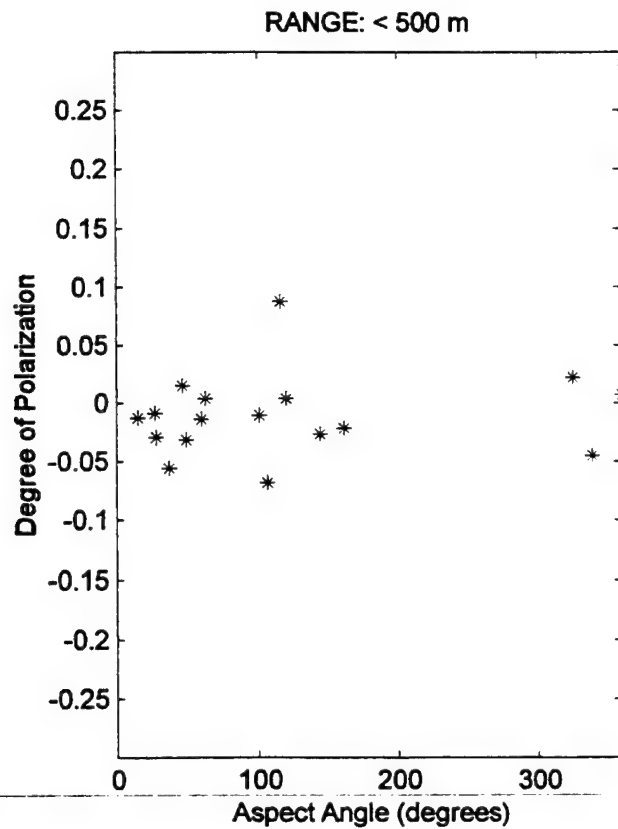
Notes :

Column “range” in the table presented in Appendix E.2 corresponds to the range information used in the plots presented here (in this Appendix)

SHIP DEGREE OF POLARIZATION (ALL 70 FILES)

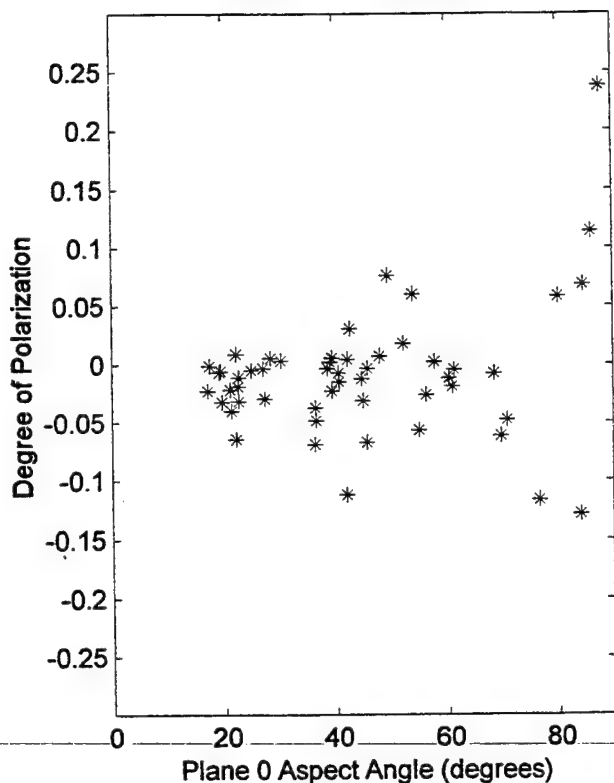


SHIP DEGREE OF POLARIZATION (BY RANGE INTERVALS)

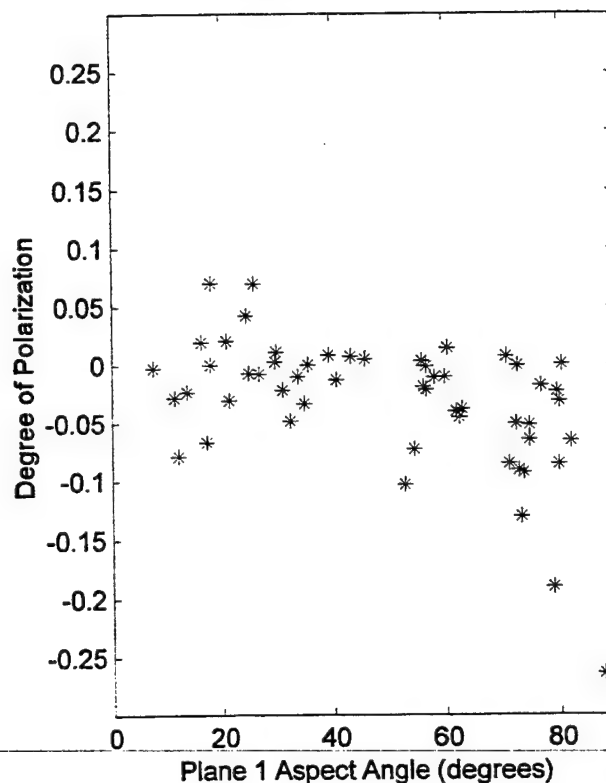


SHIP PLANES' DEGREE OF POLARIZATION (ALL 70 FILES)

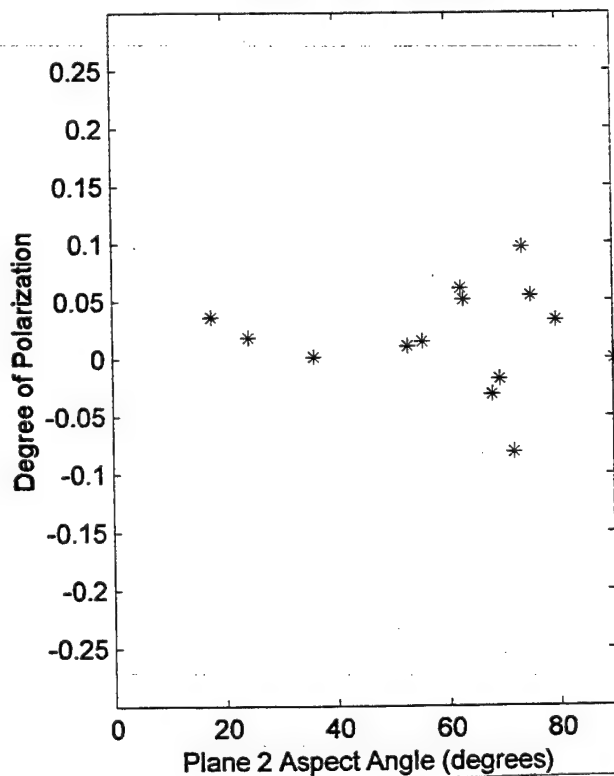
PLANE 0 : ALL RANGES



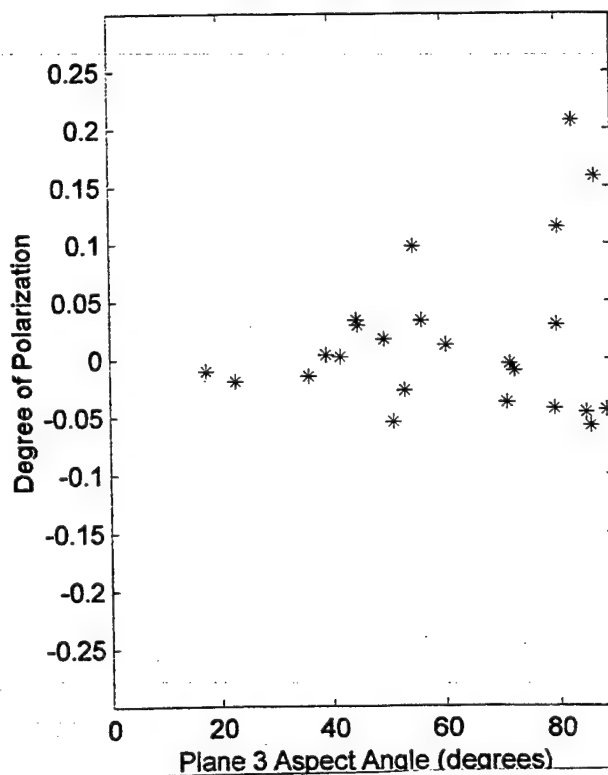
PLANE 1 : ALL RANGES



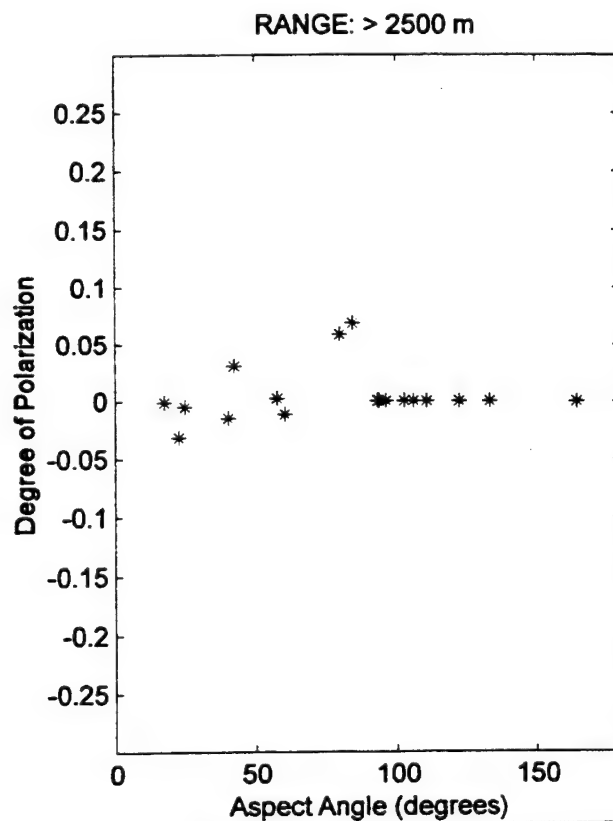
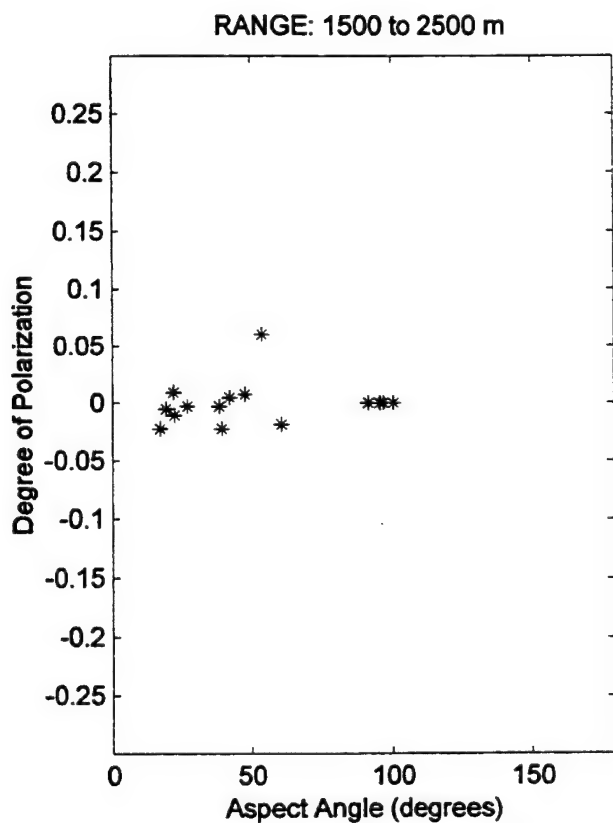
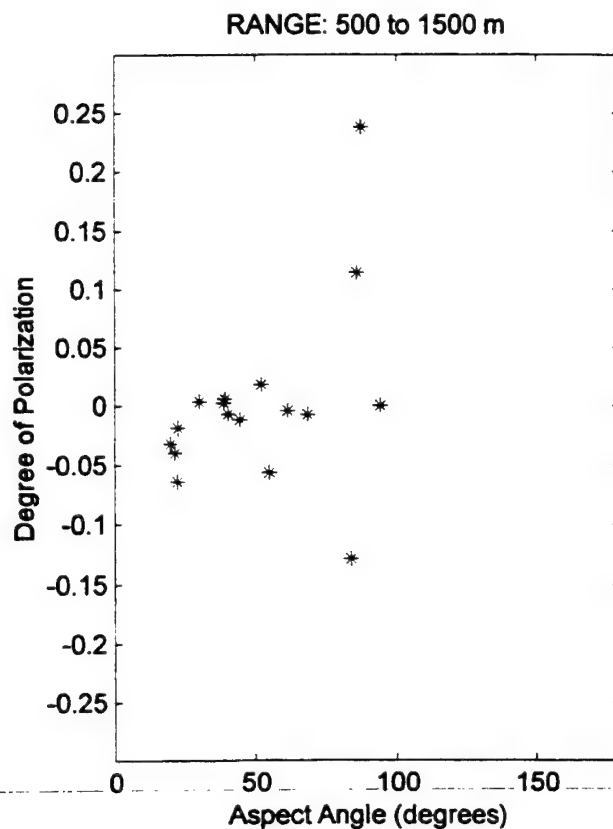
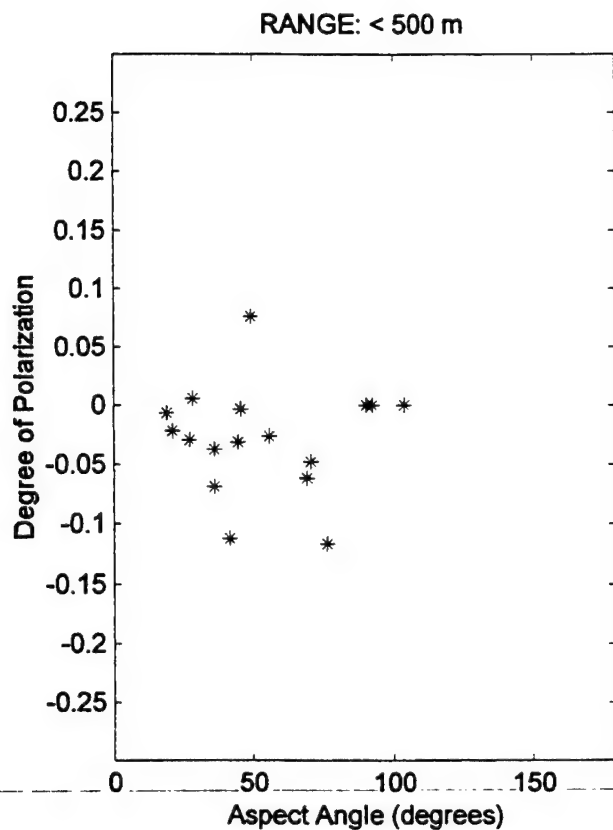
PLANE 2 : ALL RANGES



PLANE 3 : ALL RANGES

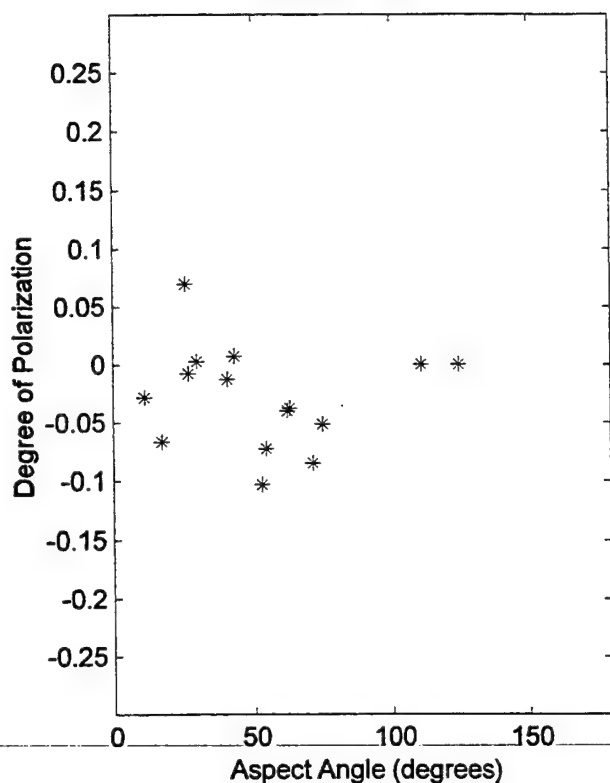


PLANE 0 DEGREE OF POLARIZATION (BY RANGE INTERVALS)

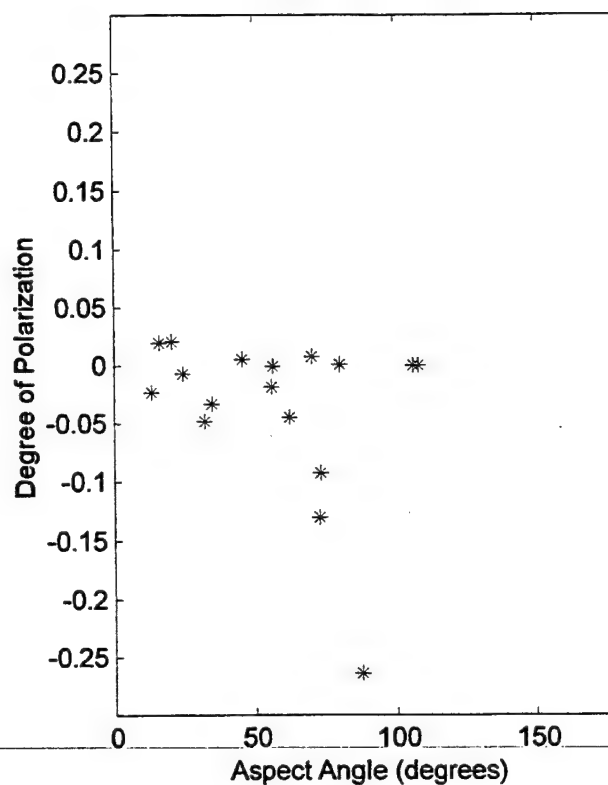


PLANE 1 DEGREE OF POLARIZATION (BY RANGE INTERVALS)

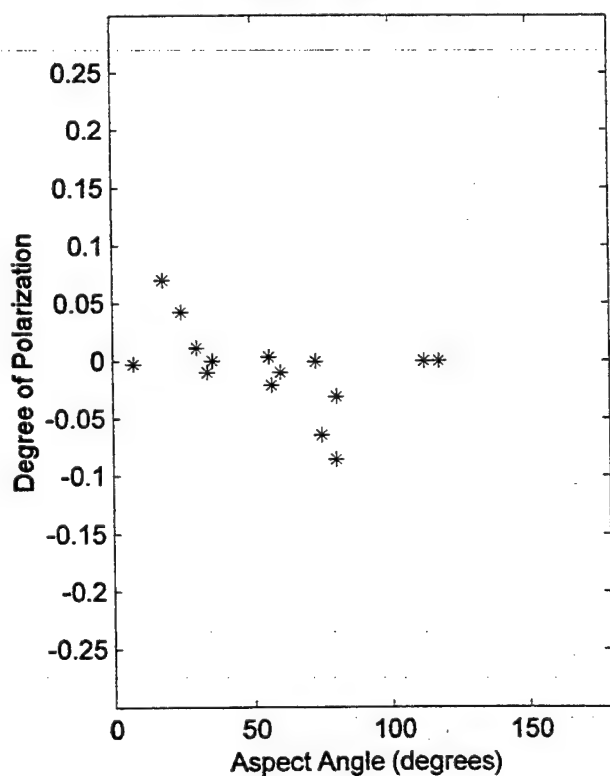
RANGE: < 500 m



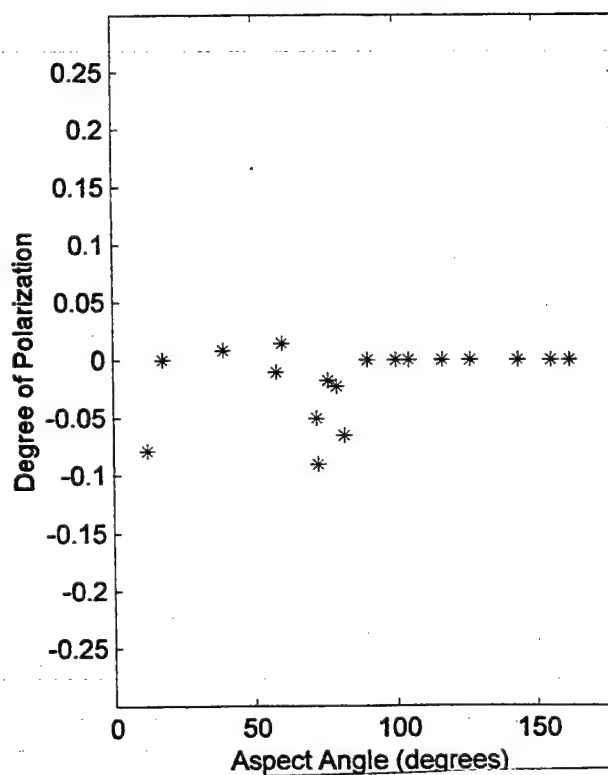
RANGE: 500 to 1500 m



RANGE: 1500 to 2500 m

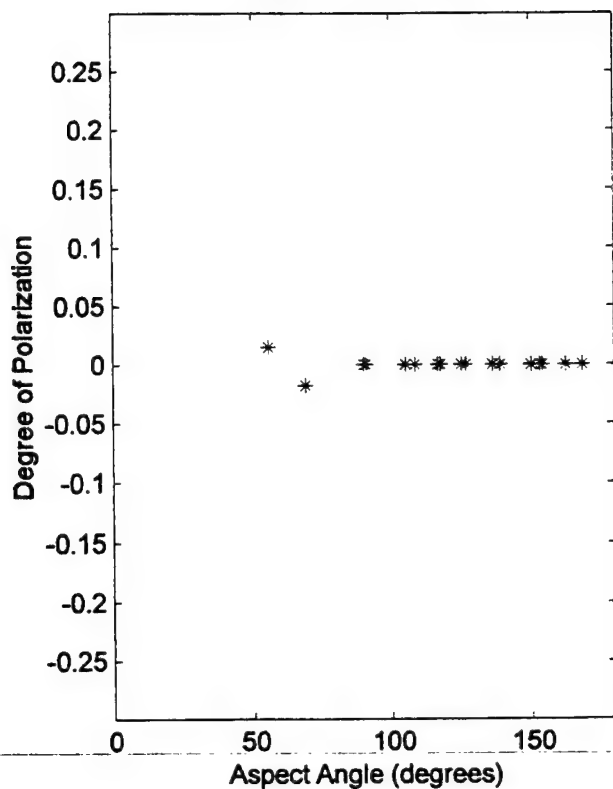


RANGE: > 2500 m

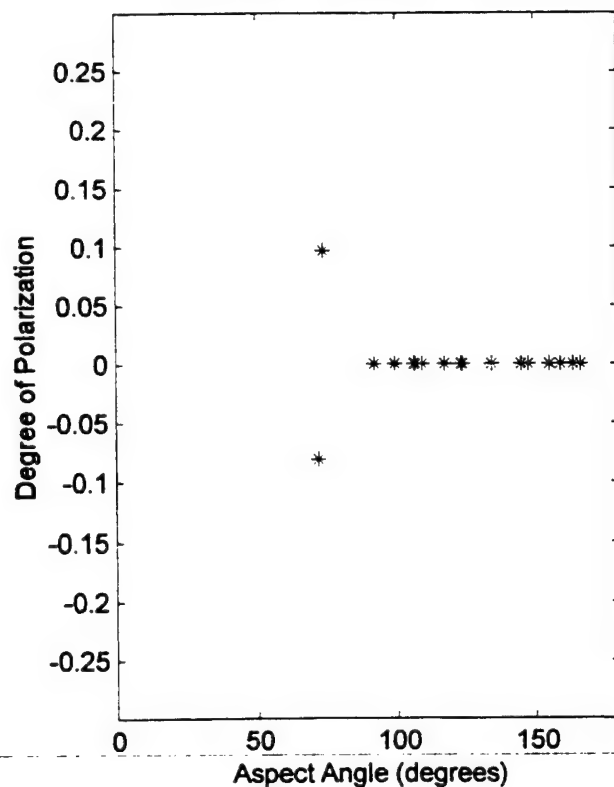


PLANE 2 DEGREE OF POLARIZATION (BY RANGE INTERVALS)

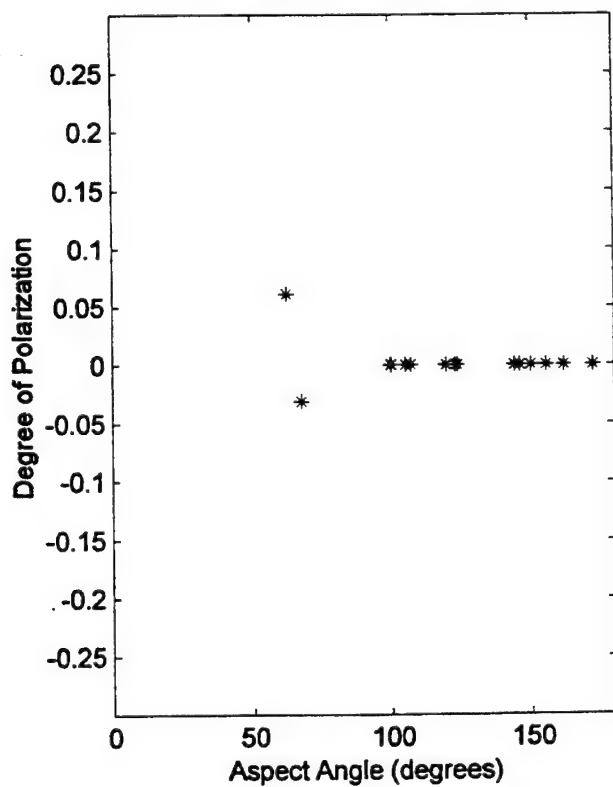
RANGE: < 500 m



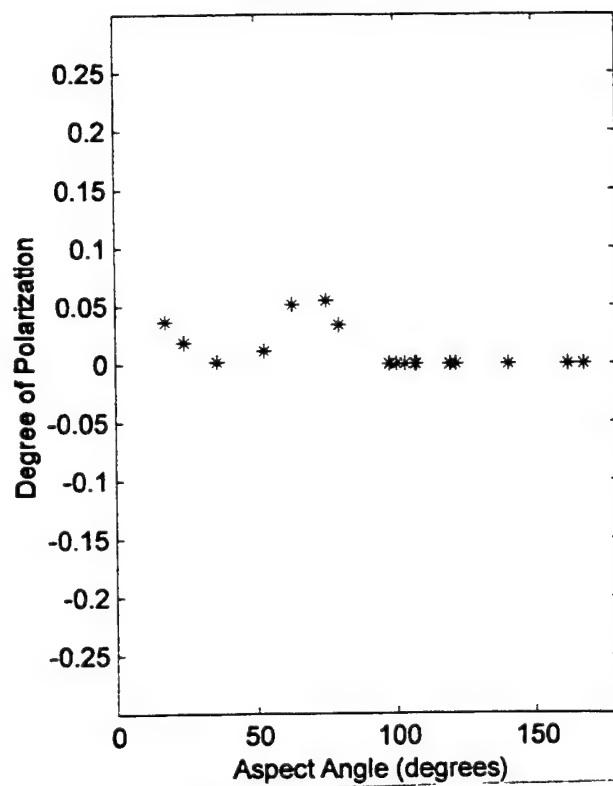
RANGE: 500 to 1500 m



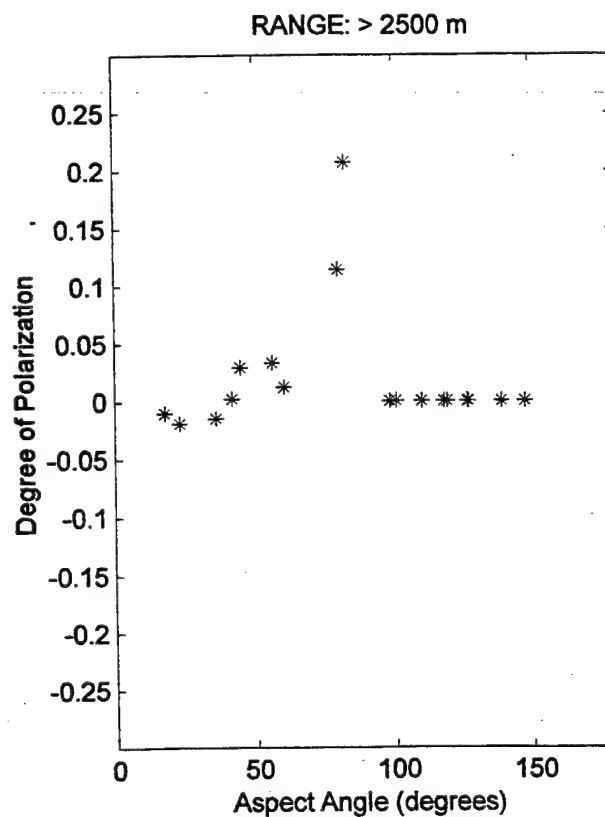
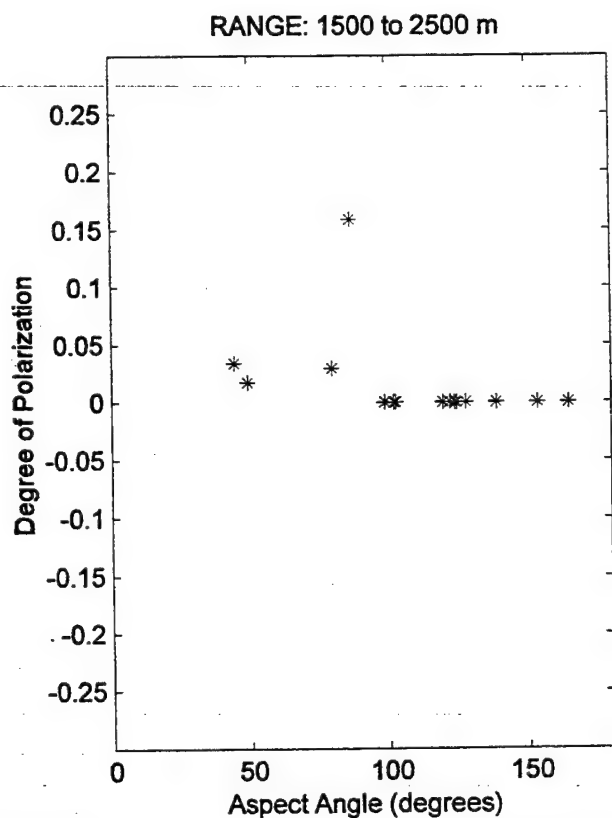
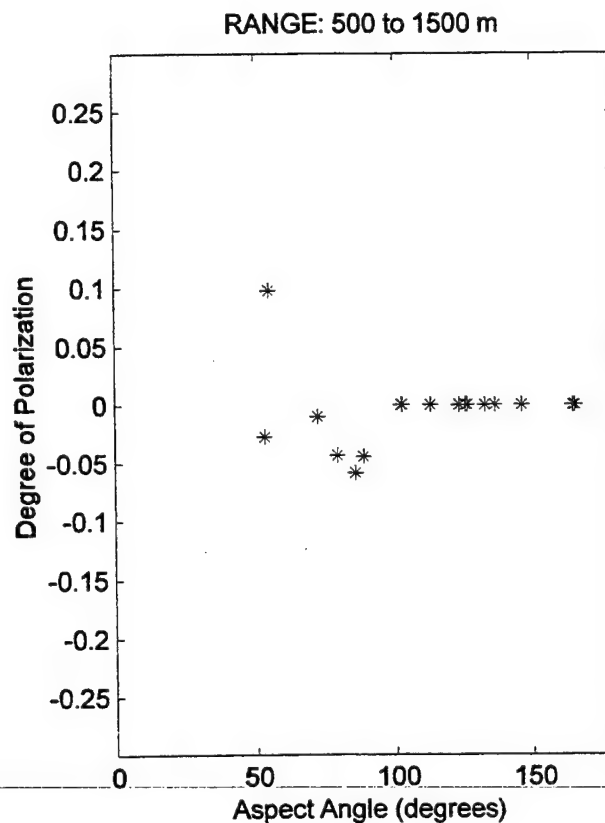
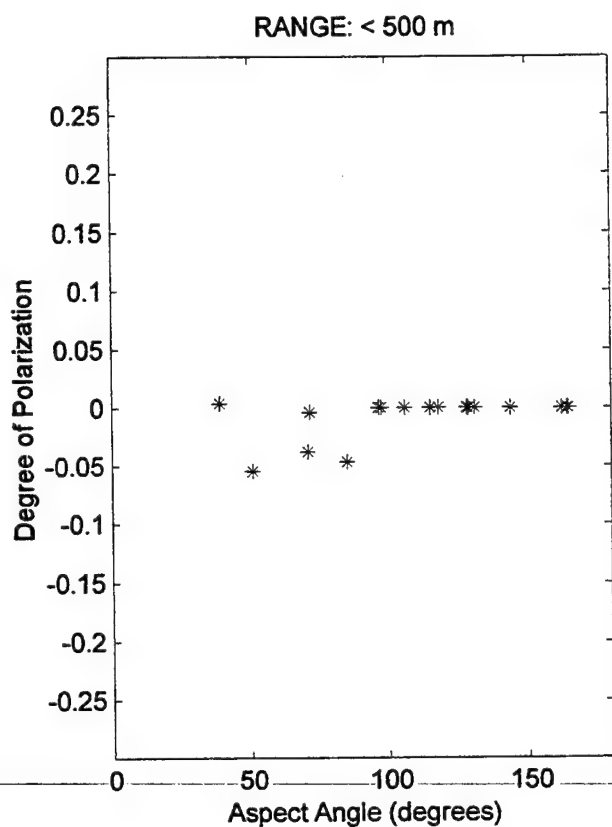
RANGE: 1500 to 2500 m



RANGE: > 2500 m



PLANE 3 DEGREE OF POLARIZATION (BY RANGE INTERVALS)



LIST OF REFERENCES

1. Chan, P.M., "Experimental Investigation of Infrared Polarization Effects in Target and Background Discrimination," Master's Thesis, Naval Postgraduate School, December, 1993.
2. Moretz, D.G., "Analysis of Target Contrast Improvement Using Polarization Filtering in the Infrared Region," Master's Thesis, Naval Postgraduate School, December, 1994.
3. Gregoris, Dennis J., Yu, Simon, Cooper, Alfred W., Milne, Edward A., "Dual-band Infrared Polarization Measurements of Sun Glint from the Sea Surface," *SPIE Proceedings*, Vol. 1687, 1992.
4. Heisey P. H., "Split-Field And Internally Filtered Imaging Polarimeter Development And Testing," Master's Thesis, Naval Postgraduate School, June, 1996.
5. Cooper, A.W., Lentz, W.J., Walker, P.L., Chan, P.M., "Infrared Polarization Measurements of Ship Signatures and Background Contrast," *SPIE Proceedings*, SPIE International Symposium on Optical Engineering in Aerospace Sensing, Orlando, FL, April, 1992.
6. Walker, P.L., Lentz, W.J., Cooper, A.W., "Atmospheric and Sea State Dependence of Polarized Infrared Contrast," *SPIE Symposium on Electro-Optics in Aerospace Engineering*, Orlando, FL, April 1995, SPIE Proceedings, Vol. 2469, 1995.
7. Lloyd, J.M., *Thermal Imaging Systems*, Plenum Press. New York, 1975.
8. *AGA Thermovision Operating Manual*, AGA Thermovision Systems AB, Publication No. 556 492, ed. II, 1980.
9. Cooper, A.W., Crittenden, E.C., "Electro-optic Sensors and Systems," Naval Postgraduate School, Naval Academic Center for Infrared Technology, February, 1995.
10. Wolfe, W.L., Zissis, G.J., *The Infrared Handbook*, Environmental Research Institute of Michigan, United States Government Printing Office, 1978.
11. Sidran, M., "Broadband Reflectance and Emissivity of Specular and Rough Water Surfaces," *Applied Optics*, Vol. 20, No. 18, September 1981.
12. Basener, R.F., McCoyd G.C., "Polarization of Infrared Light Emitted by the Sea," *Grumman Research Department Memorandum* RM-360, April 1967.

13. Saunders, P.M., "Radiance of Sea and Sky in the Infrared Window 800-1200cm⁻¹," *Journal of the Optical Society of America*, Vol. 58, No. 5, May 1968.
14. Jordan, D.L., Lewis, G., "Infrared Polarization Signatures," *AGARD Meeting on Atmospheric Propagation Effects through Natural and Man-made Obscurants for Visible to MM-Wave Radiation*, May 1993.
15. Bramson, M.A., *Infrared Radiation : A Handbook for Application*, Plenum Press, New York, 1968.
16. Collett E., *Polarized Light Fundamentals and Applications*, Marcel Dekker, Inc., New York, 1993.
17. Cooper A.W., Crittenden E.C., class notes for PH4253, Sources, Signals and Systems, Naval Postgraduate School.
18. Coulson, K.L., *Polarization and Intensity of Light in the Atmosphere*, A. Deepak Publishing, Hampton, Virginia, 1988.
19. Grum, F. And Becherer, R.J., *Optical Radiation Measurements*, Academic Press, New York, 1979.
20. Hackforth, H.L., *Infrared Radiation*, McGraw-Hill, New York, 1960.
21. Lloyd, J.M., *Thermal Imaging Systems*, Plenum Press, New York, 1975.
22. Skowronek, P.J., *Infrared Polarization Imaging Characteristics*, Master's Thesis, Naval Postgraduate School, September, 1994.
23. Sandus, O., "A Review of Emission Polarization," *Applied Optics*, Vol. 4, No. 12, December, 1965.
24. Rosell, F., and Harvey, G., Editors, *The Fundamentals of Thermal Imaging Systems*, Electro-optical Technology Program Office, Naval Research Laboratory, Washington, D.C., 1979.
25. Schade W.J., and Law, D.B., "IR Sky Radiance Distribution in the Marine Boundary Layer," *SPIE Proceedings*, Vol. 926, 1988.

INITIAL DISTRIBUTION LIST

	No. Copies
1. Defense Technical Information Center 87725 John J. Kingman Rd., STE 0944 Ft. Belvoir, VA 22060-6218	2
2. Dudley Knox Library Naval Postgraduate School 411 Dyer Rd. Monterey, CA 93943-5101	2
3. Professor Alfred W. Cooper Code PH/Cr Naval Postgraduate School Monterey, CA 93943-5101	2
4. Professor David D. Cleary Code PH/CI Naval Postgraduate School Monterey, CA 93943-5101	1
5. Naval Sea Systems Command PEO- Theater Air Defense, Ship Self Defense ATTN: Mr J.E. Misanin, PEO-TAD D-234 Washington, DC 20363-5100	1
6. Naval Space and Naval Warfare Systems Center Propagation Division ATTN: Dr. J.H. Richter, Code 88 53570 Silvergate Ave. San Diego, CA 92152-5230	1
7. Naval Space and Naval Warfare Systems Center RDT&E Division ATTN: Dr. D.R. Jensen 53570 Silvergate Ave. San Diego, CA 92152-5230	1

8. Naval Air Warfare Center 1
Research and Technology Group, Physics Branch
ATTN: Dr. J. Bevan
China Lake, CA 93555-6100
9. Capt. Marcos Cesar Pontes 1
National Aeronautics and Space Administration
Lyndon B. Johnson Space Center
Houston, TX 77058